# Micelle-forming Macromolecular Conjugates of Methotrexate and Paclitaxel: Structural Effects on Micellar Properties and Drug Release

by

Yu Li

A dissertation submitted in partial fulfillment of

the requirement for the degree of

Doctor of Philosophy

(Pharmaceutical Sciences)

at the

UNIVERSITY OF WISCONSIN-MADISON

2000

AW
LH

# Micelle-forming Macromolecular Conjugates of Methotrexate and Paclitaxel: Structural Effects on Micellar Properties and Drug Release

Yu Li

Under the supervision of Associate Professor Glen S. Kwon

at the University of Wisconsin-Madison

Block copolymer micelles have been used for the solubilization of hydrophobic drugs. However, the application of polymeric micelles in drug delivery has been limited by suboptimal drug loading capacity and unpredictable drug release, which is largely related to the physicochemical properties of polymeric micelles.

The current study aimed to develop amphiphilic block copolymers containing covalently conjugated drugs. A hydrolyzable ester linkage was incorporated into the structure of the micelle-forming polymer-drug conjugates, and therefore, release of drug was potentially achievable through hydrolysis. Two anticancer drugs, methotrexate (MTX) and paclitaxel, were conjugated to a block copolymer, poly(ethylene oxide)-*block*-poly(aspartic acid), using an alkyl group as a linker. The resultant conjugates self-assembled into micelles in aqueous environments. Under physiological pH values, MTX and paclitaxel were released slowly from the conjugates.

Poly(ethylene oxide)-*block*-poly(β-benzyl-L-aspartate) (PEO-*b*-PBLA) was used as the starting material for the synthesis of drug-polymer conjugates. For the synthesis of methotrexate esters, the benzyl groups on the PBLA block were replaced by a $C_2$ or $C_6$ alkyl spacer group introduced by the aminolysis of PEO-*b*-PBLA with 2-aminoethanol or 6-

aminohexanol, yielding poly(ethylene oxide)-*block*-poly(hydroxyalkylaspartamide) (PEO-*b*-PHAA). Methotrexate was coupled to PEO-*b*-PHAA through an ester bond.

The conjugation of MTX to PEO-*b*-PHAA greatly enhanced the hydrophobicity of the block copolymer. The resultant conjugates underwent self-assembly in an aqueous environment, and the drug moieties were incorporated into the core of the micelles. The hydrophobicity of the conjugates influenced the physicochemical properties of the polymeric micelles and drug release. Eight micelle-forming MTX esters with varied hydrophobicity were synthesized. The critical micelle concentration, micelle stability, and MTX release were correlated with the hydrophobicity of the polymeric conjugates. A highly hydrophobic polymer conjugate displayed a low CMC. The conjugates that form stable micelles released MTX slowly.

MTX esters exhibited decreased inhibitory activity toward dihydrofolate reductase (DHFR) compared with free drug and decreased anticancer activity against murine leukemia L1210 cells. The presence of folate lowered the cell inhibitory activity of MTX esters toward L1210 cells, implying the altered cellular uptake pathway of MTX, as a result of conjugation to polymeric carriers.

I dedicate this thesis to my parents, my husband, Zhongren, and my son, Jarey. It is with their love and support that I have navigated my educational journey.

# ACKNOWLEDGMENTS

I would like to express my gratitude to the following individuals:

Dr. Glen Kwon, who brought me the opportunity to study in the School of Pharmacy, University of Wisconsin-Madison and to pursue in the field of drug delivery;

Dr. Kozonri Kataoka, who consistently supported this study;

Drs. George Zografi, Ralph Abrecht, Indig, and Joe Robinson, members of my thesis committee. I thank them for their time and interest in this project;

Ms. Bing Li. I thank her for her friendship, companionship and aid in the past years;

Ms. Monica Adams. I thank her for her precious time on revising all my writings, especially the first chapter of this thesis;

Ms. Lavasefar Afsaneh, a graduate student in the University of Alberta, who assisted me in some of the TEM studies;

All the staffs in the instrumental service office, in the general office, and in the stockroom;

Finally, the sources of funding without which this study would not have been possible: NIH Grant AI43346-01 and the New Investigator Program of the Burroughs Wellcome Fund and the American Association of Colleges of Pharmacy.

# Table of Contents

# List of Tables

# List of Figures

# List of Abbreviations

| | |
|---|---|
| BOP | benzotriazolyl-N-oxy-tris(dimethylamino)-phosphonium hexafluorophosphate |
| CBz | benzyloxycarbonyl |
| CMC | critical micelle concentration |
| CWC | critical water concentration |
| DCC | dicyclohexylcarbodiimide |
| DHFR | dihydrofolate reductase |
| DLS | dynamic light scattering |
| DMAc | dimethylacetamide |
| DMAP | dimethylaminopyridine |
| DMEM | Dulbecco's Modified Eagle's medium |
| DMF | dimethylformamide |
| DMSO | dimethylsulfide |
| DOX | doxorubicin |
| EPR | enhanced permeability and retention |
| GPC | gel permeation chromatography |
| 2-HP | 2-hydroxypyridine |
| HPLC | high performance liquid chromatography |
| LCST | low critical solution temperature |
| MTX | methotrexate |
| MW | molecular weight |
| NMP | N-methylpyrolidone |
| NMR | nuclear magnetic resonance |

| | |
|---|---|
| PEO | poly(ethylene oxide) |
| PEO-*b*-PAsp | poly(ethylene oxide)-*block*-poly(aspartic acid) |
| PEO-*b*-PLAsp | poly(ethylene oxide)-*block*-poly(L-aspartic acid) |
| PEO-*b*-PBLA | poly(ethylene oxide)-*block*-poly(β-benzyl-L-aspartate) |
| PEO-*b*-PHAA | poly(ethylene oxide)-*block*-poly(hydroxyalkyl aspartamide) |
| PMS | phenazine methosulfate |
| SEC | size exclusion chromatography |
| TEM | transmission electron microscopy |
| TLC | thin layer chromatography |
| TMS | tetramethylsilane |
| UV-Vis | ulatraviolet-visible |
| XTT | 2,3-bis(2-methoxy-4-nitro-5-sulphonyl-5-[(phenelamino)carbonyl]-2H-tetrozolium hydroxide |

# CHAPTER 1

# Introduction

Recent advances in genomics have expanded the range of potential drug targets (1). The application of genome-based technology will greatly speed up the development of new therapeutic agents (2). A variety of structurally unrelated, novel agents with new mechanisms of action are continually being generated by increasingly efficient drug discovery programs. Therefore, the development of appropriate drug delivery systems must keep pace with the progress of drug discovery. Although numerous investigators are aggressively exploiting innovative drug delivery systems, the effective delivery of drugs to their target site still limits the success of therapeutics.

## 1.1. Basic components of an ideal drug delivery system

An ideal drug-delivery system is expected to transport a drug to a desired site within the body and then liberate the drug. The carrier should then be degraded to non-toxic substances and eliminated from the body. Examples of transporting vehicles with desirable functions are natural molecule transport systems such as lipoproteins and viruses, which transport biologically active substances.

### *1.1.1. Natural molecule transport systems*

#### *1.1.1a. Lipoproteins*

Plasma lipoproteins are nanoscopic endogenous colloids which transport lipids such as cholesterol in blood. Low-density lipoprotein (LDL) consists of a hydrophobic core comprised of triglyceride, cholesterol, and the hydrophobic regions of apolipoprotein and a hydrophilic shell of the polar region of phospholipids and hydrophilic regions of apolipoprotein. LDL enters cells via receptor-mediated endocytosis (3). When bound to LDL receptors in the coated pits, the LDL particles are rapidly internalized via coated vesicles. Upon shedding the clathrin coats, these vesicles then deliver their contents to early endosomes located near the cell periphery. Once in the endosomal compartment, LDL is delivered via late endosomes to lysosomes, where the cholesteryl esters in the LDL particles are hydrolyzed to free cholesterol. This free cholesterol then becomes available to the cell for membrane synthesis. LDL is being actively investigated as a carrier for water insoluble drugs.

#### *1.1.1b. Viruses*

Viruses are supramolecular complexes that can replicate themselves inside appropriate host cells. A virus consists of a nucleic acid molecule surrounded by a protective shell, or capsid, made up of protein molecules, and in some cases, a membranous envelope. Viruses efficiently transport the enclosed nucleic acid to the host cells via receptor-mediated endocytosis. Delivery scientists are trying to utilize mechanistic information on how viral

particles infect cells. These mechanisms are beginning to be applied to drug-delivery systems, particularly gene delivery systems (4).

In general, these natural transport systems possess an environmentally separated microcontainer formed by supramolecular assembly and a binding moiety on the surface. They exhibit excellent biocompatibility and are able to promptly release biological substances in response to a series of biological events (5).

### *1.1.2. Models of drug delivery systems*

There are numerous elements that enable drug delivery to the correct site at a predetermined time and rate of release. The ultimate aim of such systems is tailoring drug formulations to meet the individual requirements under the control of pathophysiological or *in vivo* conditions. The clinical utilization of many therapeutic agents has been limited due to poor water solubility, insufficient stability and low specificity. Therefore, the development of novel drug-delivery technologies that can efficiently deliver problematic drugs to the desired site at a desired time is necessary.

In principle, a drug delivery system consists of three basic components: a transporting device, drug moieties, and a targeting device, as proposed by Ringsdorf (6). Each component possesses unique functionality required for optimal drug delivery. The transporting device is a molecular (Figure 1.1) or vesicular (Figure 1.2) carrier for drug molecules containing segments to make the whole system soluble and nontoxic. Furthermore, the system can improve drug solubility or protect the drug from degradation. The drug molecules are incorporated to a transporting carrier through physical interaction or a chemical bond, and are

expected to exert a pharmacological effect upon release. The targeting device directs the carrier and drug to the targeted cells. Sugars and antibodies have been exploited as pilot molecules for the delivery of drugs to targeted organs or tissues which can drastically decrease the side effects of the drug (7, 8). Consequently, the therapeutic index of the drug can be improved and toxicity minimized.

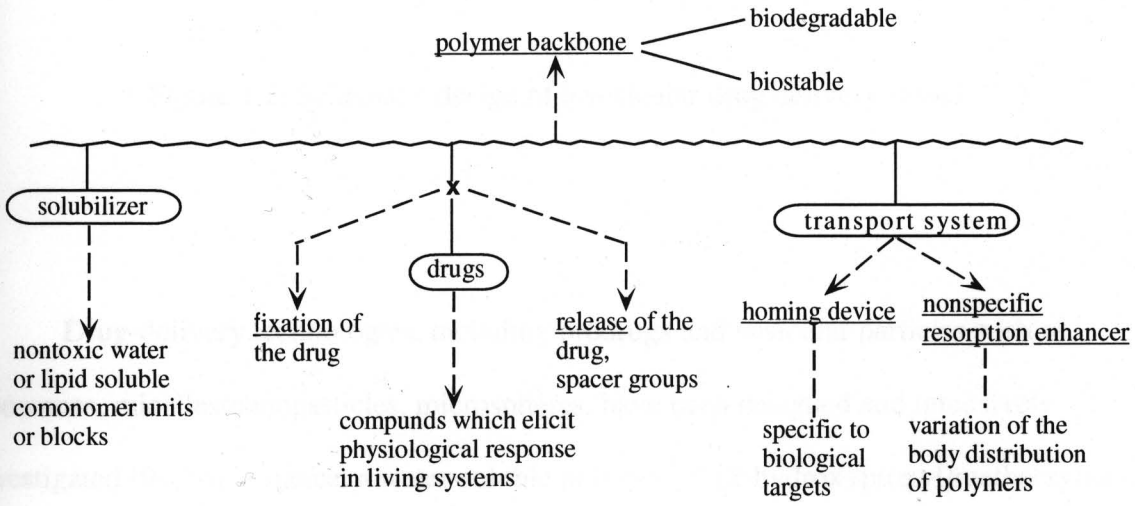


Figure 1.1. Ringsdorf's model for a pharmacologically active polymer.

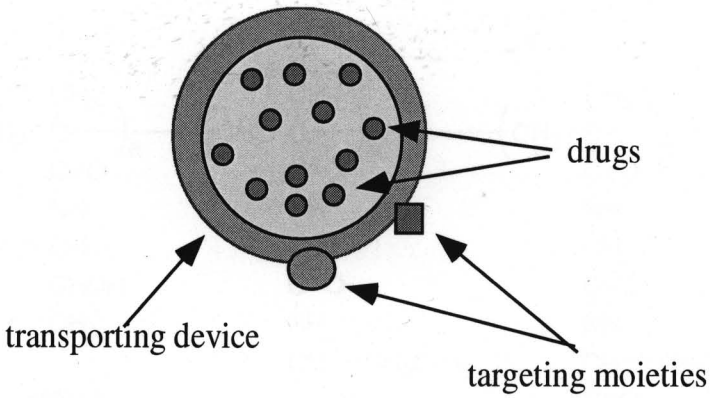


Figure 1.2. Schematic design of a vesicular drug delivery vehicle.

Drug-delivery technologies, including prodrugs and vesicular particles such as liposomes, micelles/nanoparticles, microspheres, have been designed and intensively investigated (9). For instance, a water-soluble polymer, N-(2-hydroxypropyl)methacrylamide (HPMA) copolymer, has been designed as a molecular-basis drug-carrier. The conjugation of doxorubicin (DOX), an anticancer drug, to HPMA copolymer results in a water-soluble polymer-drug conjugate (10). Using peptidyl spacers, the conjugate can be cleaved by lysosomal enzymes. Consequently, the solubility of DOX is greatly enhanced and its side effects are greatly reduced. Moreover, attaching a sugar molecule, galactosamine (GalN), to the conjugate makes it possible to mediate liver targeting (Figure 1.3) (11).

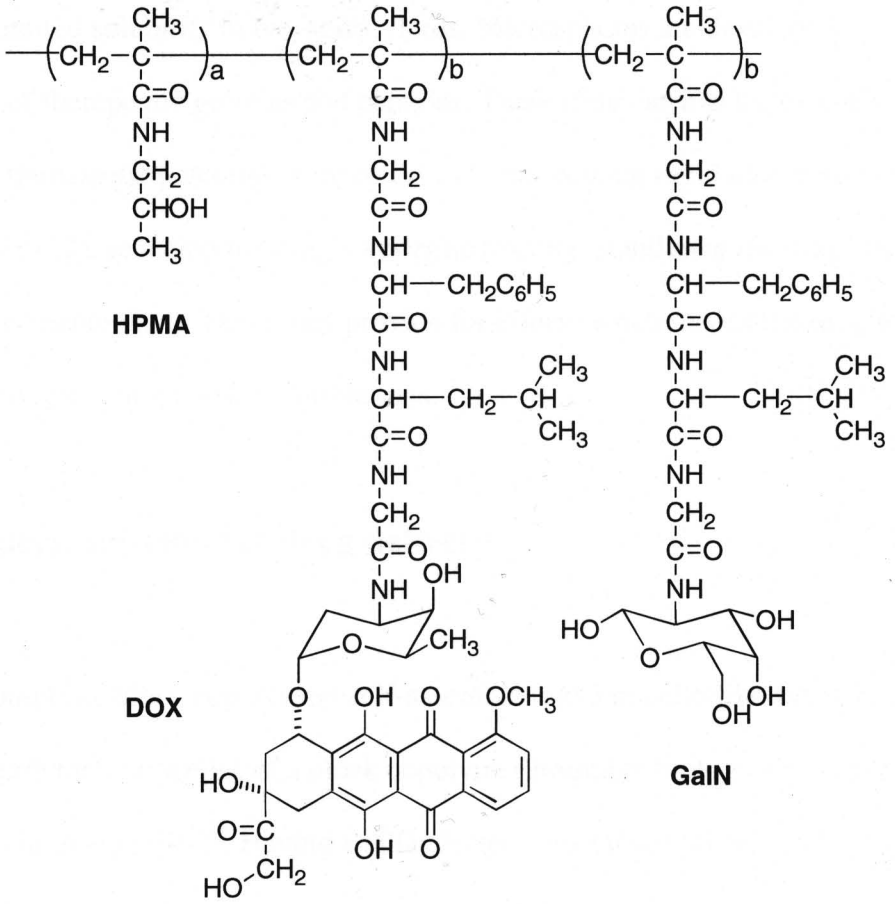


Figure 1.3. Chemical structure of HPMA copolymer-doxorubicin conjugate. The weight average molecular weight is approximately 30,000 g/mol.

Liposomes and micelles/nanoparticles are vesicle based drug carriers. While the exteriors of the vesicles are water compatible, they may be used for the administration of drugs with limited solubility in biological fluids. Microspheres are developed primarily for the delivery of therapeutic proteins and peptides. These drug carriers have been shown to enhance the therapeutic potential of many drugs by preventing rapid elimination of the drug from the body (12), reducing the drug's systemic toxicity, stabilizing the drug, and optimizing its metabolism. These may provide for effective delivery of the drug to a target site, thereby overcoming transport limitations.

## 1.2. Polymeric micelles for drug delivery

Amphiphilic block copolymers self-assemble into a micelle-like structure in aqueous media. The polymeric micelles of a block copolymer resemble biological transport systems such as LDL in many aspects. Having similar dimensions (about 20 nm) and analogous structural features to LDL, polymeric micelles have been investigated for drug delivery (13).

### *1.2.1. Milestones in the development of polymeric micelles for drug delivery*

Much of the interest in exploiting polymeric micelles for drug delivery is frequently traced to Ringsdorf's pioneering studies (14). For the first time, he introduced the concept that a micelle-forming block copolymer can serve as a lipoprotein-like drug carrier (Figure 1.4). He and coworkers attached hydrophobic palmitoyl or cyclophosphamide onto a polymer, poly(ethylene oxide)-*block*-poly(lysine). Micelle formation of the block copolymer

was evidenced by the solubilization of a dye, sudan red 7B. The micelles exhibited similar behaviors to low molecular weight surfactant micelles. *In vivo* studies of the conjugate revealed a prolonged life span for L1210 tumor-bearing mice.

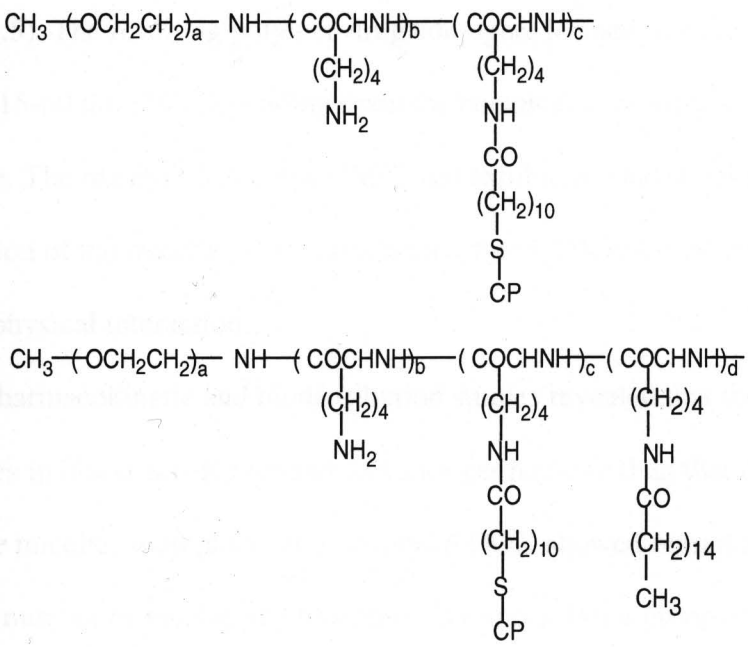

Figure 1.4. Chemical structure of a micelle-forming block copolymer drug conjugate (Ringsdorf's first example).

Kataoka and coworkers have conducted extensive studies on polymeric micelles for drug delivery (15). They synthesized an AB block copolymer, poly(ethylene oxide)-*block*-poly(β-benzyl L-aspartate) (PEO-*b*-PBLA) through a ring opening polymerization of β-benzyl-L-aspartate-N-carboxylanhydride using ω-methyl-α-aminopolyethylene oxide as an initiator. Hydrolysis of PEO-*b*-PBLA produced poly(ethylene oxide)-*block*-poly(aspartic acid) (PEO-*b*-PAsp). DOX was then attached to PEO-*b*-PAsp through an amide linkage (Figure 1.5). The resulting polymer-drug conjugate formed micelles in aqueous solution with a size of 15-60 nm (16), depending upon the chemical composition of the polymeric conjugate. The micelles had a low CMC, and exhibited good stability in terms of slow dissociation of the micelle (17). Furthermore, free DOX could be entrapped into the micelles through physical interaction.

Pharmacokinetic and biodistribution studies revealed that the concentration of conjugates in blood was higher and had a longer half-life than that of free DOX. The conjugate micelles with physically entrapped DOX showed remarkable anti-cancer activity against a number of murine and human solid tumors. For a group of mice bearing C26 tumors, complete disappearance of the tumors was observed. However, subsequent studies revealed that the chemically bound DOX did not have antitumor activity. Instead, the observed activity was due to physically entrapped drug (18). These results revealed that the conjugated DOX could not be released from its carrier owing to stability of the amide bond, which is inert toward hydrolysis.

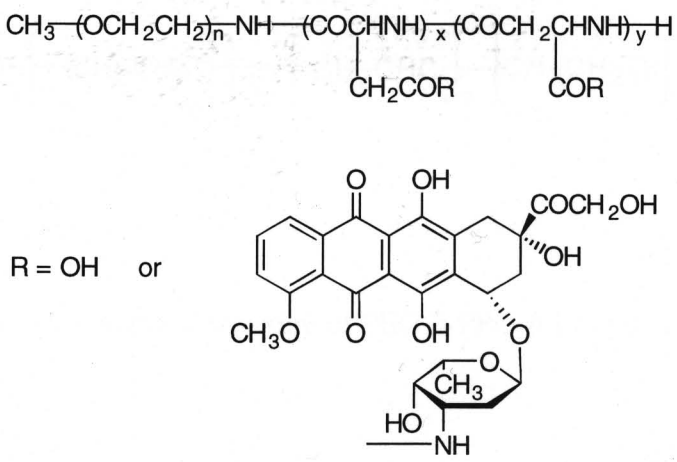


Figure 1.5. Chemical structure of PEO-*b*-PAsp-DOX.

In the meantime, the remarkable biological properties of Pluronic triblock copolymers, poly(ethylene oxide)-*block*-poly(propylene oxide)-*block*-poly(ethylene oxide) (PEO-*b*-PPO-*b*-PEO) (Figure 1.6), were explored by Kabanov and coworkers. Specifically, they demonstrated that Pluronic micelles could be used as a delivery vehicles for hydrophobic drugs (19, 20) and that Pluronics are able to enhance the delivery of haloperidol to the brain (21). The group also found that Pluronics could overcome multidrug resistance due to the inhibition of the P-glycoprotein mediated drug efflux (22).

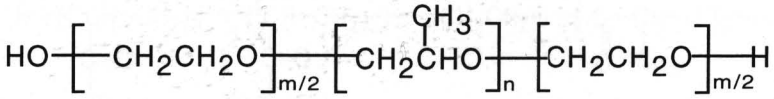


Figure 1.6. Chemical structure of PEO-*b*-PPO-*b*-PEO (Pluronic).

Functional block copolymers greatly extend the scope of polymeric micelles in drug delivery. Thermo-responsive block copolymers have been reported (23). Poly(N-isopropylacrylamide) (PIPAAm) is a thermally sensitive polymer which exhibits reversible hydration-dehydration changes in aqueous media in response to small temperature changes. The transition temperature, called the lower critical solution temperature (LCST), of PIPAAm is 32°C in water (24). Below the LCST, PIPAAm is water soluble in an extended chain form. Above the LCST, it becomes hydrophobic and precipitates from water. Block copolymers with PIPAAm as the shell-forming block form micelles that exhibit reversible changes in optical properties in response to changes in solution temperature. Polymeric micelles composed of PIPAAm-*block*-polystyrene (23), P(IPAAm-*block*-D,L-lactic acid) (25), and P(IPAAm-*co*-N,N-dimethylacrylamide)-*b*-poly(D,L –lactic acid) (P(IPAAm-*co*-DMAAm)-*b*-PDLLA) (26) (Figure 1.7) have shown thermoresponsive properties. Dynamic light scattering and atomic force microscopy studies of poly(N-isopropylacrylamide)-*block*-D,L-lactic acid) indicated that the micelles were approximately 40 nm in diameter below the

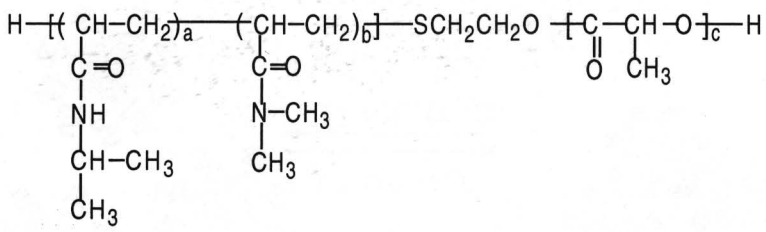

Figure 1.7. Chemical structure of P(IPAAm-*co*-DMAAm)-*b*-PDLLA.

LCST. Above this temperature, the polymeric micelles were shown to undergo reversible aggregation. The LCST could be controlled by altering the chemical composition of the polymer, allowing the development of systems that aggregate at temperatures between 30-50 °C, but exist as stable nanoparticles below these temperatures. These systems may have potential use in the development of thermo-controlled drug delivery systems (Figure 1.8).

Adriamycin (ADR) has been loaded into polymeric micelles of P(IPAAm-*co*-DMAAm)-*b*-P(D,L-lactic acid). Turbidity studies found the LCST of the micelles to be 40°C. It was found that the micelles exhibited distinct properties above and below the LCST, and that the release of drug was closely related to the temperature. Above the LCST, drug is released more rapidly than below the LCST. Thus, the ADR-loaded micelles had higher cytotoxicity above the LCST than below it.

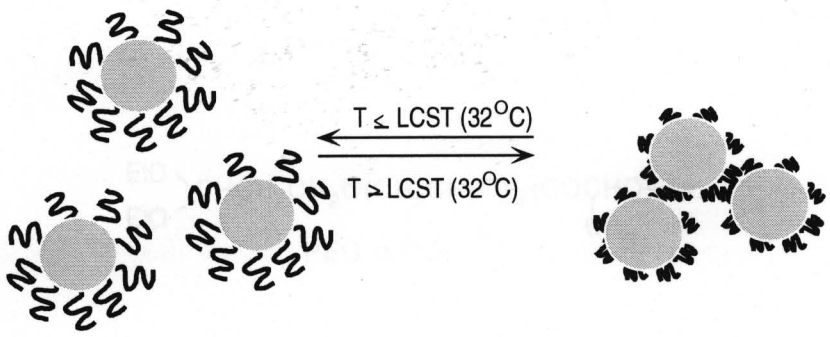


Figure 1.8. Thermo-responsive micelles above and below LCST.

Another type of functional block copolymer contains chemical functional groups which may be potentially useful for the introduction of targeting moieties. Poly(ethylene oxide-*block*-poly(lactic acid) (PEO-*b*-PLA) has a reactive aldehyde group and can form micelles with the aldehyde groups on the surface (27) (28). The exposed aldehyde groups may then be conjugated with targeting molecules. Avidin, a model protein, has been conjugated to aldehyde-PEO-*b*-PLA micelles (Figure 1.9) (29).

Polymeric micelles based on PEO-*b*-PBLA with hydroxyl groups have also been developed (28). Pluronic micelles with conjugated insulin or brain-specific antibodies can effectively deliver the entrapped haloperidol to the brain in vivo (30). Such pioneering work has explored and demonstrated the feasibility of efficient targeting to cells with various physiological or pathological properties.

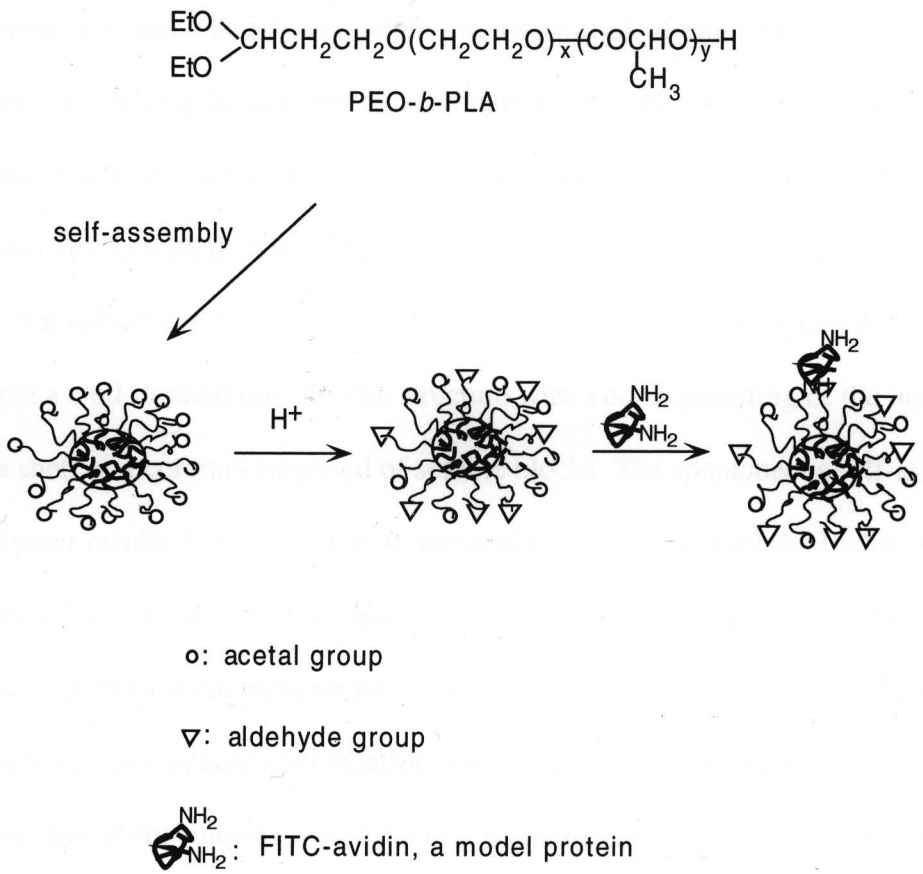


Figure 1.9. Functional PEO-*b*-PLA micelles.

### *1.2.2. Physical properties of polymeric micelles*

#### *1.2.2a. Self-assembly of block copolymers*

Amphiphilic block copolymers represent a new class of functional polymers that consist of unique building blocks serving a number of applications related mainly to the energetic and structural control of material interfaces. An amphiphilic block polymer consists of at least two blocks with different chemical natures, constituting an amphiphilic character. In solvents that selectively dissolve one of the blocks, amphiphilic block copolymers self-assemble into a well-defined micelle-like structure with a core consisting of the insoluble block and a shell or a corona comprised of soluble blocks. The spontaneous self-assembly of block copolymer results from the physical interactions among the amphiphilic molecules. In aqueous media, the central core is predominantly hydrophobic due to the expulsion of the hydrophobic segments of the polymer from the polar medium, which is believed to be an important driving force behind micellization. The hydrophilic segments orient on the surface and form the shell of the micelle, thereby acting as an interface between the micelle core and the surrounding aqueous phase (Figure 1.10) (31).

The hydrophilic block of a block copolymer should have good blood and tissue compatibility. Since the endothelial surfaces of the blood vessels are covered with negatively charged components, the polymers with neutral or slightly negative electric charge are more suitable than polycationic polymers, which can be rapidly captured by cells of the reticuloendothelial system (RES) during circulation. The micelle shell acts as a stabilizing

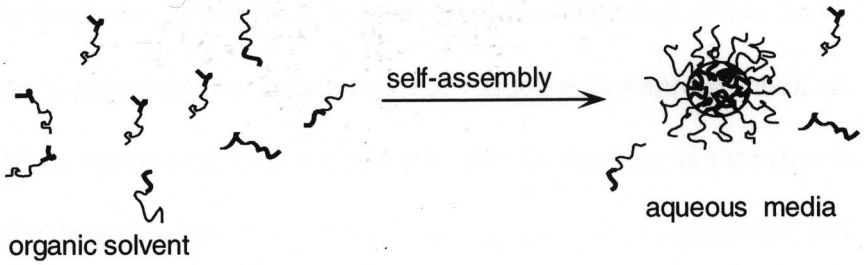


Figure 1.10. Self-assembly of block copolymers.

interface between the hydrophobic micelle core and the external medium. Thus, the properties of the outer shell greatly affect the biodistribution of the incorporated drug as well as its pharmacokinetic parameters. In most cases, the hydrophilic block has been poly(ethylene oxide) (PEO) with a molecular weight in the range of 1,000-12,000 g/mol. PEO has unlimited solubility at room temperature for all degrees of polymerization due to extensive hydrogen bonding with water molecules. Because of its remarkable water solubility, PEO has been widely used for the structural modification of a variety of molecules including low molecular weight drugs, therapeutic proteins and liposomes. Studies have shown that pegylation of proteins or liposomes can prolong their blood circulation time, increase their resistance to proteolysis, reduce their antigenicity and immunogenicity, and improve their water solubility (32). Furthermore, micelles with PEO surfaces may have a low tendency toward adsorption with biological components.

The hydrophobic block is the source for the uniqueness of a block copolymer system. The hydrophobic counterpart of an amphiphilic block copolymer may be poly(amino acids), polyesters, poly(styrene), poly(propylene oxide), poly(caprolactone), etc. Each hydrophobic block imparts the unique properties for the micelles and the diverse functionality for drug delivery. For instance, poly(amino acid) hydrophobic blocks provide block copolymers with functional groups for further structural modification. Moreover, poly(amino acids) and polyesters, especially poly(aspartic acids) or poly(glutamic acids), are degradable in biological systems. It has been shown that PEO-*block*-polystyrene micelles have a glassy core and are extremely stable with negligible chain exchange between the unimers and micelles (33).

*1.2.2b. Morphology*

A variety of morphologies have been found for the amphiphilic block copolymer aggregates. The interfacial curvature and packing symmetry are largely controlled by the copolymer composition. These morphologies include spheres, rods, vesicles, lamellae, tubules. For example, Pluronic micelles of P103 (propylene oxide (PO) units of 60 and ethylene oxide (EO) units of 34) and P123 (PO units of 69 and EO units of 39) have short hydrophilic segments and form cylindrical micelles. In contrast, block copolymers with a long hydrophilic segment tend to form spherical micelles (34). The factors affecting polystyrene-*block*-poly(acrylic acid) (PS-*b*-PAA) micelle morphology have been extensively studied by Eisenberg's group (35). The morphology of the PS-*b*-PAA aggregates may vary, depending on a number of different parameters, such as the block copolymer composition, the copolymer concentration, and the nature of common solvent used in micelle preparation.

The morphologies of block copolymer micelles may influence the drug-loading capacity, as polymeric micelles with different morphologies have varied effective core volume. Indeed, the results available in the literature suggest that Pluronics of different compositions produce micelles with distinct structures, particularly different core and corona volumes. Typically, increases in the length of the PPO block are accompanied by an increase in aggregation number, size of the hydrophobic core, and solubilization of hydrophobic substances. On the contrary, an increase in PEO content usually lowers the solubilization of hydrophobes.

*1.2.2c. Size*

The size of polymeric micelles is primarily determined by the relative lengths of the hydrophobic block and hydrophilic block. Hydrophilic blocks form the shell region of polymeric micelles. The length of the hydrophobic block determines the space each chain requires in the core. Therefore, a block copolymer with high molecular weight hydrophobic block is expected to require more space and may form large micelles. The pattern of packing of the hydrophobic segments also influences micelle size. However, due to technical limitations and structural complexity, additional studies are needed in order to fully understand packing phenomena. Typically, the size of polymeric micelles is in the range of 10-100 nm, and the solvent used in micelle preparation also has a notable effect on micelle size. For PEO-*b*-PBLA, DMAc yields micelles with a small size and narrow size distribution, while micelles formed from DMF and methanol are large (36). Polymeric micelles of small size and appropriate surface properties are believed less recognizable by mononuclear

phagocytotic system (MPS). Moreover, these smaller particles are able to traverse the capillaries with discontinuous characteristics.

*1.2.2d. Association and dissociation kinetics*

The spontaneous self-assembly of amphiphilic block copolymers often operates cooperatively under equilibrium control. The equilibrium can be described as an open (e.g., Pluronic micelles) or closed association model (e.g., PS-*b*-PAA) with an association–dissociation equilibrium between the unimers and micelles. For most polymeric micelle systems that follow the closed association model, a discontinuity of physical properties at the critical micelle concentration (CMC), which is defined as the concentration at which micelles start to form, indicates the formation of polymeric micelles, as a result of the association process.

A CMC is determined by many factors, particularly by the chemical nature of a block copolymer and the length of its hydrophobic and hydrophilic block. The polymeric micelles with low CMC may serve as an efficient drug vehicle. Below the CMC, the micellar structure becomes unstable and breaks apart. Under *in vivo* conditions, the dilution by the biological fluid, e.g., blood in the systemic circulation, causes a rapid drop of the polymer concentration, which may result in the burst-release of any entrapped drug. Micelle systems with a low CMC are more tolerant upon dilution. For example, utilizing amphiphilic block copolymers containing a glassy hydrophobic segment may greatly stabilize the molecular assembly, resulting in a stable *in vivo* system.

*1.2.2e. Dynamics*

The dynamics of exchange of block copolymer molecules between the micelles, formed in aqueous solution, depends on many factors. Because of the low mobility of polymeric amphiphiles and the strong adhesive force among their hydrophobic segments, their diffusion into the surrounding media is slowed. The dynamic stability of the aggregated structures is also sensitive to the chemistry and block length. In contrast to classical low molecular weight surfactants, which are known to easily exchange, the exchange between unimers and micelles of block copolymer is substantially slowed down. Pluronic micelles have an exchange rate constant larger than $3 \times 10^3$ $s^{-1}$ in aqueous solution, which is slow in comparison with what is found for low molecular weight surfactant micelles with an exchange rate constant between $10^6$ and $10^8$ $s^{-1}$ (37). Block copolymers based on polystyrene as the hydrophobic block have an even slower exchange rate. Compared to the millisecond exchange of low molecular weight aggregates, the lifetime of block copolymer micelles can easily be adjusted to be in the second, minute, or hour region (20).

The process for the exchange involves the escape of the unimers from the micelles. In order to escape, the hydrophobic block has to diffuse from the outer layer of the micelle to the bulk solution. This process will cause the temporary disturbance of the micelle structure, which may affect the loaded drug molecules or have an impact on drug release. Ideally, the exchange rate should be adjustable in such a way that the requirement for a slower or a faster drug release can be achieved.

### *1.2.3. Biological aspects of polymeric micelles*

*1.2.3a. Fate of micelle drug-carriers*

The plasma circulation time of micelle particles is determined by their size and surface properties (Figure 1.11). Usually, a particle with a hydrophobic or positively charged surface can be rapidly cleared from the circulation by the mononuclear phagocytotic system (MPS). The MPS is a collection of phagocytic cells that are present in tissues of the RES and are collectively responsible for the clearance of particles from the circulation. Typically in practice 80–90 % of hydrophobic particles are opsonized and taken up by the fixed macrophages of the liver and spleen, often within a few minutes of intravenous administration. Polymeric micelles as a drug carrier are capable of avoiding interaction with cells of the RES as a result of their nanoscopic size and their sterically stabilized PEO surface. The effect of PEO is clearly seen in a study by Hagan et al., on the biodistribution of two block copolymer micelle systems formed from PEO-*b*-PLA copolymers where one system has a PLA:PEO ratio of 1.5:2 and the other has a ratio of 2:5. The one with 1.5:2 has a higher density of PEO at the surface of micelles due to the large aggregation number in comparison to the 2:5 systems. The high PEO surface density led to an improved biodistribution with reduced liver uptake (38).

On the other hand, kidney excretion may be a major route for the elimination of the block copolymers from the body. In a polymeric micelle system, unimers and micelles are in equilibrium, and the concentration of unimers is the CMC. The molecular weight of a unimer is usually within 20,000 g/mol, lower than the threshold of renal clearance that is about 50,000 g/mol. Hence, the unimers can be gradually cleared from the body via kidney. The kidney elimination of the unimers may influence the equilibrium between unimers and

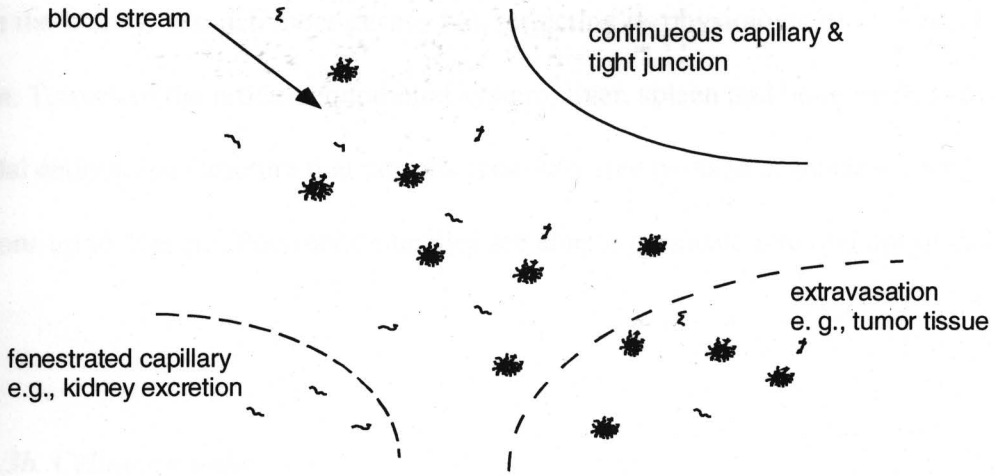


Figure 1.11. Schematic demonstration of the fate of polymeric micelles in the body.

micelles. Therefore, the CMC of polymeric micelles may be a dominant factor for the blood circulation time of a block copolymer. In principle, adjusting the composition of a block copolymer may have a great impact on the CMC and on the pharmacokinetic properties.

After intravenous injection, polymeric micelles are expected to extravasate to the targeted tissues. Extravasation is a process of transvascular exchange governed by the permeability of blood capillary walls. The extravasation of macromolecules to either extracellular or intracellular targets is dependent on the structure of the capillary wall, physiological conditions, the rate of blood and lymph supply, and the physicochemical properties of macromolecules. The extravasation of polymeric micelles is a function of their overall size and the permeability of the different vascular layers they encounter. The tightest

endothelial barrier in the body is the blood-brain barrier. Fenestrated endothelium, such as found in the kidney, is much more permeable, reflecting its physiological function of filtration. Tissues of the reticuloendothelial system, liver, spleen and bone marrow possess a sinusoidal endothelial structure that permits relatively free passage of materials without size restrictions up to 100 nm. Polymeric micelles are able to permeate into and out of those tissues.

*1.2.3b. Cellular uptake*

Passive diffusion and active transport are the major routes of cellular uptake for small anticancer drugs. However, cellular uptake of macromolecules is believed to occur via endocytosis, a process in which a small region of the plasma membrane invaginates to form a new intracellular membrane-limited vesicle about 0.05 to 0.1 μm in diameter. Endocytosis is a common term encompassing phagocytosis and pinocytosis. Phagocytosis describes the capture of vesicular material by specialized cells (macrophages and neutraphils). Pinocytosis describes the capture of extracellular fluid, all solutes dissolved therein and any material adherent to the enfolding surface. It is a process common to most cell types. Depending on the structure of the macromolecule, three types of pinocytosis may occur: fluid-phase, adsorptive and receptor-mediated pinocytosis. Fluid-phase pinocytosis occurs when no interaction of the macromolecule with cell surface takes place. Consequently, macromolecules are taken up slowly depending on their concentration in the extracellular fluid. The incorporation of hydrophobic moieties or positive charges into the macromolecular structure results in non-specific interaction with plasma membranes of different cells with a concomitant increase in the rate of macromolecular uptake. This process is known as

adsorptive pinocytosis. The introduction of moieties to the macromolecular structure that are complementary to cell surface receptors or antigens of a subset of cells renders the macromolecules biorecognizable. The macromolecule is internalized specifically by a select subset of cells. Therefore, the attachment of small hydrophobic molecules to polymeric carriers may thus change the route of cellular uptake of the drugs from passive diffusion to endocytosis. For drugs requiring transport carriers, their macromolecular conjugates may cause the carrier molecules to be less useful. Polymeric micelles and unimers may both be endocytosed by cells. Moreover, endocytosis is important for a micelle system that needs to release drugs intracellularly.

*1.2.3c. Tumor tissues*

Tumor tissues are characterized by the enhanced vascular permeability effect (EPR) (39). The effect is attributed to two factors. The tumor vasculature often displays a discontinuous endothelium, which allows macromolecular extravasation to a greater extent than seen via most other endothelial barriers. At least two substances are known to be involved in modulation of the vascular permeability: vascular permeability factor (VPF) and bradykinin (or kinin) (40). Additionally, the lack of effective lymphatic drainage in tumors prevents the clearance of penetrant macromolecules, resulting in accumulation within the tumor tissue. The effect appears to apply to all tumors so far examined, suggesting that the passive targeting of macromolecular drugs may be a universal phenomenon (41).

PEO-*b*-PAsp-DOX conjugate exhibited considerable tumor accumulation due to the EPR effect. The accumulation of the micelle-forming conjugate in tumor tissue is 50-fold higher than that in normal tissues in terms of the ratio of % dose/g organ. However, the

tumor/muscle ratio of free DOX is only 1.5, indicating a low selectivity. The EPR effect has become one of the major principles for drug targeting using macromolecular carriers (42).

*1.2.3d. Metabolism and degradation*

Although the primary route for the elimination of block copolymers is through renal clearance, degradation of the materials may also occur in the biological systems. For instance, PEO-*b*-PLA is degradable due to the hydrolysis of the ester backbone. The degradation of the unimers may cause the dissociation of the micelles, and may influence drug release.

## 1.3. Polymeric micelles with physically loaded drugs

### *1.3.1. Theoretical consideration*

The solubilization of hydrophobic drugs into polymeric micelles is influenced by the compatibility between the drugs and the core-forming block (Figure 1.12). The compatibility can be assessed by the Flory-Huggins interaction parameter, $\chi_{sp}$, as described by the following equation:

$$\chi_{sp} = (\delta_s - \delta_p)^2 \frac{V_s}{RT} \qquad (1.1)$$

Where $\chi_{sp}$ is the interaction parameter between the solute ($s$) and the core-forming polymer block ($p$), $\delta_s$ and $\delta_p$ are the solubility parameters of the solute and the core-forming polymer block, and $V_s$ is the molar volume of the solute. The lower the positive value of the interaction parameter ($\chi_{sp}$), the greater the compatibility between the solute and the core-forming block. The highest degree of compatibility will be reached when $\delta_s = \delta_p$, and the maximum drug loading capacity can be obtained. Since each drug has a unique structure, it is unlikely that any one micelle system will serve as a universal delivery vehicle for all drugs, and it is equally unlikely that any one drug will be as delivered efficiently by all block copolymer micelle systems.

The solubilization of DOX has been achieved using several polymeric micelle systems, such as PEO-*b*-PBLA (43), PEO-*b*-PAsp-DOX (18). The extent of solubilization of DOX by PEO-*b*-PBLA has reached roughly 5-18 w/w %. The micelles of PEO-*b*-PAsp-DOX with physically entrapped DOX are very stable, and only the entrapped DOX accounts for the antitumor activity of the system.

Paclitaxel, a highly hydrophobic drug with very poor water solubility, was solubilized by PEO-*b*-PLA micelle solution in which paclitaxel concentration reached up to 50 mg/mL (44). Micellar formulation of paclitaxel produced a five-fold increase in the maximum tolerated dose compared to paclitaxel formulated in the Cremophor vehicles (45). Pluronic micelles have been used to solubilize indomethacin (19), amphotericin B (46), and haloperidol (21).

Using polymeric micelles for drug delivery may revolutionize the conventional formulation methods for poorly water-soluble drugs. Because water is the only solvent for micelle solutions, the use of a cosolvent may be avoided. The overall toxicity of the

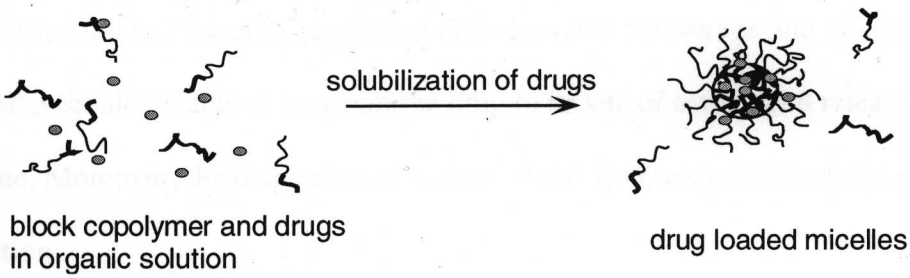


Figure 1.12. Solubilization of hydrophobic drugs into polymeric micelles.

formulation is thus reduced. Moreover, avoidance of using cosolvents eliminates the risk of leaching of plasticizer during drug infusion.

### *1.3.2. Stability of the drug loaded micelle system*

The stability of a drug loaded micelle system is a primary concern for its clinical applications. The stability during storage and after *in vivo* administration should be considered separately. The stability during storage is reflected by the change of physicochemical properties of the system, such as the degradation of block copolymers and drugs, the flocculation or coagulation of the micelle particles, and gradual drug release. The *in vivo* stability is more reflected by the tolerance of dilution by the blood, the interaction with various biological components and premature dissociation and drug release. Since the

interaction among the hydrophobic blocks and drugs are the driving force in the formation of micelles, the strength of that interaction determines the stability of the micelle-drug system. The drug-loaded micelles should not only be stable for storage and in circulating blood, but also should be able to transport the drug to its site of action, and release it at an optimum rate. Moreover, the dispersion efficiency of the system should be maintained even at high dilution.

### *1.3.3. Drug release*

The mechanisms of drug release from polymeric micelles are different for individual systems. Drug release depends on the rate of degradation of the polymer, micelle stability, the physicochemical state of the loaded drug and the rate of diffusion of the drug from the micelles (Figure 1.13). The degradation of a block copolymer may occur due to hydrolysis or enzymolysis. For example, block copolymers with an ester backbone are subject to pH-dependent hydrolysis. The degradation usually leads to a structural change of a block copolymer, which greatly changes the physicochemical properties of the micelle and causes drug release. The change in the physicochemical state of the loaded drug may significantly alter the rate of drug release. Depending on the pH of the media, indomethacin exists in the salt form or acid form. Solubilized by PEO-*b*-PBLA micelles, faster drug release was observed at higher pH, as a result of ionization of the drug. The weak interaction between the drug and the core-forming block results in a micelle system with low stability and relatively rapid drug release as a result of micelle dissociation or drug diffusion. However, the factors that govern drug release have not been well evaluated.

## 1.4. Block copolymer micelles with chemically loaded drugs

### *1.4.1. Micelle-forming drug-polymer conjugates*

A micelle-forming drug-polymer conjugate consists of a hydrophilic block and a hydrophobic block comprised of the hydrophobic segment and the bound drug moieties. Sometimes a spacer group is used to bridge the drug and the polymeric backbone. During the micellization process, the hydrophobic segment of block copolymer, along with the drug moieties and the spacers, form the core of micelles. Unlike physical drug loading micelle systems in which the drug molecules may reside not only in the core of micelles but also in

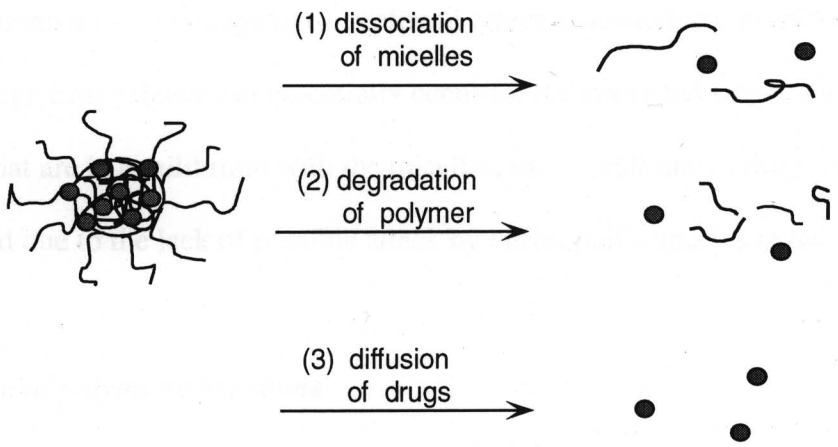


Figure 1.13. Mechanisms of drug release from polymeric micelles.

the corona region, the drug moieties reside only in the core of micelles for chemical drug loading micelle systems. The segregation of drugs with the surrounding media efficiently prevents the drugs from degradation, which is especially beneficial for drugs lacking stability. Moreover, attaching a drug to a macromolecular carrier will allow the conjugated drug to have a prolonged circulation. It may also alter the biodistribution, and cellular uptake pathway of the drugs.

Although polymer-drug conjugate technology has been quite successful on its own especially owing to the development of oligopeptido-linkages which are specifically hydrolyzed within the lysosomal compartment, micelles formed from block copolymers with covalently linked drugs have not been very satisfactory. The micelle-forming PEO-*b*-PAsp-DOX conjugate does not have anti-tumor activity because the amide bond that is used as the linkage is too stable to release the conjugated DOX. Therefore, coupling a drug to a block copolymer through a labile linkage has a profound effect in achieving controlled drug release. Although drug release can potentially occur for the coexisted single polymer chains (or unimers) that are in equilibrium with the micelles, the overall rate of drug release may be greatly reduced due to the lack of possible attack by nucleophilic species in the micelle core.

### *1.4.2. Selection of polymeric backbone*

The development of polymeric micelles with covalent incorporated drugs is strictly dependent on the selection of an appropriate polymeric backbone and a linkage for drug attachment. Poly(amino acids) can be used as the hydrophobic segment for a block copolymer.

Poly(amino acids) have been widely used as drug carriers for low molecular weight drugs, and are usually tolerated when implanted in animals since poly(amino acids) may be metabolized to relatively nontoxic products despite the intrinsic hydrolytic stability of the amide bond which must rely upon enzymes for bond cleavage (47). Some studies suggest that poly(amino acids) have good biocompatibility; but the antigenic nature of the materials makes their widespread application uncertain. The expense and inconvenience in the production of elaborate polypeptides has limited its application, homopolymers are thus commonly used. Poly(amino acids) are attractive due to the functionality they can provide a polymer backbone. Poly(lysine) provides pendent amino groups. Poly(aspartic acid) or poly(glutamic acid) provides carboxylic groups on the side chains. These functional groups can be employed as the reaction sites for further structural modification or drug conjugation. PEO-*b*-PAsp, in which poly(aspartic acid) is the hydrophobic segment, has been used for the conjugation of DOX. Having pendent carboxylic groups, it can react with a variety of drugs that have hydroxyl or amino groups.

### *1.4.3. Selection of chemical bonds*

The utilization of micelle-forming polymer/drug conjugates has been restricted by poor control over the polymer-drug bond, which is determined by the chemical structure of polymers and drugs. In addition, preparation of micelle-forming polymer-drug conjugates requires straightforward chemical reactions with good yield. The covalent linkage should be designed so that the conjugated drug can be released via hydrolysis or enzymolysis to exert its activity. Moreover, the structure of the conjugates should contain elements controlling drug release.

A variety of chemical bonds can be used to bind drugs to polymeric carriers, such as ester, amide, carbonate, urethane, hydrazone, and thioether bonds. All these bonds may be hydrolyzable under certain conditions, but the rate of hydrolysis varies from very fast to almost insignificant.

For the attachment of drugs to a polymeric backbone, conditions must be mild enough to allow for attachment without any adverse effect on the biological activity of the drug. For this purpose, various coupling methods, which are well known in the field of peptide synthesis, can be applied.

### *1.4.4. Selection of spacers*

Drug molecules can be directly attached to the polymeric backbone or through the use of a linker. The nature of the linker used to conjugate drugs is a key factor in releasing the drugs. For some purposes it might be necessary to prepare polymers in which the drug is firmly attached to the polymer by means of a linkage which is completely stable under all normal body conditions. Alternatively one may wish to use a linkage from which the drug can be released rapidly in the body either by hydrolysis or via an enzymatic process. For these purposes, permanent or temporary spacer groups may be used. The influence of spacer groups on drug release is schematically summarized in Figure 1.14.

A permanent spacer group is a distance holder that merely separates the active drug from the polymeric backbone or coil so that the latter does not interfere with the biological activity of the bound material. A temporary spacer group is one from which the active material can be readily released. This is necessary because the majority of drugs are inactive

in the macromolecular form and, thus, their links to the polymer must be reversible or degradable

The stability of a drug-carrier linkage and its capacity for controlled degradation is the overriding factor determining the usefulness of a drug-carrier conjugate. If the linkage is sufficiently unstable to maintain the integrity of a drug conjugate before it reaches its target (extra- or intracellular) the carrier becomes functionally unnecessary. Similarly, when the drug conjugate is simply designed as an extracellular depot, the drug must be liberated in a predictable manner without dumping the entire dose immediately after administration. Therefore, the selection of spacers with desired function is very important in the design of a drug delivery system.

## 1.5. Statement of Problem

Current research has been focused on polymeric micelle systems for the physical solubilization of hydrophobic drugs. There is no doubt that the physicochemical properties of a polymeric micelle system determine its performance in drug delivery. The physicochemical properties of polymeric micelles have been extensively studied by physical chemists, and the application of polymeric micelles in drug delivery has attracted pharmaceutical scientists. However, few studies have bridged the physicochemical properties of polymeric micelles, such as their kinetic and dynamic stability, with research on micelle-drug delivery systems. The application of such a system is limited by systemic stability, unsatisfied drug loading capacity, and unpredictable drug release. In principle, those limitations can be overcome by tailoring the structure of micelle forming block copolymers to satisfy the structural

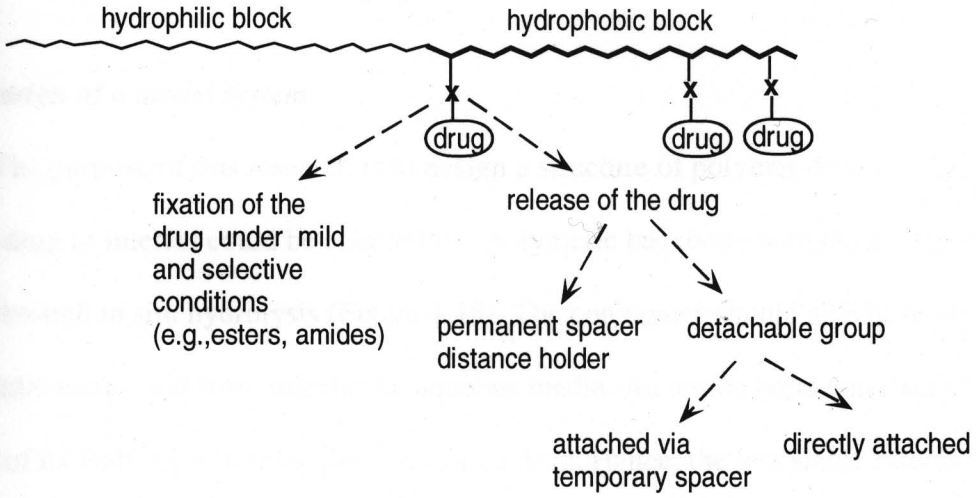


| | principle | example |
|---|---|---|
| Various spacers | drug, stable | $-(CH_2)_n-$ |
| | x-drug, hydrolyzable | x: ester, |
| | y-drug, enzyme cleavage | y: -N = N-, oligopeptides |

Figure 1.14. Functions of spacer groups.

requirement for the delivery of a drug. In this study, effort is focused on the exploration of the factors in optimizing micelle-drug delivery systems by modifying the structure of block copolymers.

### *1.5.1. Design of a model system*

The purpose of this research is to design a structure of polymer-drug conjugates, in which a drug of interest could be coupled to a polymeric backbone with the potential of release through in situ hydrolysis (Figure 1.15). The conjugates should also have an amphiphilic nature and form micelles in aqueous media. An amide bond was excluded because of its inability to release the conjugated drug. Hence, the less stable ester bond was chosen to conjugate the polymeric carrier with drug moieties.

Ester bonds are particularly useful for the preparation of prodrugs. An ester bond is susceptible to hydrolysis, which allows liberation of the covalently coupled drug to exert its function. However, the major problem for most ester prodrugs is their insufficient stability during prolonged circulation. Most ester prodrugs exhibit a relatively short half-life in the range of hours to days depending upon the chemical structure of the individual prodrug. The application of prodrugs in therapeutics to achieve sustained release is thus limited. However, because of the unique structure of a micelle, adopting ester bonds to a micelle forming block copolymer may provide a novel drug-polymer conjugate system. Chemically bound drug moieties are part of the hydrophobic segment, and may play an important role in micelle formation and stability. Bound to the hydrophobic block through an ester linkage, drugs may be released by hydrolysis of the ester bonds under physiological conditions. In addition, upon self-assembly of amphiphilic conjugates, drug moieties should reside in a hydrophobic

environment. Therefore, premature drug release may be greatly suppressed, and prolonged circulation may become attainable.

As depicted in Figure 1.15, the polymer drug conjugate is designed to have a hydrophilic PEO block and a hydrophobic block comprised of a polymeric backbone (PEO-*b*-PAsp), an alkyl spacer group, and the conjugate drugs. We developed two polymer-drug conjugate systems that form micelles in aqueous media that are able to release the conjugated drugs. We started with the anticancer drug, paclitaxel, because of its poor water solubility. Paclitaxel was successfully conjugated to a block copolymer, PEO-*b*-PAsp (discussed in Chapter 6). Methotrexate was also conjugated to PEO-*b*-PAsp via an ester linkage. In both cases, a spacer was used to bridge the drug with the polymer backbone. The major part of the thesis is based on the MTX conjugate system.

Methotrexate is an antagonist of dihydrofolic acid (Figure 1.16). It is widely used as a basic component of combination chemotherapy for the treatment of human malignancies, rheumatoid arthritis, and psoriasis. MTX is a high affinity inhibitor of dihydrofolate reductase (DHFR), thus blocking the reduction of 7,8-dihydrofolate to 5,6,7,8-tetrahyrofolate, a key cofactor in many biochemical pathways involving a one-carbon transfer reaction in biosynthesis. It results in an interference with the biosynthesis of nucleotides, causing inhibition of DNA synthesis and blocking cell reproduction. Conventional chemotherapy using MTX exhibits low specificity and selectivity of action. Undesirable side effects such as leucopoenia and nephrotoxicity are the main dose limiting factors. Many attempts have been made to decrease the toxic side effects and improve the specificity. Drug delivery systems based on antibody directed enzyme prodrug therapy or the use of macromolecular carrier have been investigated.

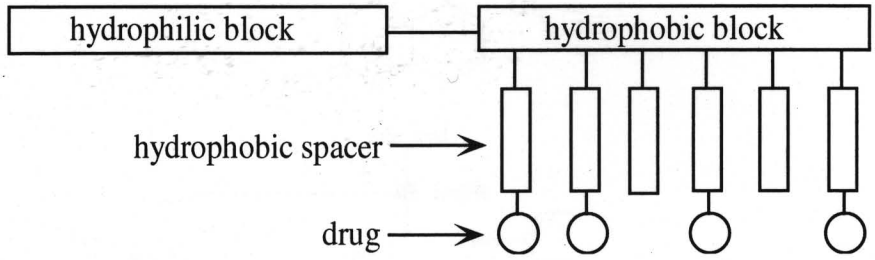


Figure 1. 15. Schematic structure of a micelle-forming drug polymer conjugate.

The conjugation of MTX to PEO-*b*-PAsp requires the utilization of a spacer group because of the structural limitations of the drug and the polymer. Introduction of an alkyl spacer with functional groups may alter the system in several aspects. The added functional groups can extend the reactivity of the polymer carrier. Moreover, the alkyl groups may greatly change the hydrophobicity of the polymer.

These studies include the synthesis and characterization of block copolymers with covalent bound drug moieties, the evaluation of the fundamental properties of the micelle systems, and the study of the structure-property relationship that influences drug release.

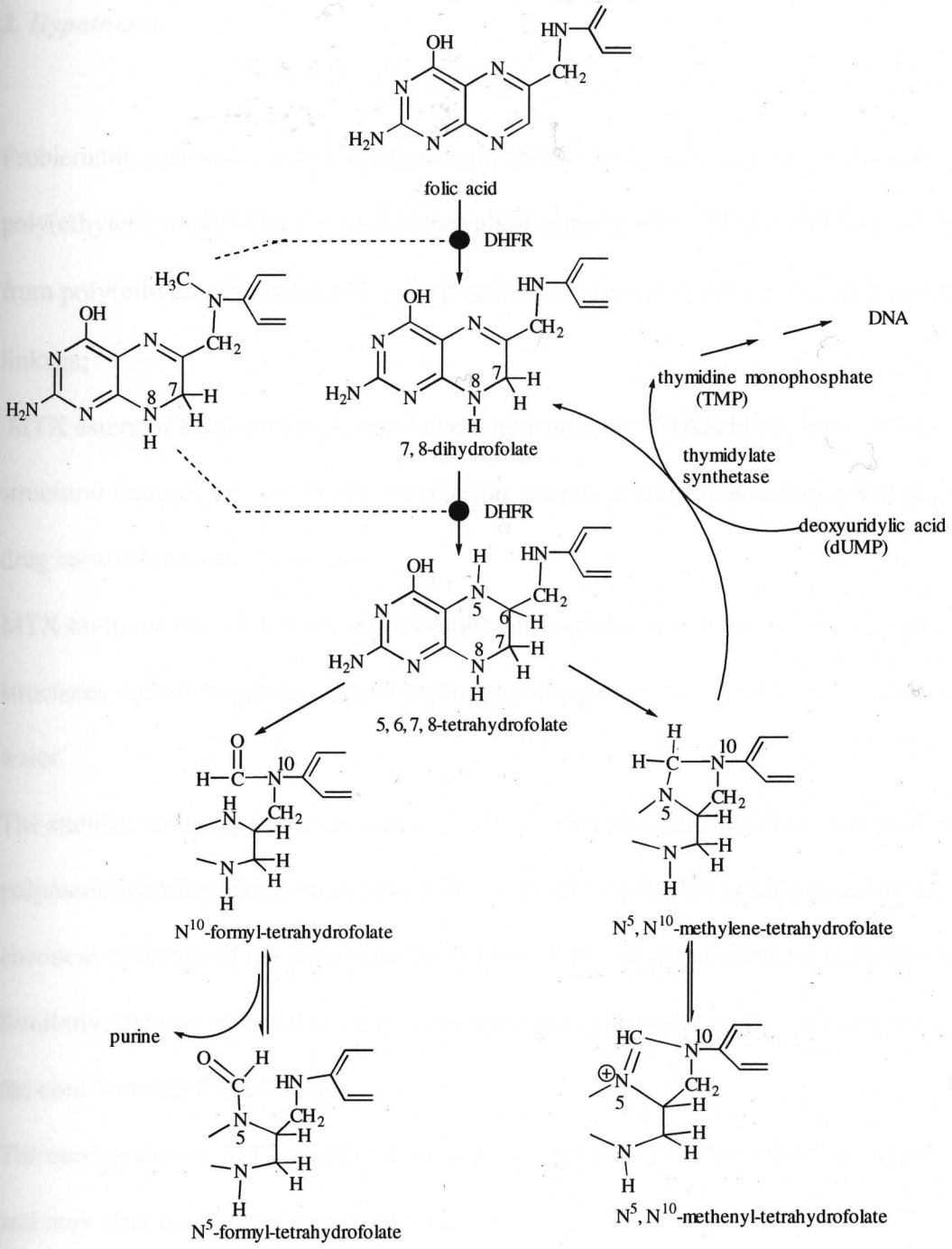


Figure 1.16. Pharmacological action of MTX.

### *1.5.2. Hypotheses*

- Problematic anticancer drugs, methotrexate (MTX) and paclitaxel, may be conjugated to poly(ethylene oxide)-*block*-poly(hydroxyalkyl aspartamide) (PEO-*b*-PHAA), converted from poly(ethylene oxide)-*block*-poly(β-benzyl-L-aspartate) via a hydrolyzable ester linkage;
- MTX esters of PEO-*b*-PHAA may have a hydrophobic PHAA block with variable structural features: degree of polymerization, length of alkyl spacer group and degree of drug substitution (methotrexate).
- MTX esters of PEO-*b*-PHAA self-assemble into spherical nanoscopic micelle-like structures during the gradual replacement of a common organic solvent, e.g. DMAc, with water.
- The stability in terms of the critical micelle concentration and the dissociation of the polymeric micelles based on the MTX esters of PEO-*b*-PHAA is influenced by the chemical structure of the core-forming PHAA block, which governs its hydrophobicity.
- Similarly, the rate of MTX release (ester hydrolysis) depends on the chemical structure of the core-forming PHAA block.
- The conjugation of MTX to PEO-*b*-PHAA may influence the biological activity of MTX and may alter its cellular uptake pathway.

### *1.5.3. Specific aims*

- To synthesize MTX esters of PEO-*b*-PHAA with a varying molecular weight of PHAA, length of alkyl spacer group and degree of drug substitution, and to characterize the conjugates by UV absorption and $^1$H NMR spectroscopy.
- To prepare micelle-like structures of MTX esters of PEO-*b*-PHAA and study their size and shape by transmission electron microscopy (TEM) and dynamic light scattering (DLS), association by $^1$H NMR, and critical micelle concentration by a light scattering method.
- To study the effect of hydrophobicity on the stability of micelles in terms of micelle dissociation under physiological pH
- To study the release of MTX at various pH values by UV spectroscopy and the effect of hydrophobicity on drug release by size exclusion chromatography (SEC).
- To evaluate *in vitro* inhibitory activity toward dihydrofolate reductase and anticancer activity toward murine leukemia L1210 cells of the MTX esters of PEO-*b*-PLAA.
- To synthesize paclitaxel conjugate of PEO-*b*-PLAsp and characterize the conjugates as well as the correspondent micelles in terms of micelle size, and study the stability of the conjugates

# CHAPTER 2.

## Synthesis and Characterization of Methotrexate Esters of Poly(ethylene oxide)-*block*-Poly(hydroxyalkyl aspartamide)

## 2.1. Introduction

The application of polymeric micelles in drug delivery demands micelle-forming block copolymers with a properly designed structure, as the chemical nature of the block copolymers dominates the physicochemical properties of the micelle. In particular, the utilization of micelle-forming drug-polymer conjugates has been restricted by poor control over the polymer-drug bond, which is determined by the chemical structure of the polymer and drug (9). A micelle-forming poly(ethylene oxide)-*block*-poly(aspartic acid)-doxorubicin conjugate has no antitumor activity, owing to the amide bond used as the linkage, which is too stable to release the conjugated DOX (18). Therefore, we have employed an ester linkage to attach a therapeutic agent to a block copolymer, poly(ethylene oxide)-*block*-poly(L-aspartic acid) (PEO-*b*-PLAA) (48).

Using methotrexate (MTX) as the first example, we have designed a synthetic route to conjugate MTX to PEO-*b*-PLAA through an ester linkage. A two- or six-carbon alkyl spacer bearing a hydroxyl group has been introduced to PEO-*b*-PLAA, yielding poly(ethylene oxide)-*block*-poly(hydroxyl alkyl aspartamide) (PEO-*b*-PHAA) (Figure 2.1). Under proper conditions, a series of MTX esters of PEO-*b*-PHAA with a varied hydrophobic block have been synthesized. These conjugates may possess multiple functions, including self-association and sustained drug release. In particular, these MTX esters may exhibit prolonged circulation time and sustained drug release after administration to biological systems. Furthermore, the novel conjugates can be used as a model system to explore the functional properties of polymeric micelles for drug delivery.

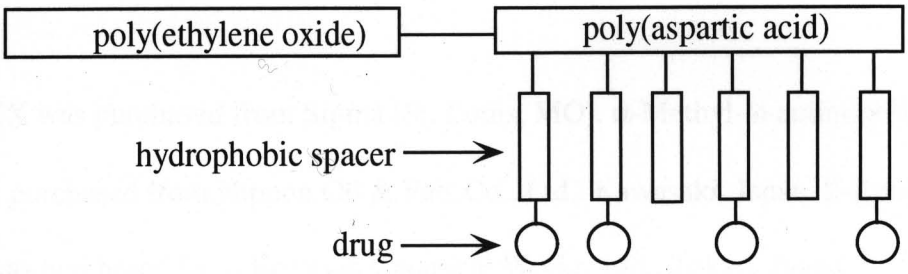


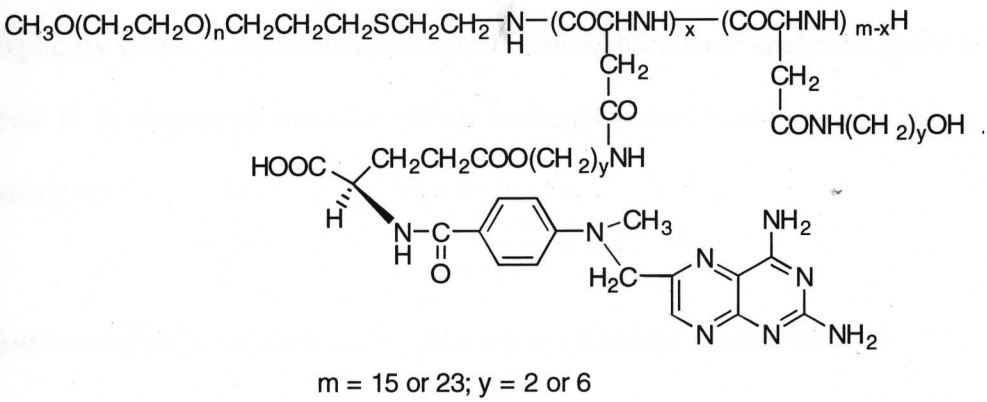


m = 15 or 23; y = 2 or 6

Figure 2. 1. Schematic and chemical structure of MTX esters of PEO-*b*-PHAA

## 2.2. Experimental

### *2.2.1. Materials*

MTX was purchased from Sigma (St. Louis, MO). α-Methyl-ω-aminopoly(ethylene oxide) was purchased from Nippon Oil & Fats Co., Ltd., Kawasaki, Japan. β-Benzyl l-aspartate was purchased from Kokusan Chemical Works, Ltd., Tokyo, Japan. Dicyclohexylcarbodiimide (DCC), dimethylaminopyridine (DMAP), 2-hydroxypyridine (2-HP), 2-aminoethanol, 6-aminohexanol, $D_2O$, and dimethylsulfoxide-$d_6$ (DMSO-$d_6$) were purchased from Aldrich (Milwaukee, WI), and used as received without further purification unless explicitly stated. All solvents purchased from Aldrich were analytical grade and used as received. N, N-dimethylformamide (DMF) and methylene chloride were dried with molecular sieves.

### *2.2.2. Synthesis of poly(ethylene oxide)-block-poly(β-benzyl L-aspartate) (PEO-b-PBLA) (49)*

#### *2.2.2.1. Synthesis of β-benzyl L-aspartate N-carboxy anhydride (BLN-NCA)*

β-Benzyl L-aspartate (25 g) was suspended in 200 mL of distilled tetrahydrofuran (THF). A portion of 1.2 M bis(trichloromethyl)-carbonate (14.4 g) solution (50 mL) in distilled THF was added to the suspension. The reaction mixture was heated at 50°C with stirring. After 30 minutes the solution became transparent, and the solvent was evaporated at reduced pressure. The crude BLA-NCA was recrystallized from distilled THF/n-hexane three

times. The purity was checked by its melting point. After the final recrystallization, BLA-NCA was dried at room temperature *in vacuo* for 6 h.

*2.2.2.2. Synthesis of PEO-b-PBLA*

Synthesis of PEO-*b*-PBLA was reported in detail previously (49). Briefly, β-benzyl N-carboxy-L-aspartate anhydride (BLA-NCA) was dissolved in anhydrous DMF followed by addition of anhydrous chloroform. Afterwards, α-methyl-ω-aminopoly(ethylene oxide) (PEO, MW = 12,000, $M_w/M_n$ = 1.04) was dissolved in distilled chloroform and added to the solution of BLA-NCA. Quantities of the solvents in the reaction mixture were adjusted to 1.5 mL of DMF and 15 mL of chloroform per 1.0 g of BLA-NCA. The reaction mixture was stirred at 35°C under a stream of dry nitrogen until BLA-NCA disappeared by the detection of characteristic peaks (1850 and 1790 $cm^{-1}$) in the IR spectrum. The reaction mixture was poured into a 10-fold volume of diethyl ether at 0°C, and the precipitate was collected by filtration, washed with diethyl ether, and dried *in vacuo*.

*2.2.2.3. Purification and characterization of PEO-b-PBLA*

The previously prepared PEO-*b*-PBLA contained a trace amount of BLA oligomer, a byproduct from the reaction as observed in gel permeation chromatography. The product was purified by repeated precipitation with a solution of chloroform and 2-propanol. PEO-*b*-PBLA (1.0 g) was suspended in 40 mL of 2-propanol and stirred at 70°C for 1.5 h, and 1.0 mL of chloroform was then added. The mixture was cooled in an ice bath. The precipitated polymer was collected by filtration and washed three times with diethyl ether followed by drying under vacuum overnight. The purity of polymer was then confirmed by gel

permeation chromatography (GPC). The composition of the polymer in terms of the degree of polymerization of PBLA was determined by $^1$H NMR (Figure 2.3).

### *2.2.3. Synthesis of poly(ethylene oxide)-block-poly(hydroxyalkyl aspartamide) (PEO-b-PHAA)*

#### *2.2.3.1. Poly(ethylene oxide)-block-poly(2-hydroxyethyl aspartamide) (PEO-b-PHEA)*

PEO-*b*-PBLA (50 mg, 0.05 mmol aspartate (Asp) residues) was dissolved in dry DMF with the aid of stirring and slight heating. Subsequently, 2-aminoethanol (130 µl, 2.2 mmol) and 2-HP (52 mg, 0.5 mmol) were added to the solution. The reaction mixture was stirred for 4 h at room temperature and poured into vigorously stirred cold 2-propanol (50 ml). The white precipitate was collected by centrifugation and thoroughly washed with 2-propanol and ether and dried under vacuum. The product was characterized by $^1$H NMR measurement in DMSO-$d_6$ (Bruker 300 MHz) and by absorption spectroscopy (Pharmacia 4000).

#### *2.2.3.2. Poly(ethylene oxide)-block-poly(6-hydroxyhexyl aspartamide) (PEO-b-PHHA)*

PEO-*b*-PBLA (50 mg, 0.05 mmol aspartate (Asp) residues) was dissolved in dried DMF with the aid of stirring and slight heating. Subsequently, 6-hydroxyl-1-hexylamine (130 µl, 2.2 mmol) and 2-HP (52 mg, 0.5 mmol) were added to the solution. The reaction mixture was stirred for 4 h at room temperature and poured into vigorously stirred cold 2-propanol (50 ml). The white precipitate was collected by centrifugation, thoroughly washed with 2-propanol and ether, and dried under vacuum.

### *2.2.4. Synthesis of MTX esters of poly(ethylene oxide)-block-poly(hydroxyalkyl aspartamide) (PEO-b-PHAA)*

MTX (1 to 2 eq), DCC (10 eq) and DMAP (10 eq) were added to a stirred solution of PEO-*b*-PHAA (50 mg) in anhydrous DMF or methylene chloride (2.0 ml). The reaction mixture was stirred and shielded from light with aluminum foil for 24 to 96 h. The mixture was dialyzed against DMSO (500 mL) with a dialysis membrane (MWCO = 3,500 g/mol, SpecPro2, Fisher Scientific, Co., PA). Absorption spectroscopy was used to monitor the disappearance of MTX in the dialysis medium. The absence of MTX in the medium outside the dialysis bag after three days of changes of DMSO was observed by UV spectroscopy (304 nm) and thin layer chromatography (chloroform:methanol:water = 1:7:2, $R_f$ = 0.21). The solution was slowly added to cold 2-propanol (50 mL), and the precipitated product was collected by centrifugation, washed with 2-propanol five times, and dried under vacuum.

### *2.2.5. Characterization of MTX esters PEO-b-PHAA*

#### *2.2.5.1. $^1H$ NMR*

The $^1$H NMR experiments were performed on a Bruker 300 MHz spectrometer operating at 300 MHz. The composition and molecular weight of PEO-*b*-PBLA was determined based on $^1$H NMR spectra in $CDCl_3$ (6.5 mg in 0.8 mL). $^1$H NMR of MTX esters of PEO-*b*-PHAA was measured in $d_6$-DMSO.

*2.2.5.2. UV-Vis spectroscopy*

The UV absorbance for each batch of exhaustively dialyzed product was measured at 304 nm, and the concentration of MTX moieties was calculated by a calibration curve of pure MTX (concentration range: 0.01-0.1 mg/mL). The level of MTX substitution was determined by dissolving the polymeric conjugate in an alkaline solution and measuring the absorbance of the liberated MTX. In a typical procedure, MTX ester (1.0 mg) was dissolved in 1.0 mL of 0.01 N NaOH solution and stirred for 5 min. The solution was neutralized and diluted 10 fold for UV measurement. The concentration of MTX was then determined ($\varepsilon_{304}$ = 2.35 x $10^4$ $dm^3mol^{-1}cm^{-1}$). The number of MTX residues on PEO-*b*-PHAA was determined by equation 2.1, where $x$ is the number of attached MTX, $MW_{MTX}$ is the molecular weight of a MTX residue, and $MW_{PEO\text{-}b\text{-}PHAA}$ is the molecular weight of PEO-*b*-PHAA.

$$\frac{[MTX]}{[Conjugate]} = \frac{(MW_{MTX})x}{MW_{PEO-b-PHAA} + (MW_{MTX})x} \qquad 2.1$$

The molar ratio of MTX substitution was thus determined by equation 2.2, where $n$ is the number of aspartic acid units in the polymer:

$$mol\%(MTX) = \frac{x}{n} \times 100\% \qquad 2.2$$

*2.2.5.3. SEC-HPLC*

The MTX conjugates were analyzed by SEC-HPLC equipped with a Ultrahydrogel™ 500 GPC column and a Ultrahydrogel™ Guard column or OHpak KB-805 SEC column (Waters, Milford, MA). The HPLC system contained a Waters 501 pump, a WISP 712 autosampler, and a 484 absorbance detector. The mobile phase was 0.1 M phosphate buffer containing 0.05 % $NaN_3$. The flow rate was 0.7 mL/min and 1.0 mL/min for Ultrahydrogel 500 and KB-805, respectively, and the detection wavelength was 374 nm.

## 2.3. Results and Discussion

### *2.3.1. Synthesis and characterization of PEO-b-PBLA and PEO-b-PHAA*

A polymer chosen as a drug carrier must meet certain criteria to maximize its potential in drug delivery. The polymer must be easily synthesized and characterized. It should also be biodegradable through hydrolysis or enzymolysis, or be able to be excreted from the body. The carrier and its metabolic products should be nontoxic and nonantigenic. The polymeric carrier should provide drug attachment/release sites. Finally, the carriers should be able to target to predetermined cell types, and, ideally, they should be biodegraded or eliminated from the organism after fulfilling their functions.

PEO-*b*-PBLA has demonstrated its potential as a drug carrier. PEO-*b*-PBLA was synthesized by polymerization of β-benzyl L-aspartate N-carboxyl anhydride, initiated by the terminal amino group of α-methoxyl-ω-aminopoly(ethylene glycol) and purified by repeated precipitation of the polymer in a solution of chloroform and 2-propanol (Figure 2.2).

The prepared PEO-*b*-PBLA was analyzed by GPC. PEO-*b*-PBLA copolymers have an identical PEO block with molecular weight of 12,000 g/mol. The degree of polymerization of BLA was determined by $^1$H NMR measurement in $CDCl_3$, from the intensity ratio of methylene protons of the benzyl group (-COOC$\underline{H}_2$C$_6$H$_5$, $\delta$ = 5.1 ppm) of the PBLA block to methylene protons (-OC$\underline{H}_2$C$\underline{H}_2$,- $\delta$ = 3.7 ppm) of the PEO block (Figure 2.3). The number of aspartate units in the PBLA block was thus calculated. PEO-*b*-PBLA with a PBLA block of 15 or 23 units of aspartic acid were used in the following studies, and it was designated as PEO-*b*-PBLA (12-15) or PEO-*b*-PBLA (12-23), whose $M_w/M_n$ is 1.07 and 1.04, respectively (results not shown).

The removal of the benzyl groups from the aspartate yields a polymer rich in carboxylic groups, which can further react with drugs possessing amino or hydroxyl groups to form an ester bond or an amide bond, respectively. For instance, DOX has been attached to poly(ethylene oxide)-*block*-poly(L-aspartic acid) (PEO-*b*-PLAsp), the product from the hydrolysis of PEO-*b*-PBLA, through an amide linkage. The removal of the benzyl groups can also be achieved by aminolysis using hydroxyalkyl amines, producing a polymer having hydroxyl groups on its side chains. Although hydroxyalkyl amines contain hydroxyl groups and amino groups, which are both nucleophiles, the aminolysis overrides transesterification because of the higher reactivity of amino groups than that of hydroxyl groups.

2-HP acted as a bifunctional catalyst possessing a basic and an acidic group, mutually situated in such a manner that a cyclic transition state, allowing a concerted displacement, might be postulated (50). Studies on the aminolysis of poly(γ-L-glutamate) revealed that

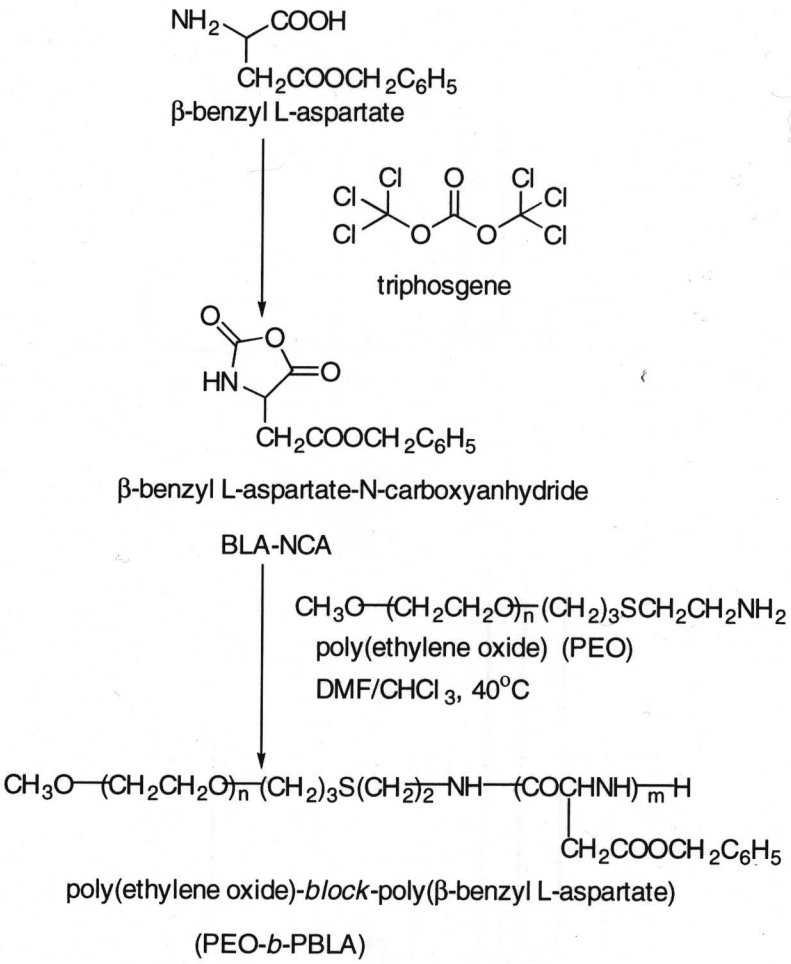


Figure 2. 2. Synthesis of PEO-*b*-PBLA

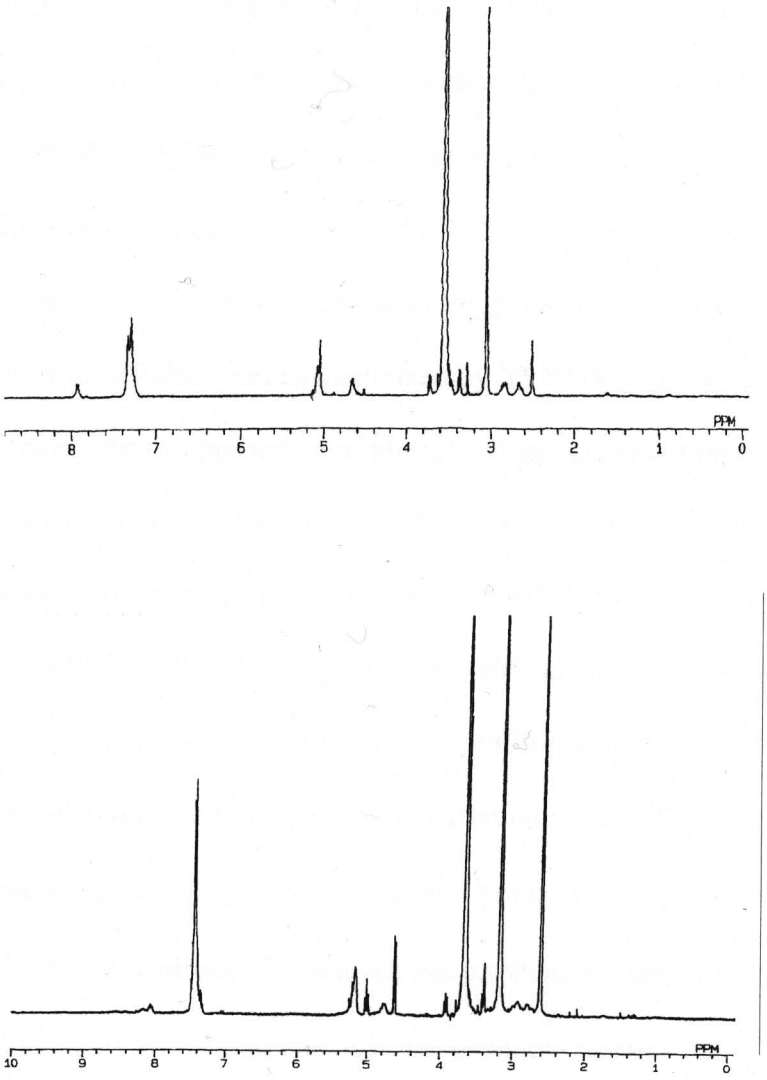


Figure 2. 3. $^{1}$H NMR of PEO-*b*-PBLA. Upper panel: 12-15. Lower panel: 12-23

using a higher ratio of 2-HP and ester decreased the reaction time for the aminolysis of poly(γ-L-glutamate) (50). Therefore, a ten-fold excess of 2-HP was used in the reaction of PEO-*b*-PBLA. The reaction time was 4 h at room temperature. It has been reported that when aminolysis was carried out at 60°C, polymer chain cleavage was significant. However, little chain cleavage occurred for the reactions carried out at room temperature in the presence of 2-HP. PEO-*b*-PHAA was purified by precipitating the polymer in 2-propanol. The unreacted 2-HP and amines were soluble in the solvent, and only polymer precipitated.

The product was collected and characterized by $^1$H NMR and UV absorption spectroscopy, following the disappearance of phenyl groups. Losses of one peak at 7.4 ppm in the $^1$H NMR spectrum and one absorption band at 280 nm in the UV spectrum indicated the complete removal of the benzyl groups from PEO-*b*-PBLA as a result of the aminolysis reaction. The yield of PEO-*b*-PHAA was greater than 90% in all experiments.

The introduction of hydroxyl groups by aminolysis to PEO-*b*-PBLA is an effective way of supplying sites for the conjugation of drugs onto hydrophilic block copolymers through hydrolytically labile linkages, e.g., esters, carbonates. Aminolysis of poly(γ-benzyl-L-glutamate) carried out with hydroxyalkyl amines has provided a water-soluble poly(γ-hydroxyalkyl L-glutamine) for conjugation of water-insoluble steroids (51). The poly(γ-hydroxyalkyl L-glutamine)-steroid conjugate was water insoluble, but it was rendered into particles capable of controlled release of steroid over a long period of time after a subcutaneous injection. Accordingly, aminolysis of PEO-*b*-PBLA with 2-hydroxyethyl amine or 6-hydroxyhexyl amine provides water soluble PEO-*b*-PHAA, which has hydroxyl groups at its side chains for the conjugation of drugs.

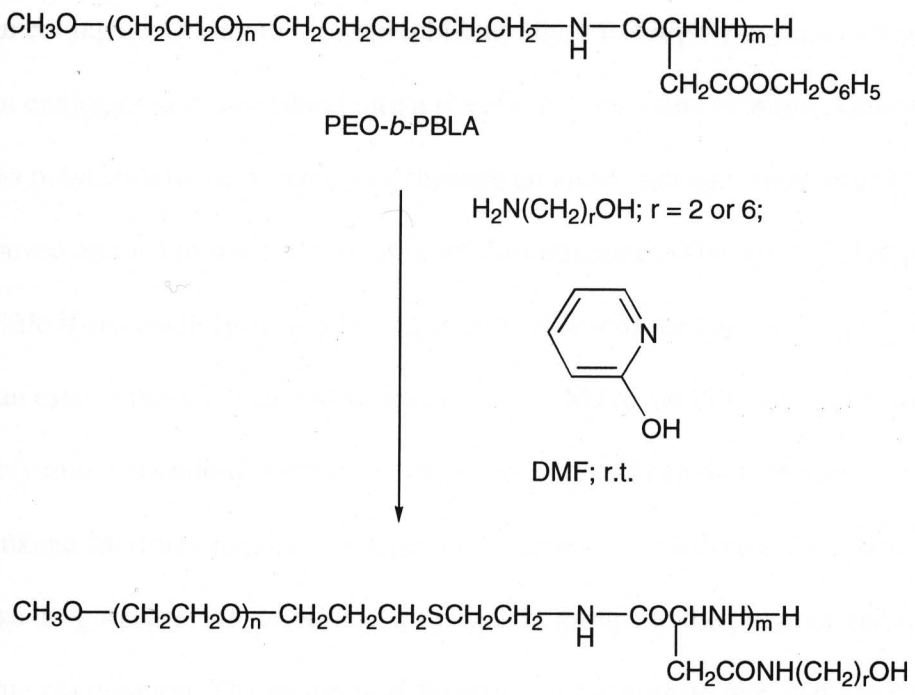


Figure 2. 4. Synthesis of PEO-*b*-PHAA

### *2.3.2. Synthesis of MTX esters of PEO-b-PHAA*

It has been reported that the attachment of doxorubicin, a hydrophobic drug, onto a hydrophilic PEO-*b*-poly(aspartic acid) leads to an amphiphilic PEO-*b*-poly(aspartic acid)-doxorubicin conjugate. Owing to its amphiphilicity, the PEO-*b*-poly(aspartic acid)-doxorubicin conjugate self-assembled into a micelle-like structure in water. Doxorubicin was attached to a poly(aspartic acid) backbone through an amide linkage. Drug conjugation at 50 % was achieved and led to micelle formation of the conjugates. The amide linkage was subject to little if any hydrolysis as part of a micelle-like structure in water. Our aim then is to explore an ester linkage for attaching drugs, such as MTX, on PEO-*b*- PHAA to achieve self-assembly into a micelle-like structure. Here, an ester linkage may be more suitable than an amide linkage for drugs requiring release for bioactivity. To increase the coupling efficacy and optimize drug release, we introduced alkyl spacer groups to the polymer and used ester bond for drug conjugation. The resulting polymeric drug conjugate may self-assemble into micelles in aqueous solution.

MTX esters of PEO-*b*-PHAA have been synthesized by the reaction of MTX with PEO-*b*-PHAA in the presence of DCC, a coupling reagent and DMAP, a catalyst (Figure 2.5). An MTX molecule has two carboxylic groups ($\alpha$ and $\gamma$ in glutamic acid residue), which can be modified and employed for its conjugation to polymers. In the coupling reaction, a carboxyl group of MTX was activated by DCC used in a 10-fold excess, resulting in an activated MTX ester. The activated ester then reacted with the hydroxyl groups of PEO-*b*-PHAA producing MTX-polymer conjugates in which MTX was attached onto PEO-*b*-PHAA through an ester linkage.

As shown in Table 2.1, the level of MTX conjugation was dependent on the initial ratio of MTX to hydroxyl residues in PEO-*b*-PHAA and the reaction medium. The level of attached MTX on PEO-*b*-PHAA increased as the initial concentration of MTX increased. Solvent also influenced the level of attachment of MTX. A higher level of substitution was more attainable for $CH_2Cl_2$ than DMF (Table 2.1). Because DMF was a good solvent for both PEO block and PHAA block, PEO-*b*-PHAA formed a clear solution in DMF in which the polymer chains exist as random coils. The steric hindrance at the reaction site might be significant because of the free movement of the extended PEO block, which might greatly decrease collisions between the MTX molecules and the hydroxyl groups. $CH_2Cl_2$, however, was a good solvent for the PHAA block but not for the PEO block. PEO-*b*-PHAA formed a translucent solution in $CH_2Cl_2$. The PEO chains might be associated, or even precipitated to reduce surface energy. The PHAA block may exist in an extended form. Consequently, the pendent hydroxyl groups may be less hindered for the reaction of MTX.

The optimal reaction time for most coupling reactions was approximately 20 h. Because of low molecular mobility of macromolecules, the coupling reaction time for MTX to PEO-*b*-PHAA was extended to 48 h-96 h, to obtain higher levels of MTX substitution.

Alkyl linkers bridged MTX and the polymeric backbone. The alkyl spacer not only provided hydroxyl groups but also changed the reactivity of the polymer. Two lengths of spacers ($C_2$ or $C_6$) were employed (Table 2.2 and 2.3). Altering the length of the spacers changes the microenvironment of the reaction sites. A long spacer group moves the reaction sites away from the polymeric backbone, which, therefore, reduces steric hindrance. As a result, a high-level drug attachment was more attainable using a six-carbon linker. Under the same reaction conditions, 36 % MTX conjugation was achieved for the conjugate with a

Table 2. 1. Coupling reaction results of MTX with PEO-*b*-PHAA ($C_2$-12-15).

| MTX esters | solvent | ratio of MTX/OH residues | Yield (%) | MTX conjugation | |
|---|---|---|---|---|---|
| | | | | mol %* | weight %** |
| LYD038 | $CH_2Cl_2$ | 2 | 90 | 54 | 20 |
| LYD010 | $CH_2Cl_2$ | 1 | 92 | 45 | 17 |
| LYD043 | DMF | 1 | 91 | 23 | 9 |

* g of MTX per gram polymer

** based on aspartic residues

Table 2. 2. MTX esters of PEO-*b*-PHAA (12-15)

| MTX esters of PEO-*b*-PHAA | spacer/ PEO-*b*-PHAA | molecular weight (g/mol)* | molecular weight of PHAA | Substitution of MTX | |
|---|---|---|---|---|---|
| | | | | mol % | weight % |
| LYD059 | $C_2$/12-15 | 15100 | 3100 | 7.4 | 3.2 |
| LYD043 | $C_2$/12-15 | 16000 | 4000 | 23 | 9.0 |
| LYD038 | $C_2$/12-15 | 18100 | 6100 | 54 | 19.4 |
| LYD050 | $C_6$/12-15 | 17800 | 7800 | 37 | 13.6 |

* calculated based on MTX substitution.

Table 2. 3. MTX esters of PEO-*b*-PHAA (12-23)

| MTX esters of PEO-*b*-PHAA | spacer/ PEO-*b*-PHAA | molecular weight (g/mol)* | molecular weight of PHAA | Substitution of MTX | |
|---|---|---|---|---|---|
| | | | | mol % | weight % |
| LYD044 | $C_2$/12-23 | 18400 | 6400 | 25 | 13.2 |
| LYD045 | $C_2$/12-23 | 21100 | 9100 | 51 | 24.3 |
| LYD051 | $C_6$/12-23 | 19200 | 7200 | 36 | 17.6 |
| LYD055 | $C_6$/12-23 | 22900 | 10900 | 55 | 26.9 |

* calculated based on MTX substitution

$C_6$ spacer (LYD050) instead of 23 % substitution for the conjugate with a $C_2$ spacer (LYD043) (Table 2.2). Moreover, the length of the alkyl linkers influences the hydrophobicity of the polymer and changes the physicochemical properties (discussed in chapter 3).

The precipitation of the reaction mixture into 2-propanol could not effectively separate the conjugate from unreacted MTX. Dialysis against DMSO proved to be the best method for purification since DMSO is a good solvent for MTX, MTX conjugate, and other substances in the reaction mixture (Figure 2.6). The removal of unreacted MTX could be observed from a gradual loss of yellow color of the dialysis medium. In the meantime, other small molecular impurities were also removed from the mixture. Dialysis was continued until no detectable MTX was present in the dialysis medium. Additional precipitation in 2-propanol was also helpful in removing trace MTX and other impurities. Free drug was not observed in the SEC-HPLC chromatogram of the conjugates, indicating that the purification method was effective (data not shown).

The $^1$H NMR spectra of MTX and a MTX ester of PEO-*b*-PHAA ($C_2$-12-15-54 % MTX) are shown in Figure 2.7. The characteristic peaks of polymer backbone as well as the MTX signals were present in the spectrum of the conjugate. The peak at 3.7 ppm was the proton signal of PEO. Proton couplings for the conjugate could not be clearly observed due to the difference between the molecular weight of PEO and other drug residues.

The UV spectra also showed the absorbance due to the MTX residues in the conjugate, indicating a successful conjugation of MTX to PEO-*b*-PHAA (Figure 2.8). MTX and MTX esters were dissolved in PBS buffer (pH 7.4) for the UV measurement. The characteristic UV absorbance peak at 305 nm is primarily due to the aminobenzoyl group and

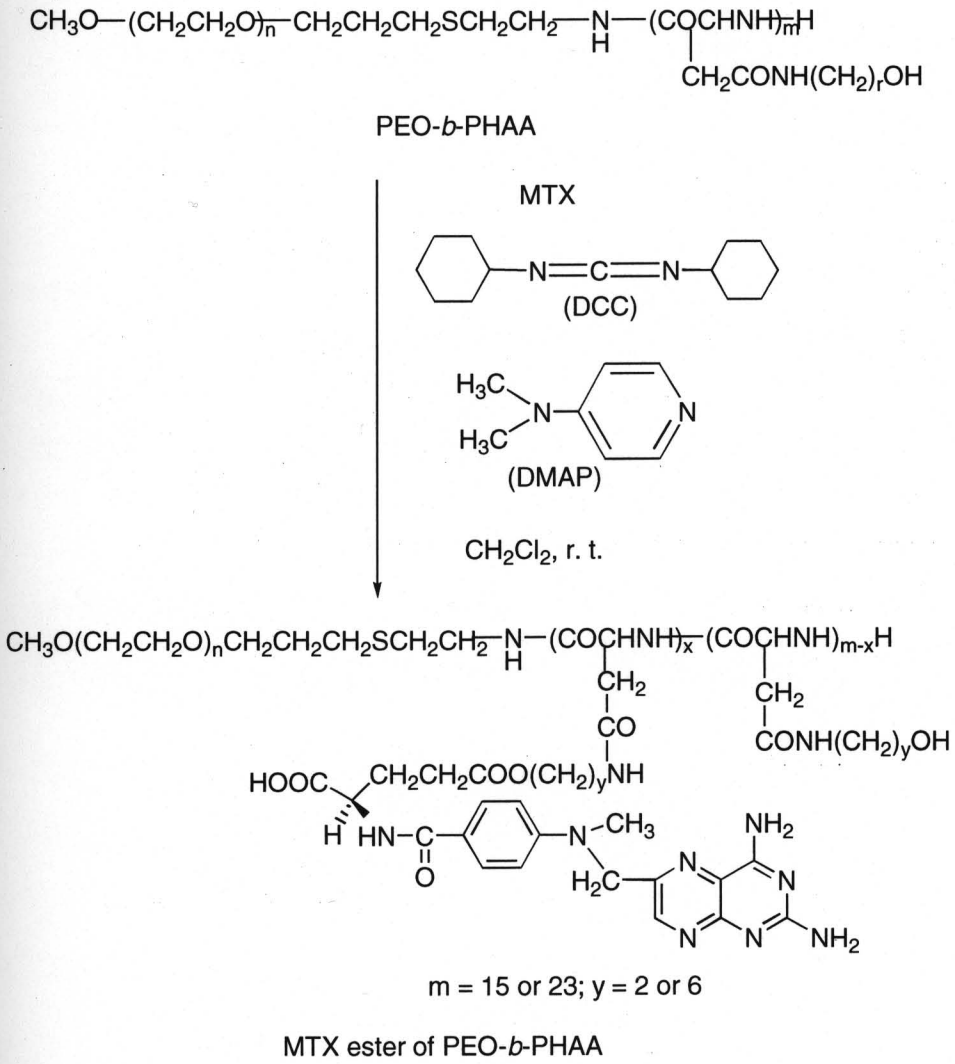


Figure 2. 5. Synthesis of MTX esters of PEO-*b*-PHAA

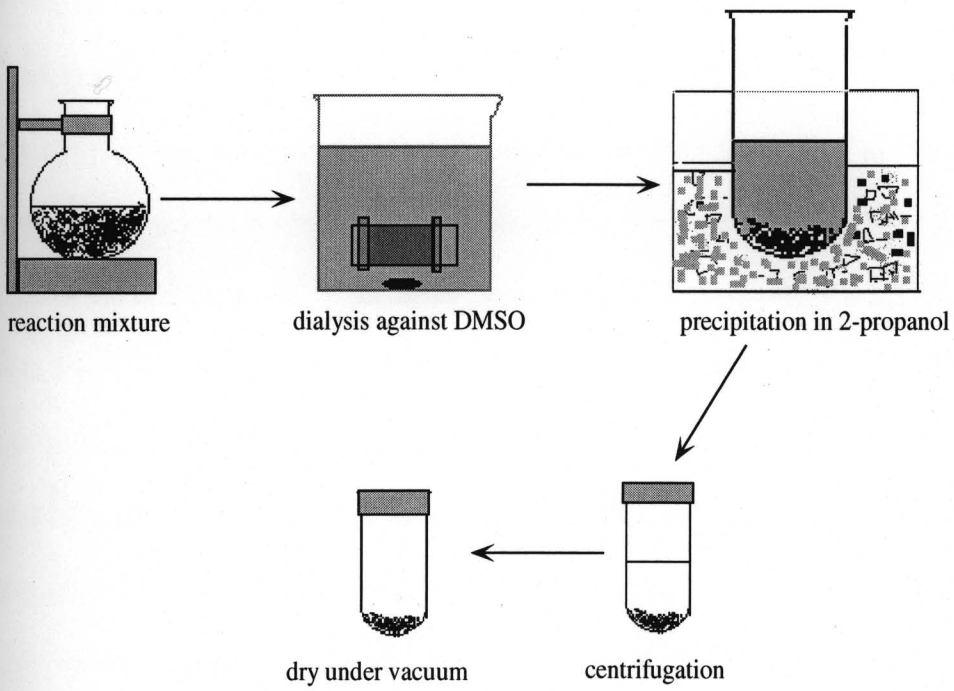


Figure 2. 6. Separation and purification of polymer product

the peak at 258 nm is due to both the diaminopteridine moiety and aminobenzoyl group in MTX molecules (52). For the conjugates of MTX with PEO-*b*-PHAA, the characteristic UV absorbance peaks of MTX moieties are notable. However, the shape of the UV spectra is different for the conjugates with varied levels of MTX substitution. This change may be caused by covalent conjugation or by intra- or intermolecular interaction in the solvent. The conjugates were designed to have two segments; PEO, the hydrophilic segment, and PHAA, the hydrophobic segment. The hydrophobic segment contains three parts: poly(aspartic acid) backbone, the alkyl spacer, and the conjugated MTX. A variety of structures with the combinations of the three parameters were synthesized. Levels of MTX substitution, expressed as an average molar ratio (mol %), were determined by UV analysis and calculated based on the number of aspartic acid residues that were coupled to MTX. Varying reaction conditions yielded a desired level of MTX substitution. For instance, the level of the attachment of MTX in its esters PEO-*b*-PHAA (e.g. 12-15-$C_2$, denoting 15 aspartic acid residues and a two-carbon spacer) expressed as the molar percentage, was 7.4, 23 or 54 % from absorption spectroscopy (Table 2.2), which was systemically consistent with $^1$H NMR (DMSO-$d_6$) results. Conjugates with other combinations such as different lengths of PHAA block and different lengths of spacer were also prepared. The compositions for the conjugates with 15 units and 23 units of aspartic acid are listed in Table 2.2 and Table 2.3, respectively. The yield of the MTX ester PEO-*b*-PHAA was greater than 90 % in all experiments.

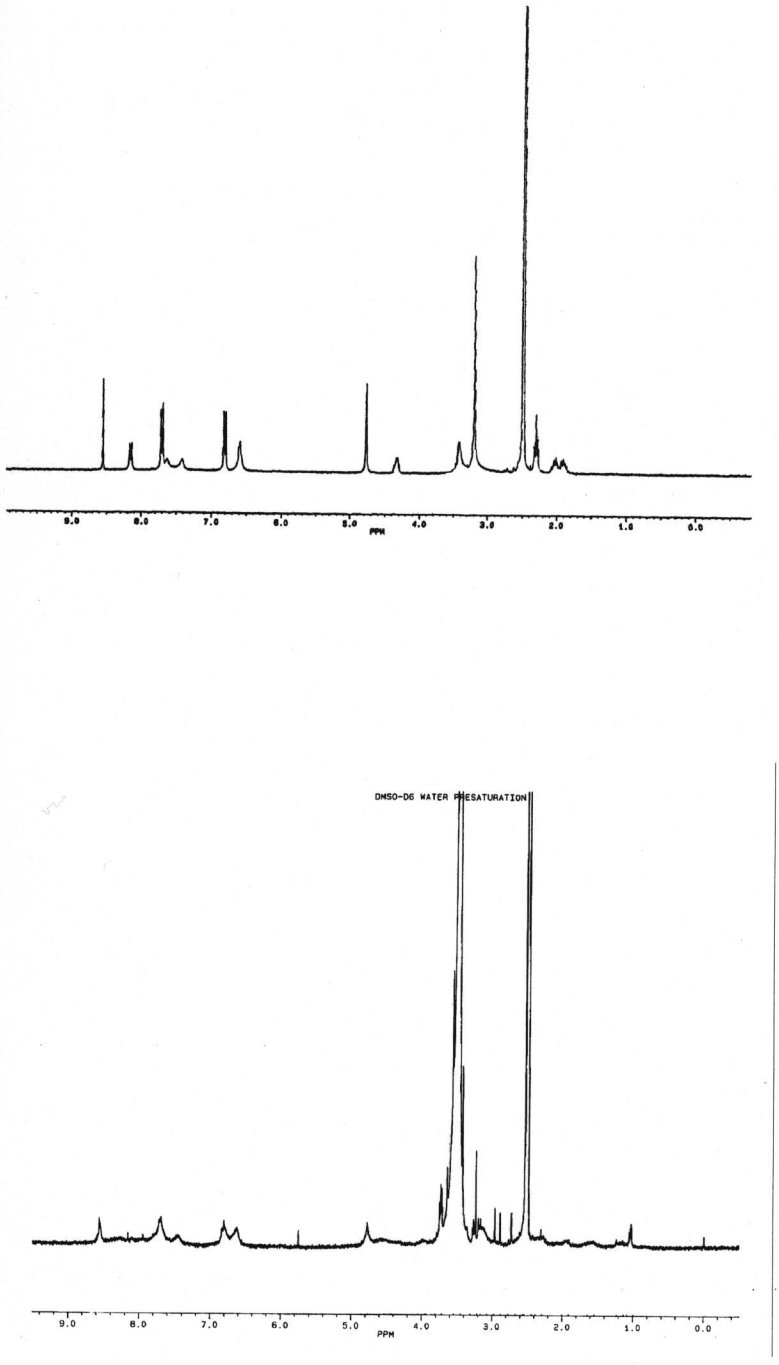


Figure 2. 7. $^{1}H$ NMR spectra of (a) MTX and (b) MTX ester of PEO-*b*-PHAA (LYD038, $C_2$-12-15-54 % MTX) in $d_6$-DMSO.

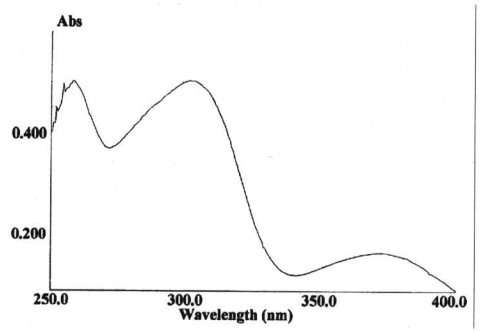


(a)

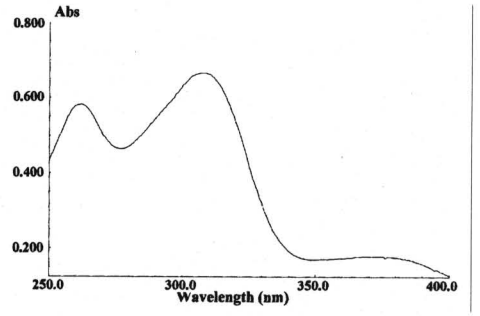


(b)

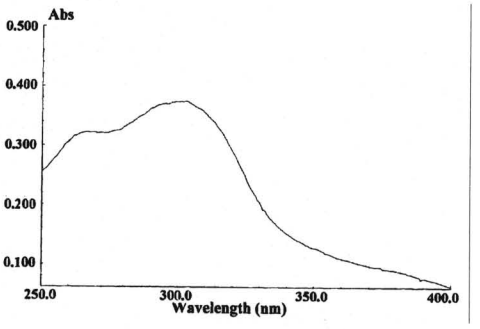


(c)

Figure 2. 8. UV spectra of MTX and MTX esters. (a) MTX; (b) LYD043 ($C_2$-12-15-23 % MTX); (c) LYD038 ($C_2$-12-15-54 % MTX).

The molecular weight of the conjugates was calculated based on the initial structure of the polymer and the level of MTX substitution. The calculated molecular weight of the conjugates correlated well with the elution time in the SEC-HPLC experiment. The SEC column was calibrated with blue dextran and a series of protein standards (Sigma, St. Louis, MO). The absolute molecular weight of the conjugates was not determined because of the structural difference between the conjugates and the standards. However, the elution time still demonstrated the relative size of the conjugates. Conjugates with high molecular weight eluted at an early time, and vise versa. The results are listed in Table 2.4.

The structural significance of the synthesized conjugates lies in the amphiphilic nature of the conjugates and the ability to gradually release MTX through hydrolysis. In summary, we have prepared a variety of amphiphilic MTX esters of PEO-*b*-PHAA. MTX was attached onto PEO-*b*-PHAA, obtained by aminolysis of PEO-*b*-PBLA. The polarity of solvents has significant effect on the level of MTX substitution. Three structural parameters were adjusted to obtain conjugates with varied physicochemical and biological properties. The hydrophilic PEO has numerous positive attributes in a biological setting, such as preventing untoward biological interactions. Hence, MTX esters of PEO-*b*-PHAA may have a prolonged blood half-life and favorable tissue biodistribution compared to free MTX.

Table 2. 4. Elution time of MTX esters of PEO-*b*-PHAA ($C_2$-12-15)

| MTX esters of PEO-*b*-PHAA | spacer/PEO-*b*-PHAA | Molecular weight calculated (g/mol) | Elution time (min)* | Elution time (min)** |
|---|---|---|---|---|
| LYD059 | $C_2$/12-15 | 15100 | 10.34 | 13.37 |
| LYD043 | $C_2$/12-15 | 16000 | 10.27 | 12.05 |
| LYD038 | $C_2$/12-15 | 18100 | 10.17 | 9.50 |
| LYD044 | $C_2$/12-23 | 18400 | 10.19 | 11.94 |
| LYD045 | $C_2$/12-23 | 21100 | 10.13 | 10.00 |
| LYD050 | $C_6$/12-15 | 17800 | n.d. | 9.16 |
| LYD051 | $C_6$/12-23 | 19200 | n.d. | 8.97 |
| LYD055 | $C_6$/12-23 | 22900 | n.d. | 8.84. |

* OHpak KB-805 column;

** Ultralhydrogel™ 500 GPC column.

# CHAPTER 3.

## Physical Properties of The Micelles of MTX Esters of Poly(ethylene oxide)-*block*-Poly(hydroxyalkyl L-aspartamide)

## 3.1. Introduction

Block copolymers with a relatively short hydrophobic block normally form spherical micelles with a core/shell structure and nanoscopic size. Based on the reported examples, the diameter of polymeric micelles fall in the range of 10-100 nm. Polymeric micelles usually exhibit relatively low critical micelle concentration (CMC) compared to low molecular weight surfactants. The CMC is defined as the threshold concentration at which micellization begins. The change in standard free energy ($\Delta G°$) of the micellization process can be estimated by the CMC. For a closed model of micellization, $\Delta G° = RT\ln(CMC)$, where R is the gas constant, and T is the absolute temperature. The threshold for micellization can be estimated by measuring the change of certain physical properties of the polymeric micelles. A certain physical property for a micelle solution usually displays a discontinuity at the CMC. Surface tension, light scattering, and solubilization of fluorescent dyes are the most commonly used techniques for determining the CMC of polymeric micelles. Although CMC values from various methods tend to be slightly different, CMC is still a valuable parameter for evaluating the thermodynamic stability of polymeric micelles.

As described in chapter 2, MTX was attached to a diblock copolymer backbone through an ester linkage. We hypothesized that the resulting MTX ester may form micelles in aqueous solution. The MTX moiety would greatly change the property of the block copolymer. Upon self-association of the conjugates, the MTX moieties would be incorporated into the core of the micelles and segregated from the aqueous media. In this section, we discuss the micelle structure of the conjugates and the physical properties of the micelles. Association of block copolymer conjugate was observed in $^1H$ NMR studies. The

shape and size of the polymeric micelles were determined by transmission electron microscopy (TEM) and dynamic light scattering (DLS). We measured the CMCs of the MTX esters of PEO-*b*-PHAA by a light scattering method and the polarity of the micelle core by a fluorescent probe, nile red. Our results demonstrated that MTX ester of PEO-*b*-PHAA formed micelles in aqueous solution. These micelles have remarkable thermodynamic stability in terms of low CMC. These properties revealed the potential for the application of MTX polymer conjugate micelles for the delivery of MTX.

## 3.2. Experimental

### *3.2.1. Materials and methods*

PEO-*b*-PHAA and MTX ester of PEO-*b*-PHAA were synthesized as described in Chapter 1. All chemicals were purchased from Aldrich (Milwaukee, WI) and were used as purchased unless explicitly stated. $^1$H NMR was operated on a Bruker 300 operated at 300 MHz. Water used for micelle preparation was purified by a SYBRON/Barnstead Pressure Cartridge System (PCS) (Boston, MA). Nitrogen gas was purchased from Matheson with labeled purity of 99.999 % and passed through a column (400 x 50 mm) packed with Dryrite (Aldrich) before use.

### *3.2.2. Preparation of the MTX conjugated block copolymer micelles*

PEO-*b*-PHAA or MTX ester of PEO-*b*-PHAA (20 mg) was dissolved in 4 mL of DMAc with stirring and slightly heated to form a clear solution. Deionized water (0.40 mL) was added dropwise to the solution of the polymer in DMAc. After stirring for 30 min, the solution was dialyzed against water (Spectra/por 2, MWCO = 12,000–14,000 g/mol, Fisher Scientific, Co., PA). The dialysis medium was replaced at 2, 4, and 24 h. The resultant polymer solution was ready for further studies or stored at 4°C after lyophilization (yield 80–85 % in weight). The micelle solution was reconstituted by dissolving the freeze-dried micelles in water or buffer with the aid of sonication.

### *3.2.3. Self-association of MTX ester of PEO-b-PHAA by $^1H$ NMR*

A MTX ester of PEO-*b*-PHAA (LYD038 ($C_2$-12-15-54 % MTX), 10 mg) was dissolved in 0.8 mL DMSO-$d_6$ with slight heating to form a clear solution. The solution was filtered and its $^1H$ NMR spectra were recorded. Subsequently, 5, 10, and 20 % $D_2O$ was added, and the $^1H$ NMR spectra were recorded after adding $D_2O$ each time. A water suppression technique was used for the measurement. The obtained $^1H$ NMR spectra are shown in Figure 3.2.

### *3.2.4. Shape and size of the micelles by TEM*

A drop of micelle solution reconstituted from freeze-dried MTX ester of PEO-*b*-PHAA ($C_2$-12-15-54 % MTX) in doubly distilled water was placed on a membrane coated electron microscopy grid. Excess fluid was removed from the grid surface with a piece of

filter paper. A drop of 1 % phosphotungstic acid was immediately added to the surface. After one minute, excess fluid was removed and the surface was air-dried. The grid was loaded in the transmission electron microscopy (Hitachi H7000, Japan), and pictures were taken at a magnification of 12,000 times (75 kV).

### *3.2.5. Size distribution of MTX ester of PEO-b-PHAA micelles by DLS*

The apparent hydrodynamic diameter and the size distribution of the polymeric micelles were measured by a COULTER® N4 Plus DLS instrument (Beckman) equipped with a 10 mW helium-neon laser source operating at 632.8 nm. Setting the light scattering angle at 90°, the measurements were performed at 25°C. All samples were filtered through a Millipore membrane (0.45 μm, Fisher Scientific, Co., PA) before the measurements. The concentration of each sample was in the range of 1.0 to 0.3 mg/ml to obtain optimum light scattering intensity. Particle size distribution was processed with the FORTRAN program "CONTIN". Briefly, the scattered light intensity signal was mathematically transformed to calculate the diffusion coefficient ($D$), which is related to the particle size according to the Stokes-Einstein equation

$$D = \frac{k_B T}{3\pi\eta d} \qquad (3.1)$$

where $k_B$ is Boltzmann constant, $T$ is absolute temperature, $d$ is diameter of a particle, and $\eta$ is the viscosity of the medium. The transformation is called the autocorrelation function

($G(\tau)$). For a sample containing a mixture of particles of different sizes (polydisperse), ($G(\tau)$) is the sum of decaying exponential for particles of each size,

$$(G(\tau)) \propto \sum a_i \exp(-2\Gamma_i(d_i)\tau) \tag{3.2}$$

Where $a_i$ is the contribution to the total scattered light intensity of particles of size $d_i$, $\Gamma_i$ is the decay constant, and is equal to $DK^2$, where $D$ is the diffusion coefficient, and

$$K = (\frac{4\pi n}{\lambda})\sin(\frac{\theta}{2}) \tag{3.3}$$

where $n$ is the refractive index of the diluent, $\lambda$ is the laser wavelength in vacuum, and $\theta$ is the angle of scattering intensity measurement. The values of $n$ and $\eta$ for each micelle solution are assumed to be equal to that of water. Polymeric micelles from dialysis or reconstituted from freeze-dried form were used for the measurement (Table 3.1)

### *3.2.6. Estimation of hydrophobicity of micelle core using a fluorescent probe*

A fluorescent probe, nile red, was used for polarity estimation for the core of polymeric micelles. A stock solution of nile red (Molecular Probes) in methanol solution was prepared at a concentration of 0.024 mg/mL (0.075 mM). Nile red solution (15 μL) was added to a vial and dried with a flow of nitrogen. A film of nile red was left after the solvent was evaporated. 1.8 mL of micelle solution was added to the vial and stirred for 30 min. The

final concentration of nile red was 0.001 mg/mL (1.4 μM). The fluorescence emission of nile red was measured with a Hitachi 3000 fluorometer with excitation and emission wavelength set at 500 nm and 630 nm, respectively. Bandpasses were set at 5 nm for excitation and 20 nm for emission. The experiments were carried out at 25°C.

### *3.2.7. Critical micelle concentration*

MTX esters of PEO-*b*-PHAA self-assembled into micelles according to a modified procedure in *3.2.2*. A series of concentrations of MTX esters of PEO-*b*-PHAA (0.001 mg/mL-1.5 mg/mL) calibrated by measuring the MTX content was prepared for the measurement of CMC. Light scattering was measured with a fluorometer (Hitachi 3000, Japan), with excitation and emission wavelengths set at 450 nm. The average intensity of scattered light from three measurements was plotted against polymer concentration, and CMC was extrapolated from the beginning of the abrupt increase of scattered light intensity (Table 3.2).

## 3.3. Results and Discussion

### *3.3.1. Preparation of the micelles of MTX esters*

In aqueous media, amphiphilic polymer molecules spontaneously associate to form various structures, depending upon the chemical structure of the polymers. Block copolymers, which have a much longer hydrophilic block than the hydrophobic block, self-

assemble into star-like micelles with a core of hydrophobic segments surrounded by a corona of soluble chains. The equilibrium size and shape of the star-like micelles is determined by the balance between the interfacial free energy characterizing the sharp core/corona interface and the conformational free energy of the chains inside the core and corona.

Poly(ethylene oxide)-*block*-poly(hydroxyaspartamide) (PEO-*b*-PHAA), the product from aminolysis of PEO-*b*-PBLA and the template for drug attachment, did not associate into a micelle-like structure at a concentration below 1.5 mg/mL, owing to its low hydrophobicity as proved by TEM and DLS studies (data not shown). This concentration was normally used for other micelle-forming MTX esters. The self-association of poly(ethylene oxide)-*block*-poly(2-hydroxyethylaspartamide) (PEO-*b*-PHEA) and poly(ethylene oxide)-*block*-poly(6-hydroxyhexylaspartamide) (PEO-*b*-PHHA) did occur at high concentration (>1.5 mg/mL) observed by abrupt increase in light scattering intensity.

The attachment of MTX to PEO-*b*-PHAA, however, greatly increases the hydrophobicity of the block copolymer, resulting in a sufficiently amphiphilic characteristic to undergo phase separation in aqueous solution. A variety of methods have been developed for the preparation of polymeric micelles. Usually, a block copolymer is dissolved in a solvent, such as DMF, DMAc, or methanol, and the solvent is then gradually replaced by water. The exchange rate of the organic solvent by water is critical for each block copolymer. For MTX esters of PEO-*b*-PHAA, DMAc was used as the solvent. As depicted in Figure 3.1, a small portion of water is slowly introduced into the polymer solution before a full exchange of solvent with water. In this step, the hydrophobic blocks start to associate weakly, and loosely packed micelles with a swollen core are formed. As the water content increases, the

cores of micelles become less swollen. Dialysis is used to remove the organic solvent from the system, and a well-defined core/shell structure is finally formed.

### *3.3.2. Self-assembly of an MTX ester studied by $^1H$ NMR*

The micellization of block copolymer can be observed by a variety of techniques. $^1H$ NMR studies provide direct evidence for micellization of MTX esters of PEO-*b*-PHAA.

$^1H$ NMR analysis of a PEO-*b*-PHAA-MTX conjugate ($C_2$-12-15, 54 % MTX) revealed the occurrence of phase separation for the block copolymer in the presence of water, observed as an absence of peaks for protons characteristic of the conjugated MTX due to the self-assembly of PEO-*b*-PHAA-MTX conjugate in $D_2O$ (Figure 3.2 (a)). Proton peaks characteristics of the PEO-*b*-PHAA-MTX block were discernible in DMSO-$d_6$. Proton peaks for MTX moieties were present at 6.6 and 6.8 ppm (benzoyl moiety) and 7.5, 7.7, 8.3 and 8.6 ppm (2,4-diamino-6-pteridinyl moiety). A peak for protons for PEO (–C$\underline{H}_2$C$\underline{H}_2$O–) was present at 3.6 ppm. Proper assignment of all the peaks was not possible, owing to poor resolution of proton peaks of MTX. This reflects the high molecular weight of PEO in comparison to the PHAA-MTX block.

When $D_2O$ was added to the solution of the PEO-*b*-PHEA-MTX conjugate in DMSO-$d_6$, the characteristic peaks of MTX lowered and became broader at 5 %, 10 %, or 15 % v/v $D_2O$:DMSO-$d_6$, and completely disappeared at 20 % v/v $D_2O$:DMSO-$d_6$ (Figure 3.2). This indicated self-aggregation of PEO-*b*-PHAA-MTX conjugate at roughly this critical solvent composition, namely critical water concentration (CWC).

$^1$H NMR studies revealed the segmental motion of the block copolymer, which reflected the microenvironment of the blocks. As shown in Figure 3.2, in pure organic solvent, DMSO-$d_6$, the characteristic signals of hydrophobic blocks, including MTX signals and aspartamide signals, were clearly seen on the $^1$H NMR spectrum. Because DMSO is a good solvent for both hydrophobic and hydrophilic blocks, the polymer chains exist in an extended state in the solvent. The signals for both blocks were thus detected. Adding $D_2O$ into the solution induced the association of hydrophobic blocks in a way to avoid their contact with water molecules. As the hydrophobic block has conjugated MTX moieties at its side chains, the microenvironment of the MTX reflected the segmental motion of the block polymer. In the $^1$H NMR spectra, protons with restricted movement due to the viscous environment often result in broader NMR signals. The movement of the hydrophobic segment became more restricted, as seen in the $^1$H NMR spectra in which the MTX signal was weaker when at 10 % $D_2O$ (Figure 3.2 (b)). As more water was introduced to the system, the tendency for hydrophobic interaction became stronger, and the motion of hydrophobic moieties was more restricted. Up to a certain point, the interaction of hydrophobic blocks reached to a point where the movement of the hydrophobic blocks was strictly restricted, and the signals completely disappeared (Figure 3.2 (c)).

On the other hand, the proton peaks of PEO are evident in both $D_2O$ and DMSO-$d_6$. An absence of proton signals for MTX of self-assembled PEO-*b*-PHAA-MTX conjugate indicates that the drug is in a core having restricted mobility. Several studies on amphiphilic block copolymers have revealed an absence of signals from a hydrophobic block after self-assembly into a micelle-like structure in water (53). By contrast, $^1$H NMR spectra reveal signals from core-forming alkyl tails of low molecular weight micelles. These micelles are in

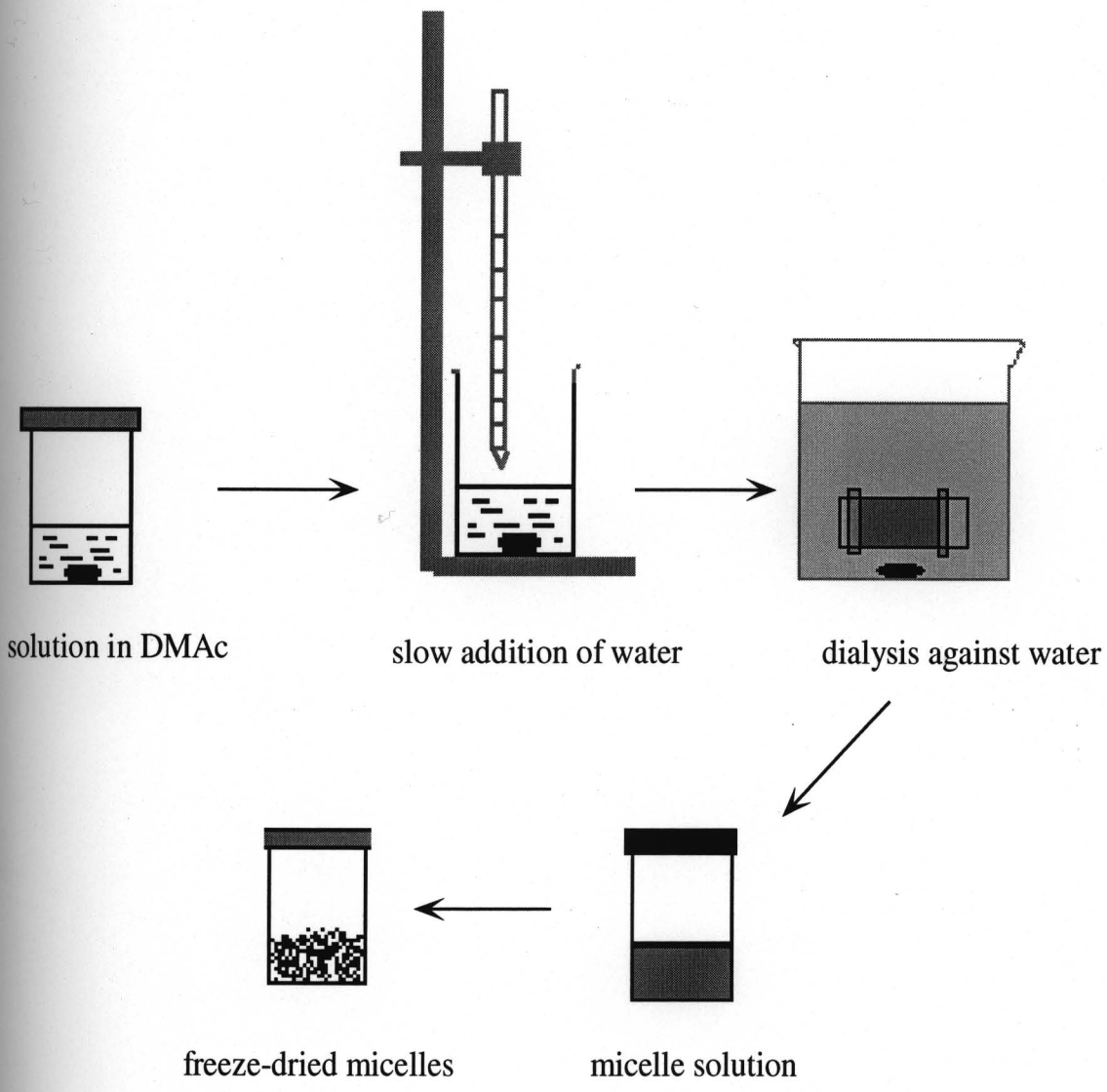


Figure 3.1. Procedure of micelle preparation.

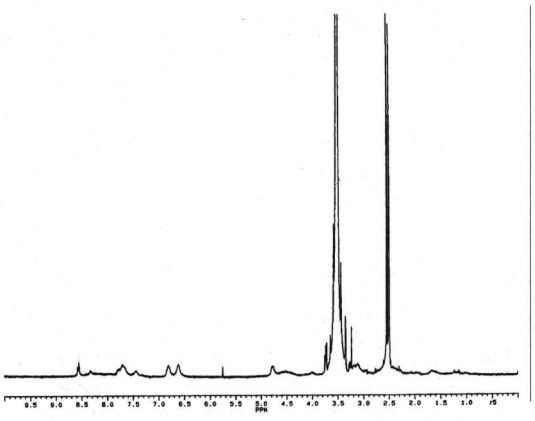

(a) 100 % $d_6$-DMSO

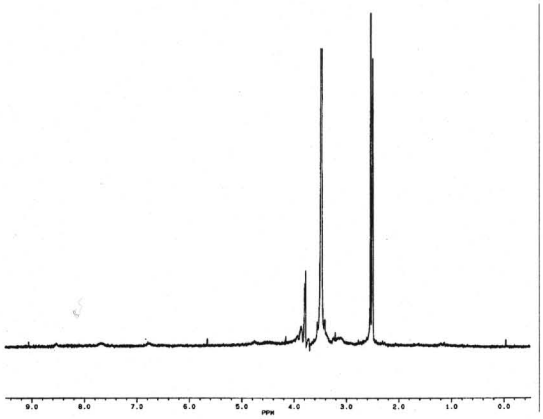

(b) 10 % $D_2O$ in $d_6$-DMSO

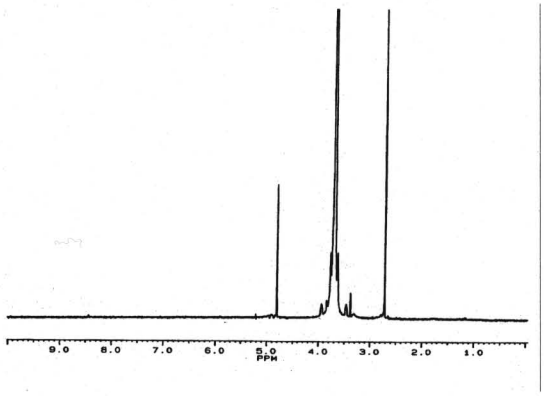

(c) 20 % $D_2O$ in $d_6$-DMSO

Figure 3.2. $^1H$ NMR of LYD038 (C2-12-15-54 % MTX) in $d_6$-DMSO or mixture of $D_2O$ and $d_6$-DMSO.

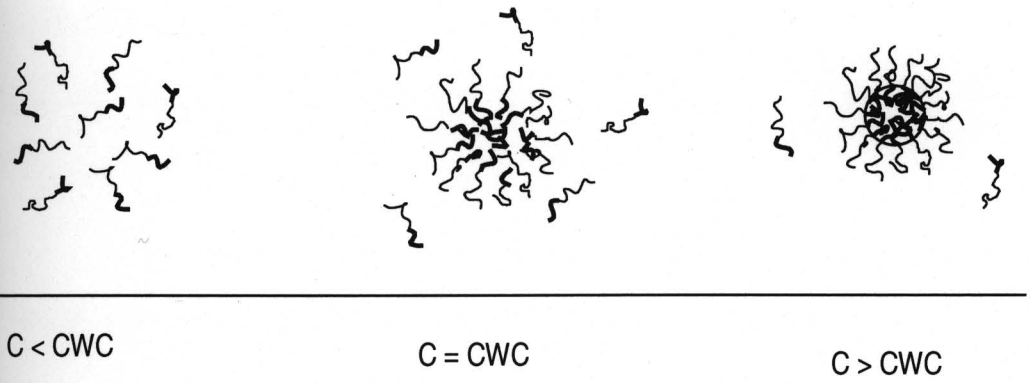


Figure 3. 3. Schematic demonstration of the association of block copolymer with water content in DMAc below, at, and above CWC.

equilibrium with the unimer. Micelle-like structures formed from block copolymers, on the other hand, may remain intact over time as opposed to being dynamic entities.

The association of block copolymers can be described in Figure 3.3. In pure organic solvent, block copolymers exist in unimer form. Adding water to the solution results in the change of the solvent polarity, inducing the micellization process. As water concentration reaches the CWC, micelles with a loosely associated core allow the free exchange of the unimers with micelles. As the water concentration is above the CWC, polymeric micelles with a defined core/shell structure are formed.

### *3.3.3. Morphology of the conjugate micelles by TEM*

The micelles of MTX esters of PEO-*b*-PHAA were freeze-dried to obtain a suitable form for long-term storage without a significant change in their properties. The micelles were reconstituted in deionized water with sonication. The resultant micelles of PEO-*b*-PHAA-MTX (12-15-$C_2$, 54 % MTX) were studied by TEM, an apparatus developed using a focused beam of electrons to "see through" the samples (Figure 3.4). The method for the preparation of polymeric micelles is more dependent on the nature of block copolymers. For block copolymers with a more hydrophilic nature, micelles are prepared by the direct dissolution of the polymers in water. Pluronic micelles are prepared by this method (54). For block copolymers with a more hydrophobic nature, an organic solvent is usually required to dissolve the polymers. Micelles are formed after the exchange of organic solvent with water. For micellization of MTX esters of PEO-*b*-PHAA, the polymers need to be dissolved in an organic solvent, DMAc, and then the solution is dialyzed against water. However, the rate of

solvent exchange is critical to obtain micelles with a small size. In this study, polymeric micelles prepared from two slightly different procedures showed different morphology. The dialysis of the conjugate in DMAc solution yielded micelles with various sizes, as well as clusters of micelle particles observed on the TEM photograph. The formation of the nanoparticles was believed to be a result of the secondary association, or intercalation of polymer chains. However, a slight modification in the micelle preparation procedure by slowly adding a small amount of water to the polymer in DMAc solution before the dialysis against water resulted in spherical micelles with small size and an absence of secondary aggregation (Figure 3.5). Size analysis for the micelles of PEO-*b*-PHAA-MTX conjugate ($C_2$-12-15-54 % MTX) revealed unimodal size distribution, and the mean diameter of micelles was 14 nm. This method for micelle preparation was used in all subsequent studies.

Slowly adding water to the polymer solution allowed the self-assembly of polymeric molecules in such a way as to minimize the free energy of the system. It is proposed that micellization is a kinetically controlled process of polymer chain exchange. If water is added slowly, the rate of the polymer chain exchange remains relatively high for long periods. As a result, the size distribution of aggregates can become unimodal instead of a broad population. On the other hand, if the water exchanges with solvent very fast, before the equilibrium resulting from polymer chain exchange can be established, the micelle cores are already frozen due to the decrease of the mobility of polymer chains in the cores as the water content increases (33). The staining process of sample preparation for TEM may result in dehydration of the surface of micelles. As a result, the micelles on the grid for TEM measurement may be in a relatively dry state. Therefore, the size of polymeric micelles obtained by TEM measurement should be smaller than the real size.

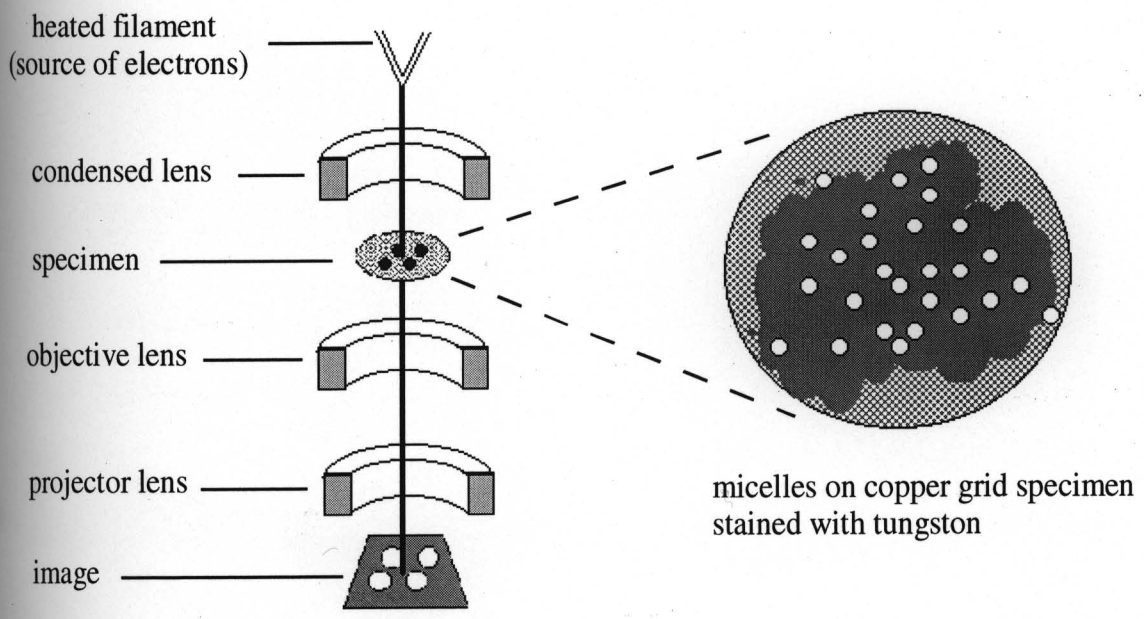


Figure 3.4. Principle features of transmission electron microscopy.

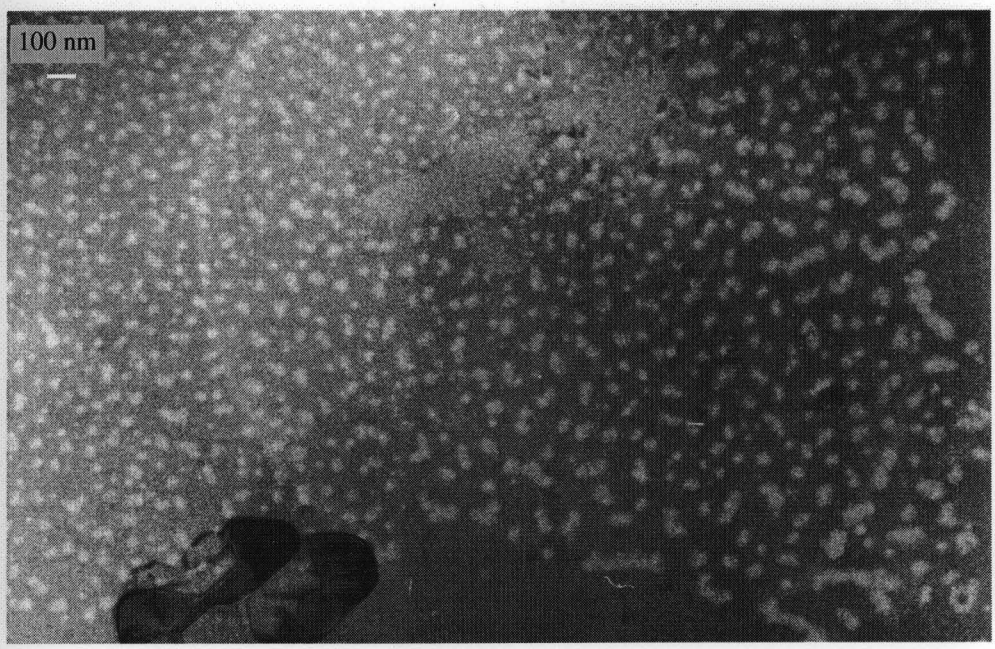


Figure 3.5. TEM photograph of LYD038 ($C_2$-12-15-54 %). Scale bar: 100 nm. Micelles were prepared by dialysis of the polymer in DMAc solution against water, omitting the step of gradual addition of water before dialysis.

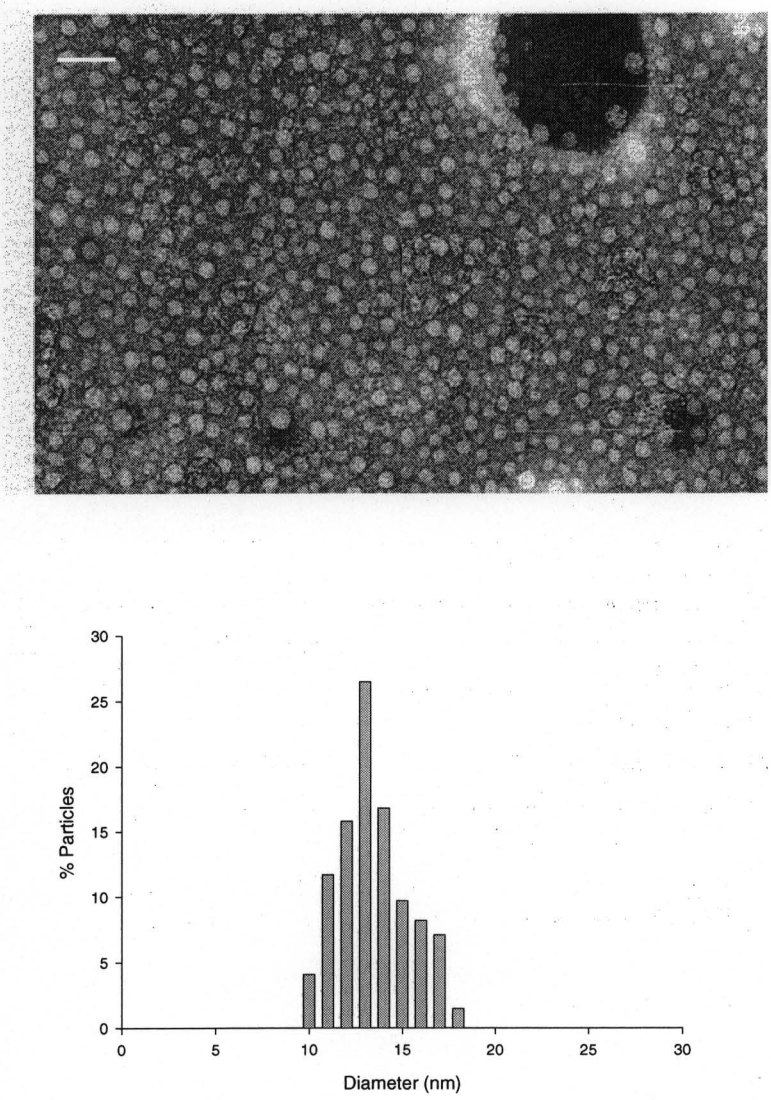


Figure 3. 6. TEM measurement of LYD038 ($C_2$-12-15-54 % MTX). Upper panel: image (scale bar: 50 nm). Lower panel: size distribution. Micelles were prepared by addition of water to polymer in DMAc solution before dialysis.

### *3.3.4. Hydrodynamic size of micelles*

In aqueous solution or biological fluid, the PEO shell of micelles is highly hydrated. Therefore, the "real" size of micelles is close to the hydrodynamic size, and is determined by dynamic light scattering measurement. Polymeric micelles are prepared by dissolving the polymer in DMAc solution, slowly adding a small amount of water and the dialysis of the solution. The resultant micelles are referred to as micelles after dialysis in Table 3.1. The micelle solution is freeze-dried. The micelles are reconstituted by dissolving the freeze-dried micelles into water or buffer, and are referred to as micelles after freeze-drying in Table 3.1.

For LYD038 ($C_2$-12-15-54 % MTX), the same sample used in the TEM measurement, the mean diameter of micelles (after dialysis) is 27 nm by DLS (Table 3.1). It is larger than the result from TEM measurement; since micelles used for TEM measurement are in a dry state, the hydrated PEO corona might not be properly detected.

The dimensions of polymeric micelles are molecular weight dependent. The MTX esters with higher molecular weight yield micelles with larger size. As shown in Figure 3.7, the three conjugates with a $C_2$ spacer and 15 units of aspartic acid have different molecular weights as a result of a varied level of MTX substitution. The micelles of LYD038, which has the highest level of MTX (54 %) and highest molecular weight (18100 g/mol), exhibit the largest diameter (27.1 nm). The sizes of micelles from LYD043 (MW: 16000 g/mol) and LYD059 (MW: 15100 g/mol) are 15.9 nm and 11.7 nm, respectively. Similarly in Figure 3.8, the three conjugates having a $C_6$ spacer in their structure exhibit an increase in size in response to an increase in molecular weight. However, molecular weight seems not the only factor in determining the size of polymeric micelles. The chemical structure of the hydrophobic block also determines the packing of the hydrophobic blocks, which may also

Table 3.1. Size distribution of the conjugate micelles.

| MTX esters of PEO-*b*-PHAA | spacer/ PEO-*b*-PHAA | molecular weight (g/mol) | micelle size (diameter, nm) | | |
|---|---|---|---|---|---|
| | | | after dialysis* | | after** freeze-dry |
| | | | primary | secondary | |
| LYD059 | $C_2$-12-15 | 15100 | 11.7±1.3 (99.1 %)*** | 153.5±32.8 (0.9 %) | n.d |
| LYD043 | $C_2$-12-15 | 16000 | 15.9±4.2 (99.4 %) | 163.4±36.9 (0.6 %) | 20.4±4.5 (0.4 %) |
| LYD038 | $C_2$-12-15 | 18100 | 27.1±3.2 (93.8 %) | 133.3±30.8 (6.2 %) | n.d. |
| LYD044 | $C_2$-12-23 | 18400 | 27.5±3.9 (99.5 %) | 188.1±32.4 (0.5 %) | n.d. |
| LYD045 | $C_2$-12-23 | 21100 | 30.7±7.8 (99.4 %) | 239.7±61.4 (0.6 %) | n.d. |
| LYD050 | $C_6$-12-15 | 17800 | 30.3±6.2 (80.3 %) | 72.7±14.8 (19.7 %) | 33.5±5.9 (98.8 %) |
| LYD051 | $C_6$-12-23 | 19200 | 37.9±9.0 (92.5 %) | 145.2±19.7 (7.5 %) | 45.5±17.6 (99.5 %) |
| LYD055 | $C_6$-12-23 | 22900 | 57.2±14.0 (86.1 %) | 199.5±22.7 (13.9 %) | 80.8±30.1 (99.5 %) |

* micelle solution after dialysis against water;

** micelles reconstituted by dissolving the freeze-dried micelles in water or buffer;

*** number in parenthesis represents the percentage of micelles within the size distribution.

affect the size of the micelles. For example, the molecular weight of LYD045, which has a $C_2$ spacer, 23 unit of aspartic acid, and 51 % MTX substitution, is 21100 g/mol. The size of micelles of LYD045 is about 30 nm, close to the size of micelles of the conjugates with lower molecular weight, such as LYD050, which has a $C_6$ spacer, 15 units of aspartic acid and 54 % MTX. The micelle size of LYD050 is 30 nm, while the molecular weight is 17800 g/mol.

The micelles of MTX esters of PEO-*b*-PHAA exhibited a certain degree of secondary association (Table 3.1, numbers in parenthesis). Micelles of the conjugates with low level of drug conjugation and a $C_2$ spacer revealed a low tendency for secondary association. Contrarily, MTX esters with a more hydrophobic nature, in terms of a higher level of drug conjugation and a longer spacer, exhibited a higher tendency for secondary association, observed as a bimodal distribution for the polymeric micelles (after dialysis) (Figure 3.9). LYD043 has 23 % MTX substitution, and the population of its micelles is composed of 99.4 % micelles with small size (about 15.9 ± 4.2 nm) and only 0.6 % micelles with a larger size (163.4 ± 36.9). However, 93.8 % of LYD038 ($C_2$-12-15-54 % MTX) micelles exhibited small size (27.1 ± 3.2 nm), and 6.2 % micelles appeared as large size (133.2 ± 30.8 nm). Polymeric micelles from the conjugates with a $C_6$ spacer exhibited notable bimodal size distribution. LYD050 ($C_6$-12-15-37 % MTX), LYD051 ($C_6$-12-23-36 % MTX), and LYD055 ($C_6$-12-23-55 % MTX) showed 19.7 %, 7.5 %, and 13.9 % secondary association, respectively (Figure 3.9).

The sizes of the micelles after dialysis and micelles reconstituted from freeze-drying were compared. Freeze-drying only slightly increased the size of the micelles (Figure 3.11). For instance, the size of LYD055 ($C_6$-12-23-55 % MTX) was changed from 57 nm before

dialysis to 81 nm after dialysis. The size change is not significant if the standard deviations of the values are considered. Interestingly, polymeric micelles reconstituted from freeze-drying showed a low degree of secondary association. As seen from DLS of LYD050, the second peak referred to the secondary association decreased for the micelles after freeze-drying (Figure 3.12). This phenomenon was also observed for other samples (Table 3.1). The results suggest that storage of micelles in a freeze-dried form does not significantly increase the size of the micelles, which is important for the use of micelles in pharmaceutics.

The secondary association is believed to be the clusters of individual primary micelles, which have aggregated due to hydrophobic-hydrophobic interactions between the core of the micelles (9). It is important that micelle preparation methods be able to produce small micelles with a unimodal size distribution. The sonication of polymer solutions and a decrease of polymer concentration are helpful in reducing secondary association (55) (56). In general, the micelle sizes of the MTX esters of PEO-*b*-PHAA are in the range of 10-200 nm.

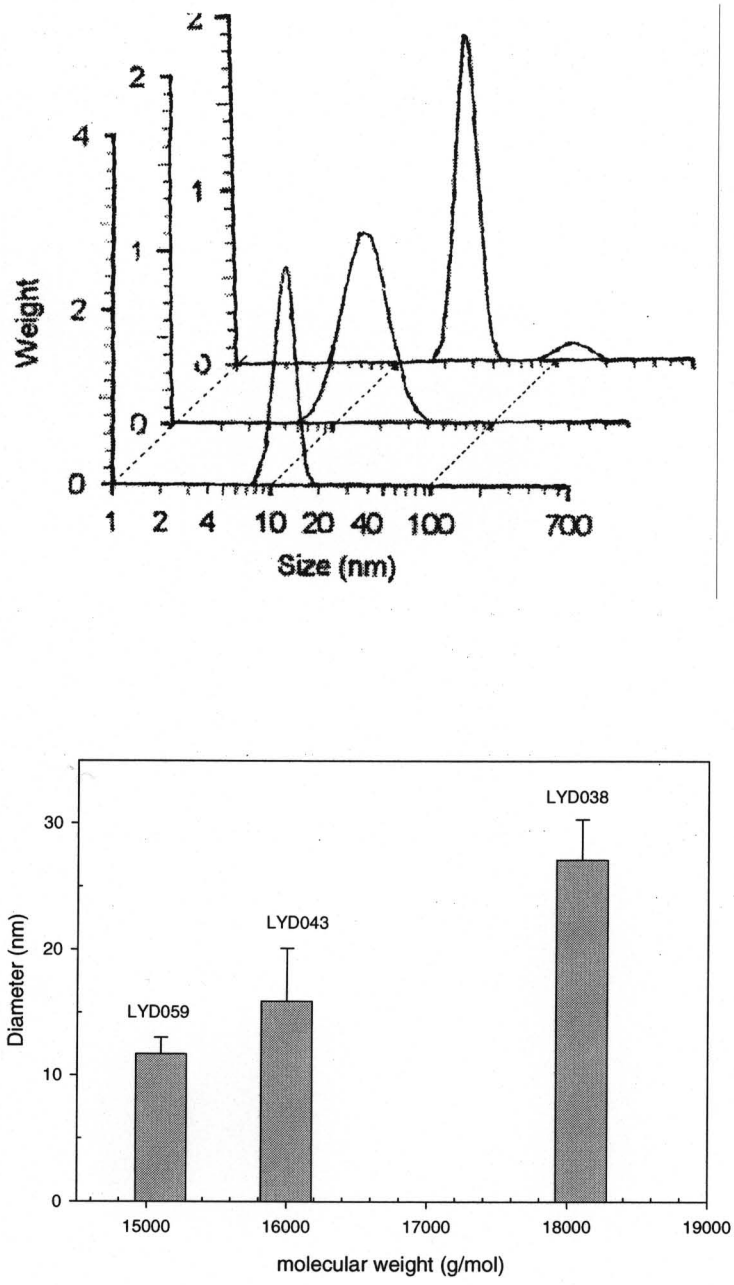


Figure 3.7. Hydrodynamic size distribution of micelles. Samples measured: LYD059 ($C_2$-12-15-7.4 %), LYD043 ($C_2$-12-15-23 %), LYD038 ($C_2$-12-15-54 %). Upper panel: size distribution from DLS. Lower panel: relationship between size and molecular weight.

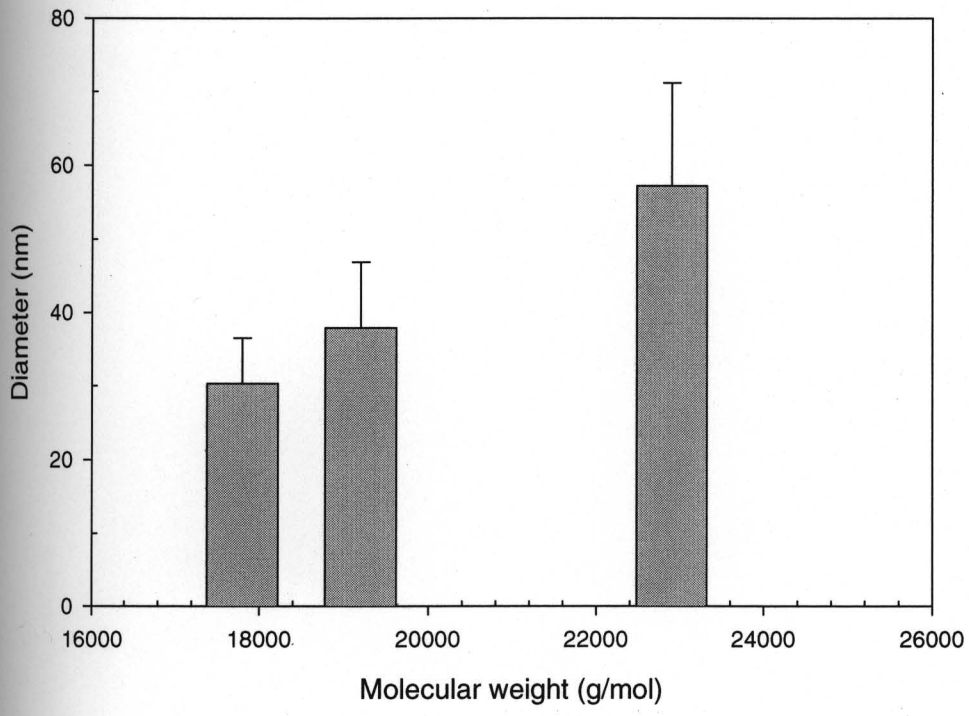


Figure 3.8. The dependency of micelle size on molecular weight of the conjugates. LYD050 ($C_6$-12-15-37 % MTX), LYD051 ($C_6$-12-23-36 % MTX), LYD055 ($C_6$-12-23-55 % MTX).

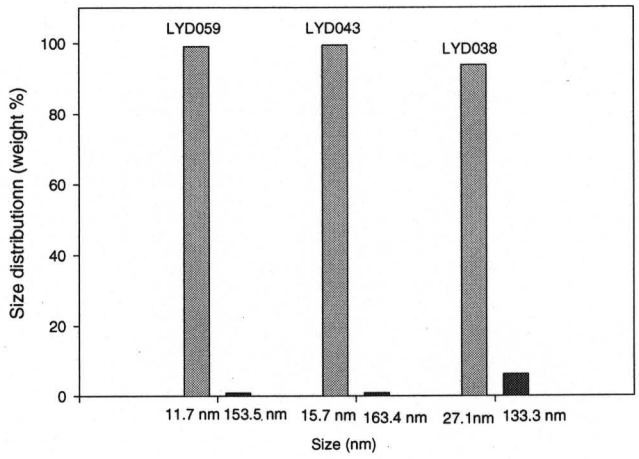


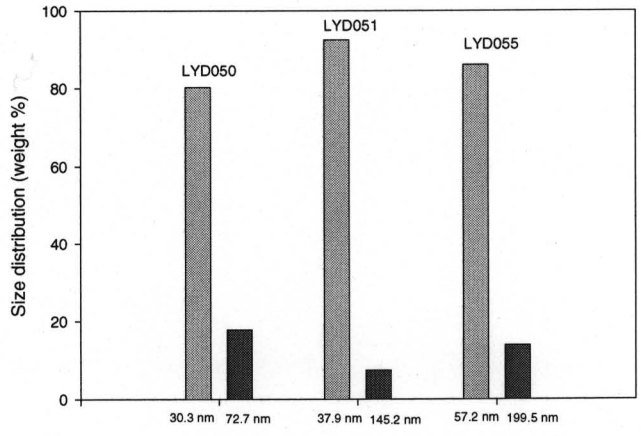


Figure 3. 9. Micelle size distribution. Upper panel: three conjugates with relatively low hydrophobicity. Lower panel: conjugates with relatively high hydrophobicity.

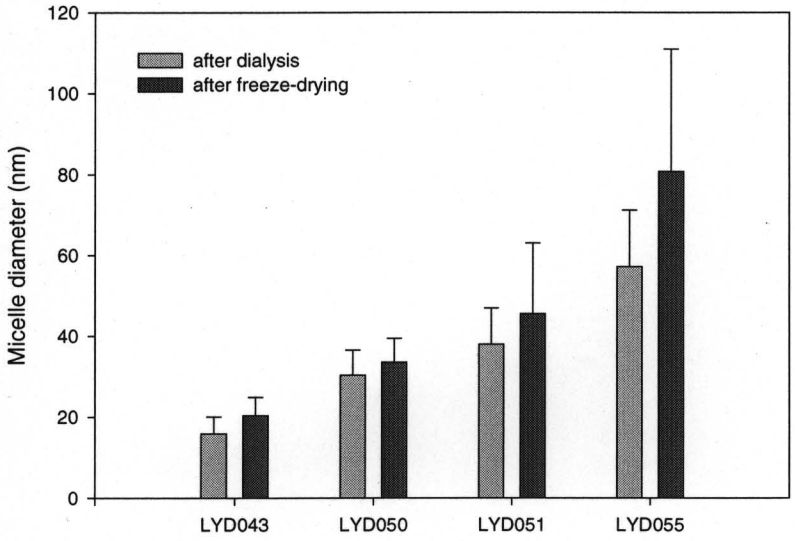


Figure 3. 10. Effect of freeze-drying on micelle size. LYD043 ($C_2$-12-15-23 % MTX), LYD050 ($C_6$-12-15-37 % MTX), LYD051 ($C_6$-12-23-36 % MTX), LYD055 ($C_6$-12-23-55 % MTX).

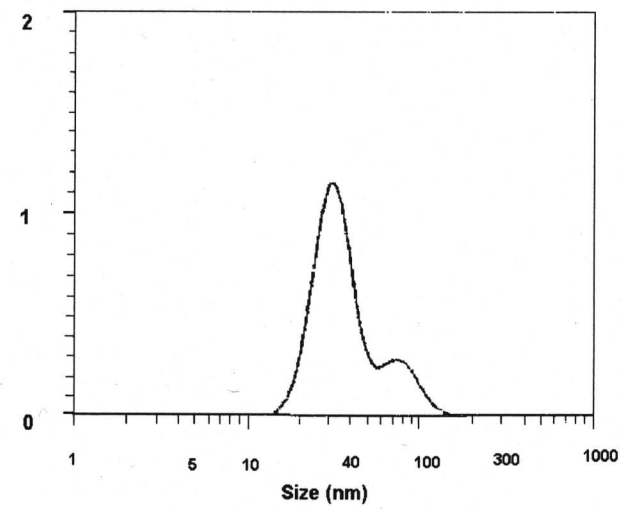


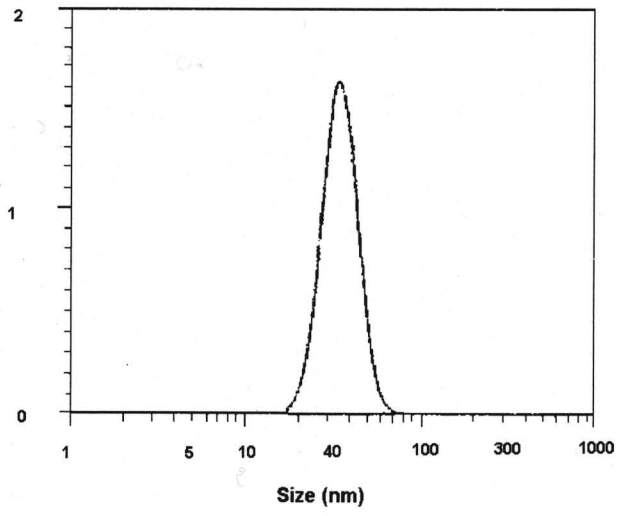


Figure 3.11. Size distribution of LYD050 (C6-12-15-37 % MTX) micelles from DLS. Upper panel: after dialysis. Lower panel: after freeze-drying.

### *3.3.5. Solubilization of nile red by the conjugate micelles*

Fluorescence probe techniques have been used to detect the association of amphiphilic molecules and to characterize the aggregates in terms of apparent microviscosity and micropolarity. Changes in micropolarity can be used to detect the onset of association based on the emission spectrum of the probe, which is strongly dependent on solvent polarity. Nile red (Figure 3.10), an uncharged phenozazone dye, has been used as a fluorescence probe in the studies of protein surfaces. It has a high oil/water partition coefficient (57) (58); it is photochemically stable, and its fluorescence is strongly dependent on the polarity of its environment. In cholesterol ester droplets or hydrocarbon solvents, nile red fluoresces to a yellow gold color, while in ethanol or phosphotidylcholine vesicles, the dye fluoresces as a red color (59). In aqueous media, it is relatively insoluble and its fluorescence is red shifted, but strongly quenched.

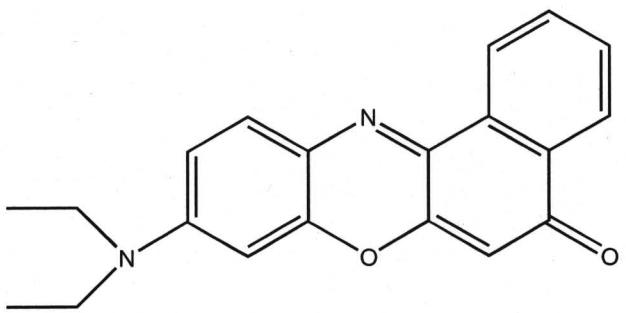


Figure 3.12. Chemical structure of nile red.

The self-assembly of the MTX conjugates is also evidenced by the solubilization of nile red. At low polymer conjugate concentrations, the fluorescence intensity is relatively low, as the probe is in a polar environment. However, when the concentration of polymer reaches the CMC, nile red molecules partition into micelles. A significant increase of fluorescence intensity is thus observed, as the Nile red molecules are transferred to a relatively non-polar environment, the core of the micelles (Figure 3.13). The CMC of the LYD038 micelles ($C_2$-12-25-54 % MTX) is extrapolated from the fluorescence intensity versus concentration curve, and is consistent with the value obtained from the light scattering method (0.014 mg/mL).

The core of the micelles is predominantly hydrophobic in nature, as indicated by the emission spectra of Nile red. The polarity change of the microenvironment of nile red molecules causes a blue shift of the maximum emission wavelength. The maximum emission wavelength was 627 nm for the polymer conjugate, PEO-*b*-PHAA-MTX (12-15-C2, 54 % MTX), at a concentration of 1.0 mg/mL (Figure 3.12). This polarity is close to that of dimethylformamide (emission maximum: 625 nm), as reported in the literature (59). In aqueous solution, however, the maximum wavelength of Nile red is about 650 nm.

### *3.3.6. Critical micelle concentration*

Although properly selected fluorescent probes can be used to estimate the CMC of the surfactants, the CMC values obtained are closely related to the compatibility of the probe and the micellar core, and are influenced by the probe used. Therefore, the CMCs of MTX

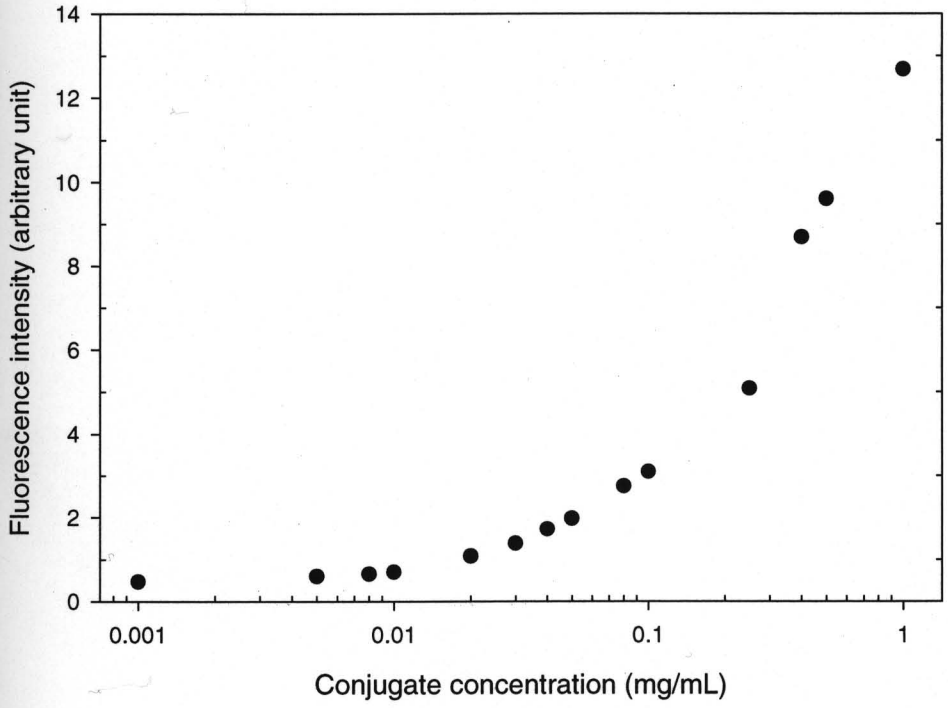


Figure 3.13. Fluorescence intensity as a function of concentration of LYD038 ($C_2$-12-12-54 % MTX)

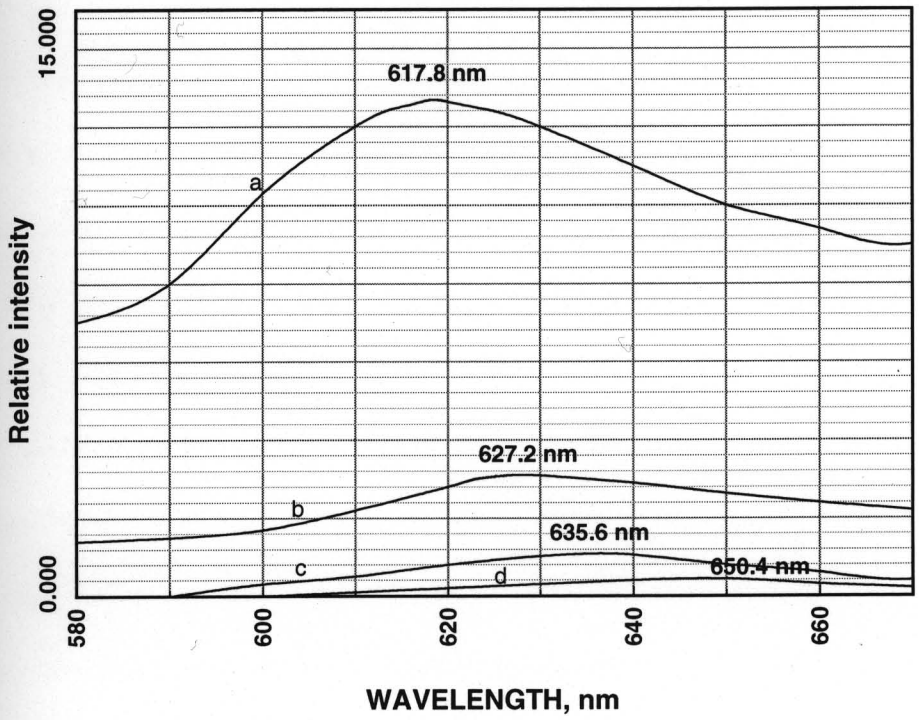


Figure 3.14. Fluorescence spectra of nile red in various concentrations of LYD038. (a) 0.5 mg/mL; (b) 0.08 mg/mL; (c) 0.02 mg/mL; (d) pure water.

esters of PEO-*b*-PHAA are determined by light scattering measurements using a fluorometer. Setting the excitation and emission at the same wavelength, the detected photo signals mainly result from the scattered light by the samples including the solvent and solute molecules, or large particles as a result of self-association of polymers (60). However, the effects of large particles prevail in the system observed as a high intensity of light scattering.

When the concentration of a block copolymer conjugate is below the CMC, the solution produces a scattered light signal at low intensity. However, when the concentration reaches the CMC, the unimers start to assemble into micelles, and an abrupt increase in the intensity of scattered light is detected (Figure 3.13-3.15). The CMCs of the MTX esters of PEO-*b*-PHAA are determined by extrapolation of the intensity versus concentration plots, and summarized in Table 3.2.

The CMC is an indication for the tendency toward self-assembly of the amphiphilic molecules, and is largely determined by the hydrophobicity of block copolymers. At concentrations below CMC, all the block copolymers are in the single chain form. At the CMC, the hydrophobic blocks begin to associate to form loose aggregates. In this stage, the insoluble blocks remain in their individual collapsed states in order to maintain equilibrium with the single chains. Above the CMC, a well-defined micelle structure with a distinct hydrophobic core is formed. Block copolymers with high hydrophobicity tend to form micelles at a low polymer concentration, exhibited as low CMCs.

A variety of structures of MTX esters with varied hydrophobicity were prepared for the study of the effect of chemical structures on the CMCs. MTX esters with different level of drug conjugation showed significant differences in their CMCs. For the conjugates with a polymeric backbone having 15 units of aspartic acid and a $C_2$ spacer for bridging drug

moieties to polymers, a higher level of MTX substitution results in a low CMC (Figure 3.15). For the conjugate with 54 % MTX, micellization starts at 0.019 mg/mL. However, the conjugates with 23 % MTX and 7.4 % MTX start to form micelles at 0.081 mg/mL and 0.19 mg/mL, respectively. Similarly, for the conjugates with 23 units of aspartic acids and a $C_2$ spacer, the onset of micellization for the conjugate with 51 % MTX substitution occurred at a lower concentration than the one with 25 % MTX (Figure 3.15, lower panel).

The effect of the length of spacer group is not obvious for the conjugates with 15 units of aspartic acid because the level of MTX conjugation is not generalized for comparison. However, the lengths of spacer groups showed a larger effect on the conjugates with 23 units of aspartic acids. Having a similar level of drug conjugation (54 % vs. 51 %), the conjugate with a $C_6$ spacer exhibited much higher hydrophobicity, observed as a low CMC (0.008 mg/mL), compared to the one with a $C_2$ spacer (0.045 mg/mL) (Figure 3.16).

A high degree of polymerization of polymer backbone (more units of aspartic acids) also increased the hydrophobicity of the polymer conjugates (Figure 3.17). With a similar level of drug conjugation and same length of spacer ($C_2$ or $C_6$), LYD044 with longer poly(aspartic acid) block (23 units of aspartic acid) showed a CMC of 0.065 mg/mL, lower than LYD043 with a shorter PHAA block (15 units of aspartic acid), whose CMC is 0.081 mg/mL (Figure 3.15). Similarly, for LYD050 and LYD051 having same length of spacer ($C_6$) and a similar level of MTX (37 % and 36 %, respectively), the CMC of LYD051, which has 23 units of aspartic acid, is 0.018 mg/mL; while the CMC of LYD050, which has 15 units of aspartic acid, is 0.027 mg/mL. The effect of the hydrophobic block on the CMC is observed in a number of systems. Usually a long hydrophobic block results in micelles with a low

Table 3.2. Critical micelle concentrations of MTX esters of PEO-*b*-PHAA

| **MTX esters of PEO-*b*-PHAA** | **spacer/PEO-b-PHAA-MTX %** | **Critical micelle Concentration (mg/mL)** |
|---|---|---|
| LYD059 | $C_2$-12-15-7.4% | 0.140 |
| LYD043 | $C_2$-12-15-23% | 0.081 |
| LYD038 | $C_2$-12-15-54% | 0.019 |
| LYD044 | $C_2$-12-23-25% | 0.065 |
| LYD045 | $C_2$-12-23-51% | 0.045 |
| LYD050 | $C_6$-12-15-37% | 0.027 |
| LYD051 | $C_6$-12-23-36% | 0.018 |
| LYD055 | $C_6$-12-23-55% | 0.008 |

CMC (34). The CMC determines thermodynamic stability of the micelles against possible dilution of the drug delivery system in the body fluids.

In summary, covalently attaching MTX to PEO-*b*-PHAA through an alkyl spacer greatly enhanced the hydrophobicity of PEO-*b*-PHAA. The resultant MTX esters with altered hydrophobic blocks revealed varied hydrophobicity. MTX esters self-assembled into spherical micelles with core/shell structure in aqueous media. The micelle preparation method is critical to achieving micelles with small size. The hydrodynamic size of the micelles was in the range of 10–200 nm, largely depending on the molecular weight of the block copolymer. The core of micelles exhibited relatively low polarity based on fluorescence measurements. The CMCs of the micelles depend upon the hydrophobicity of the micelles, and are influenced by altering the structure of the hydrophobic blocks, such as the level of MTX substitution, and lengths of alkyl spacer groups and the polymeric backbone. MTX esters of PEO-*b*-PHAA with high hydrophobicity demonstrate a low CMC, indicating good thermodynamic stability. The physical properties of the micelles of MTX esters are the basis for their applications in drug delivery.

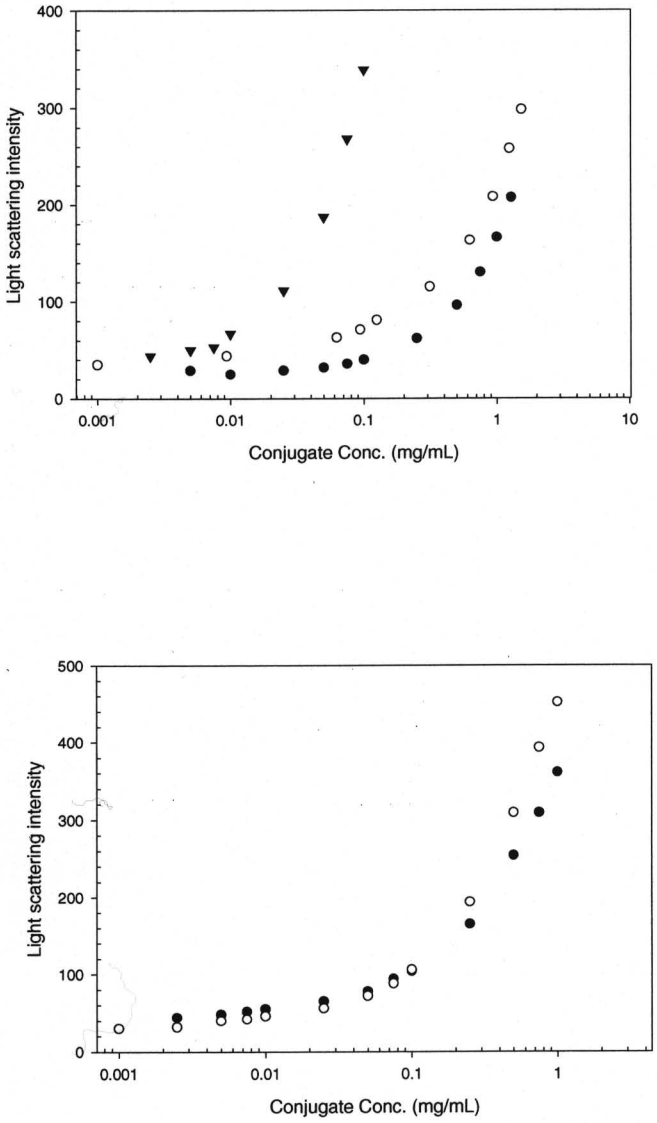


Figure 3.15. Light scattering intensity of MTX esters with varied levels of MTX substitution. The samples had same length of PHAA backbone and spacer, but different level of MTX substitution. Upper panel ($C_2$-12-15): (●) LYD059 (7.4 % MTX); (○) LYD043 (23 % MTX) (▼) LYD038 (54 % MTX); lower panel ($C_2$-12-23): (●) LYD044 (25 %); (○) LYD045 (51 % MTX).

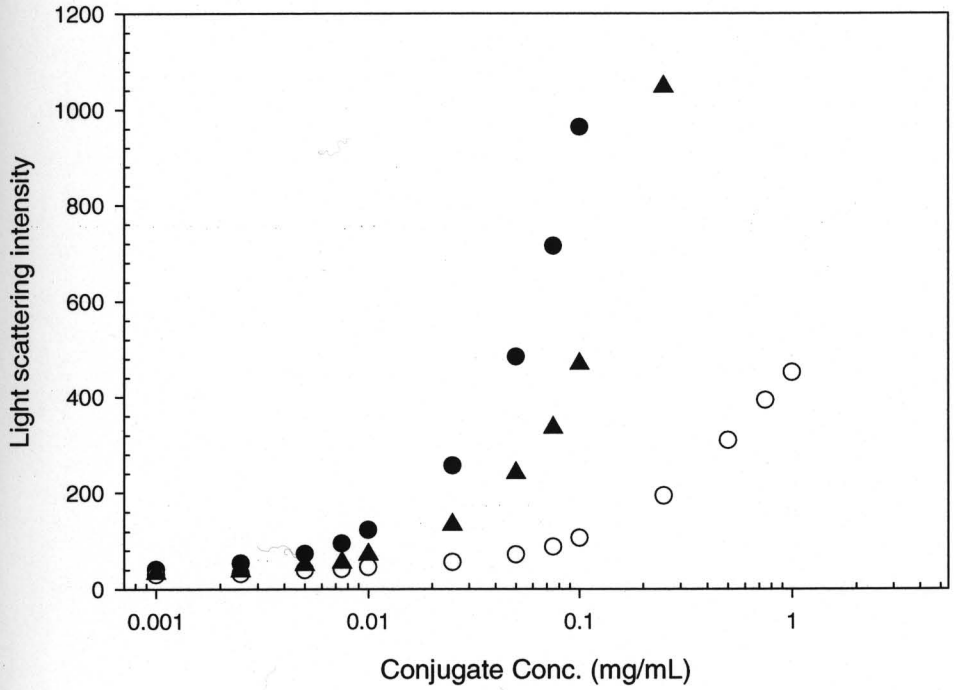


Figure 3.16. Light scattering intensity of MTX esters with varied lengths of alkyl spacer. (●) LYD055 ($C_6$-12-23-55 % MTX); (▲) LYD051 ($C_6$-12-23-36 % MTX); (○) LYD045 ($C_2$-12-23-55 % MTX).

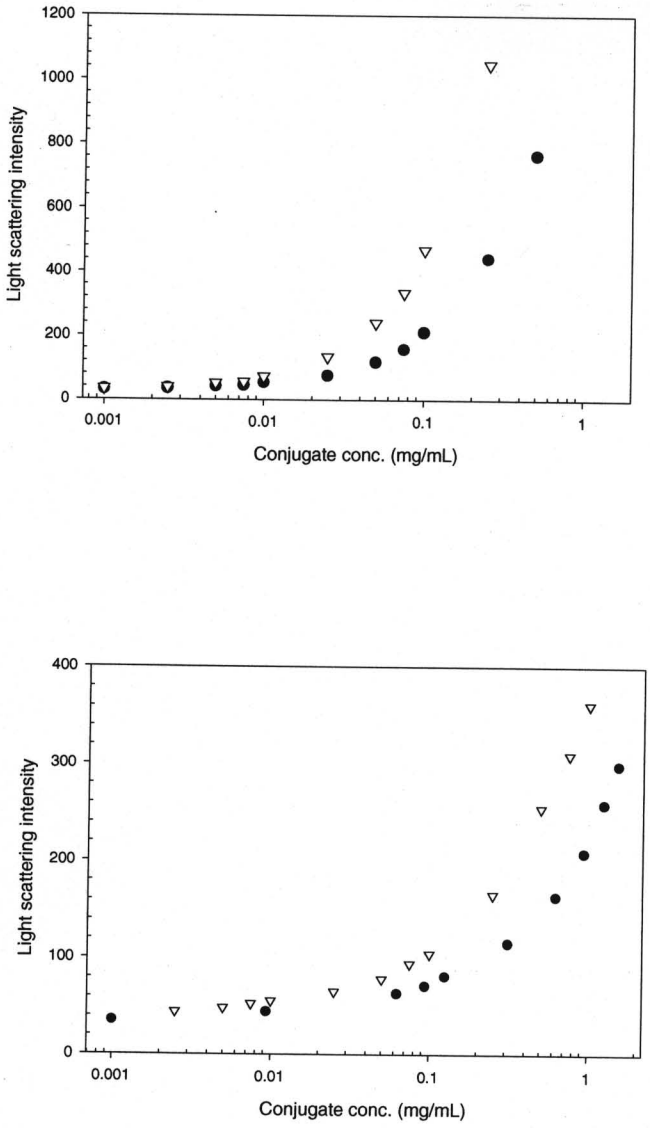


Figure 3.17. Light scattering intensity of MTX esters with varied lengths of PHAA backbone.

Upper panel: (●) LYD050 ($C_6$-12-15, 37 % MTX); (▽) LYD051 ($C_6$-12-23, 36 % MTX);

Lower panel: (●) LYD043 ($C_2$-12-15, 23 % MTX); (▽) LYD044 ($C_2$-12-23, 25 % MTX).

# CHAPTER 4.

## Structural Effects of MTX Esters of Poly(ethylene oxide)-*block*-Poly(hydroxyalkyl L-aspartamide) on Micelle Stability and Drug Release

## 4.1. Introduction

Studies on drug delivery using polymeric micelles have focused on the characterization of physicochemical properties (61) (62) (37, 54), solubilization of hydrophobic drugs (63) (64) (43), and biological activities of drug/carrier systems (12) (44). Few studies have addressed the issue of stable and reliable long-term release of active substances. The use of polymeric micelles in drug delivery has been limited by a low drug loading capacity and suboptimal drug release.

We have found that the hydrophobicity of a polymer-drug conjugate has a profound effect on the thermodynamic stability of polymeric micelles, in terms of the CMC in chapter 3. In this chapter, we discuss the effect of hydrophobicity of MTX esters of PEO-*b*-PHAA on the stability of micelles in terms of micelle dissociation and on drug release. MTX esters of PEO-*b*-PHAA with varied structures have been synthesized. We hypothesized that structural modifications on the hydrophobic block of a block copolymer conjugate by altering the degree of polymerization of PBLA, the length of spacers and the level of MTX conjugation may influence the physicochemical properties of the micelles, including their thermodynamic stability in terms of CMC, the equilibria between micelles and single polymer molecules (unimers), and the release of MTX. Accordingly, experiments were performed to study systematically the relationship between the chemical structure and the physical and functional properties of polymer-drug conjugates, MTX esters of PEO-*b*-PHAA. The results reveal that the degree of hydrophobicity of a block copolymer significantly influences micelle stability and release of MTX.

## 4.2. Experimental

### *4.2.1. In vitro release of MTX at varied pH values*

The micelles of MTX esters of PEO-*b*-PHAA were lyophilized and stored at 4°C. The lyophilized PEO-*b*-PHAA-MTX conjugate micelles ($C_2$-12-15-54 % MTX, 10 mg) were reconstituted in 0.10 M phosphate buffer, pH = 7.0 and placed in a dialysis bag (MWCO = 6,000–8,000 g/mol). The dialysis bag was equilibrated with 0.10 M phosphate buffer (100 mL) at varied pH (2.0, 5.0, 7.4 and 9.9). The released MTX diffused into the dialysis medium, and the polymeric conjugate remained in the dialysis bag. At proper time intervals, 100 μL of the release medium was sampled and replaced by an equal volume of fresh release medium. The *in vitro* release experiment was carried out at room temperature. As a control, the loss of free MTX from the dialysis bag was measured. All the samples were assayed spectrophotometrically at 304 nm using free MTX as a standard.

### *4.2.2. Micelle stability and in vitro drug release at pH 7.4*

The micelles were reconstituted by dissolving the freeze-dried conjugates in 0.10 M phosphate buffer (pH 7.4) containing 0.10 % $NaN_3$ with the aid of sonication in a water bath for 20 min. The resulting solution was filtered through a 0.45 μm nylon membrane (Fisher Scientific, Co., Pittsburgh, PA). The concentration of conjugates was calibrated by MTX content determined by UV-Vis measurement, and the conjugate concentration was in the range of 0.3-1.0 mg/mL that was above the CMC. The prepared micelle solutions were

incubated in a shaking water bath (Yamato, YB521, Japan) at 37 ± 0.5°C and mildly agitated at a rate of 100 times/min. Chromatographic analyses of the aqueous solution of MTX esters of PEO-*b*-PHAA were carried out on a Waters HPLC system consisting of a Waters 501 pump, a WISP 712 autosampler, and a 484 absorbance detector. SEC columns (Shodex® OHpak KB-805 with a KB-800P precolumn or Ultrahydrogel™ 500 GPC with a Ultrahydrogel™ Guard column, Waters, Co., Milford, MA) were used for the analysis. PBS buffer (0.10 M, pH = 7.4) was used as the mobile phase, which was degassed by sonicating the vacuum filtered solution through a 0.45 μm Millipore membrane before use. The flow rate was 1.0 mL/min for KB-805 and 0.7 mL/min for Ultrahydrogel column. The columns were calibrated with a series of molecular weight markers (Sigma, St. Louis, MO). The molecular weight of the markers was in the range of 500 to 2,000,000 g/mol (Table 4.1). The concentration of the markers was 1.0 mg/mL, and the detection wavelength was 280 nm. The calibration experiments only demonstrated that the columns were in good working condition. The molecular weight of the polymeric conjugates and micelles could not be determined because of the structural difference between the molecular weight markers. The molecular weight markers mainly are proteins with a defined molecular weight; while the polymeric molecules are characterized by the intrinsic polydispersity. The elution time of molecular weight markers was listed in Table 4.1. At predetermined time intervals, aliquots of the micelle solutions (5-30 μL, depending on the concentration) were injected to the SEC column. The eluent was detected at a wavelength of 372 nm. Each sample was assayed three times.

Table 4.1. Molecular weight markers used for column calibration

| molecular weight marker | molecular weight (g/mol) | elution time*** (min)* | elution time*** (min)** |
|---|---|---|---|
| Blue dextran | 2,000,000 | 9.28 | n.d. |
| Thyroglobulin | 669,000 | 9.47 | 12.01 |
| Apoferritin | 433,000 | 9.72 | 12.14 |
| Alcohol dehydrogenase | 150,000 | 10.16 | 14.18 |
| Bovine albumin | 66,000 | 10.20 | 14.21 |
| Carbonic anhydrase | 29,000 | 10.60 | 14.60 |

* detected by OHpak KB-805 column

** detected by Ultrahydrogel 500 GPC column

*** the average of three measurements

## 4.3. Results and discussion

### *4.3.1. Structural differences of MTX esters of PEO-b-PHAA*

The hydrophobicity of a block copolymer can be regulated by modifying the chemical structure of the polymer. To demonstrate the effect of hydrophobicity on the dissociation of polymeric micelles and on drug release, the hydrophobic block of MTX esters of PEO-*b*-PHAA has been altered to have different lengths of poly(aspartic acid) backbone and alkyl spacer, and varied levels of MTX conjugation. By fixing two of the three structural variables and varying the third, we have been able to differentiate the effect of each variable on the physicochemical properties of the conjugate micelles and the potential of the micelles for controlled drug delivery. For example, to demonstrate the effect of level of MTX substitution, polymers with same lengths of polymeric backbone and spacer group were used for the comparison. The structural properties of MTX esters of PEO-*b*-PHAA are summarized in Table 2.2 and Table 2.3.

Polymer micelles were reconstituted from the freeze-dried form for the stability and drug release studies. The dissociation of micelles and the release of MTX were analyzed by SEC-HPLC. SEC separates the molecules based on their size. In SEC, the stationary phase consists of porous beads. Therefore, molecules with larger size or higher molecular weight are excluded from the interior of the beads and thus elute at an earlier time. The smaller compounds are allowed to enter the beads and elute according to their ability to exit from the pores. Polymeric micelles are composed of the aggregated unimers; therefore, they have

higher molecular weight than unimers, and are eluted from the SEC column preceding unimers and free drugs (Table 4.2).

### *4.3.2. Effect of hydrophobicity on micelle stability*

In an aqueous solution of a chemically nondegradable block copolymer, micelles and unimers exist in equilibrium, and the concentration of each species is constant. Although the dynamic exchange between micelles and unimers may occur constantly in solution, and the rate of the exchange may vary, the concentration of unimers remains constant at the CMC (65) (66). On the contrary, MTX esters of PEO-*b*-PHAA are degradable due to the release of MTX. Therefore, the concentration of each species in the solution system of MTX esters changes over time. The gradual release of MTX from the conjugates results in structural change of the unimers in the direction of decreasing hydrophobicity, which, in turn, would decrease the stability of micelles exhibited as an increase of CMC, the concentration of unimers. In this study, micelle dissociation is referred as to as the increase of the unimer concentration as a result of decreased stability of the micelles. SEC-HPLC was used to monitor the appearance and accumulation of unimers. By monitoring the peak change of micelles and unimers, the relative stability of polymeric micelles for each MTX ester of PEO-*b*-PHAA was compared.

The level of MTX conjugation influenced the stability of conjugate micelles significantly. For the conjugates with 15 units of aspartic acid and a two-carbon spacer, the micelles of the conjugate with a low level of MTX substitution showed low stability. The micelle peak for LYD059 with 7.4 % MTX was not detected in SEC-HPLC under the

Table 4.2. Elution time of the MTX esters of PEO-*b*-PHAA (SEC column, KB805)

| MTX esters | spacer/ PEO-*b*-PHAA | molecular weight (g/mol) | elution time* (min, micelle) |
|---|---|---|---|
| LYD059 | $C_2$/12-15 | 15100 | n.d. |
| LYD043 | $C_2$/12-15 | 16000 | 9.12 |
| LYD038 | $C_2$/12-15 | 18100 | 8.69 |
| LYD044 | $C_2$/12-23 | 18400 | 9.09 |
| LYD045 | $C_2$/12-23 | 21100 | 8.85 |
| LYD050 | $C_6$/12-15 | 17800 | 8.41 |
| LYD051 | $C_6$/12-23 | 19200 | 8.38 |
| LYD055 | $C_6$/12-23 | 22900 | 8.10 |

* the average of three measurements by OHpak KB0805 column.

experimental conditions (Figure 4.1). Only the unimer peak was observed at day 0 at a retention time of 10.34 min. After 26 days, besides the unimer peak, the released MTX peak also appeared at about 13 min. The peak at about 11 min might be due to the partially degraded conjugate. The injection of the micelles into SEC column resulted in instant dilution by the mobile phase. The conjugate has a relatively high CMC (0.14 mg/mL), indicating poor tolerance upon dilution; therefore, micelle peak was not detectable, and only a unimer peak was observed.

On the other hand, LYD043, which had 23 % MTX, showed a major micelle peak at 9.12 min and a shoulder unimer peak at 10.27 min on day 1 (Figure 4.2). Accompanying the decrease of the micelle peak, the unimer peak increased significantly over time. After 4 days, the unimer peak prevailed in the conjugate solution. After 8 days, unimers became dominant, and the micelle peak became much lower. The micelle was not detectable after 12 days. In addition, the peak of released MTX appeared at about 13 min.

For LYD038 with 54 % MTX, only micelles were detected in HPLC at day 0, and the elution time of micelles was 8.69 min. At day 4 a small shoulder peak due to unimers appeared. The elution time of unimers was 10.17 min. Although the unimer peak was getting bigger over time, associated conjugate concentration was still much higher than unimer concentration after 26 days, which means that the conjugate molecules mainly existed in micelle form (Figure 4.3).

The changes of micelle and unimer in the solution were clearly depicted in Figure 4.4 for LYD043 and LYD038. After 20 days, approximately 80 % of LYD038 molecules were still in micelle form; however, almost all LYD043 conjugates appeared in unimers in HPLC

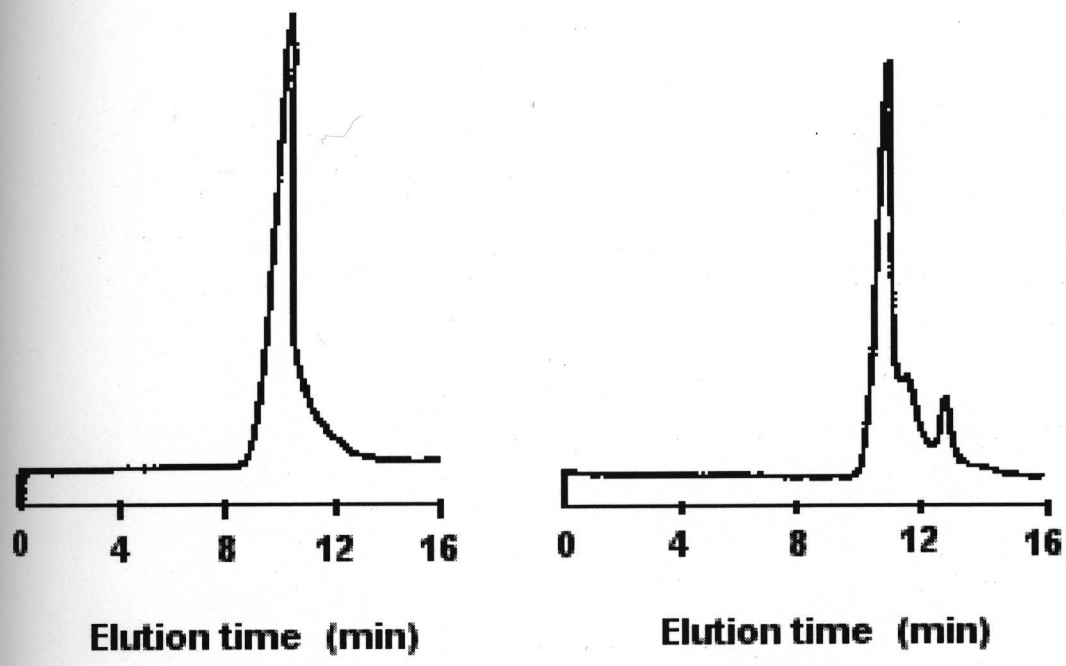


(a) (b)

Figure 4.1. SEC chromatograms of LYD059 ($C_2$-12-15-7.4 % MTX). (a) day 0; (b) day 26). OHpak KB-805 column was used. Unimer peak eluted at 10.344 min; micelle peak is not detected.

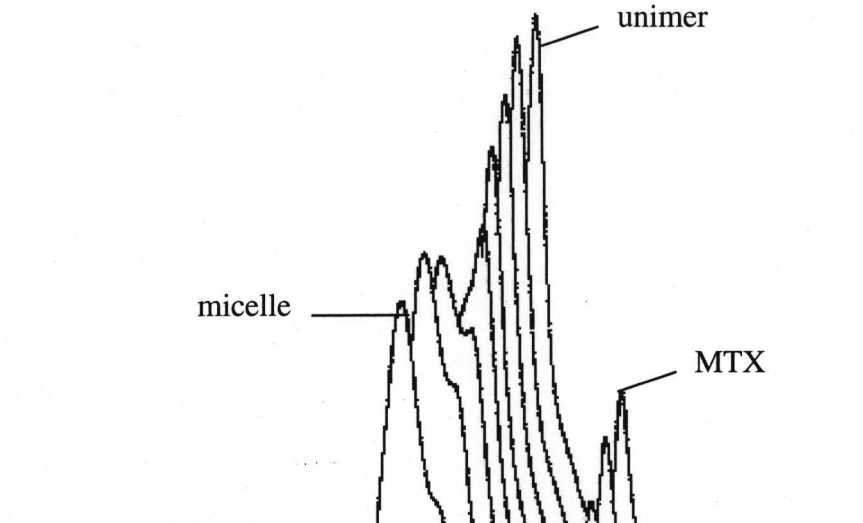


Figure 4.2. SEC chromatograms of LYD043 ($C_2$-12-15-23 % MTX). OHpak KB-805 column was used. Micelle peak eluted at 9.12 min, and unimer peak eluted at 10.27 min.

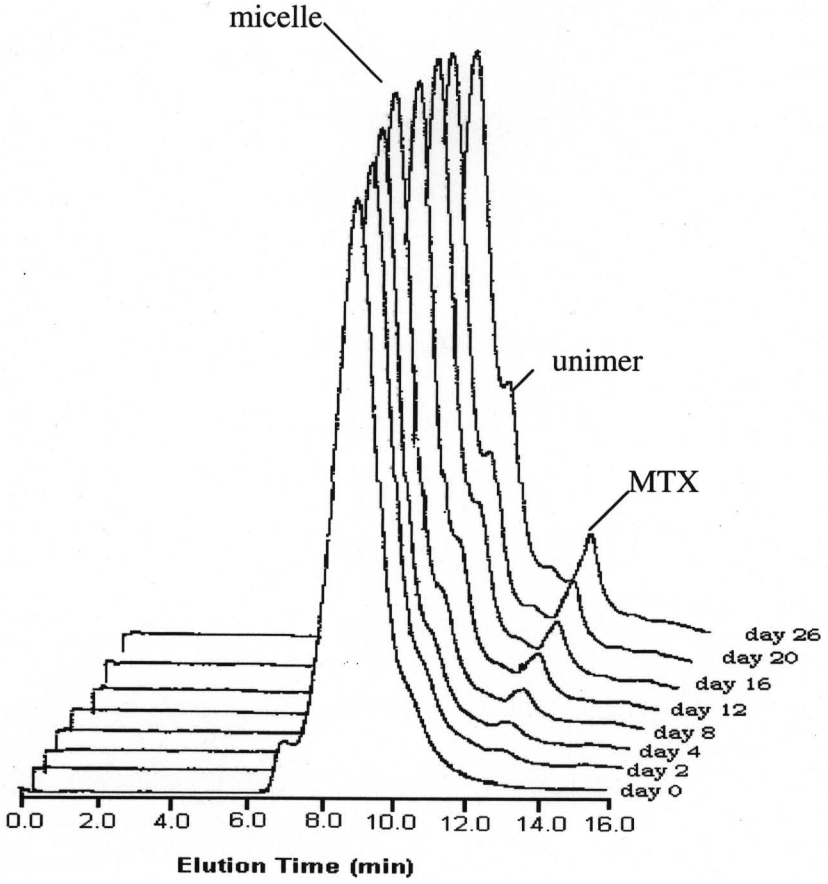


Figure 4.3. SEC chromatograms of LYD038 ($C_2$-12-15-54 % MTX). OHpak KB-805 column was used. Micelle peak eluted at 8.69 min, and unimer peak eluted at 10.17 min.

chromatogram. Accordingly, the unimer peak of LYD038 increased slowly and steadily compared to LYD043, whose unimer peak increased rapidly, reached the maximum on day 12, then decreased gradually (Figure 4.4).

Consistent results were obtained for the conjugates LYD044 and LYD045 which had 23 units of aspartic acid and a $C_2$ spacer. LYD045 had 51 % MTX substitution, while LYD044 had 25 % MTX. Micelles of LYD045 appeared more stable than LYD044 (Figure 4.5). Although both conjugates revealed a significant decrease in the micelle peak and increase in the unimer peak, micelles of LYD044, which has a lower level of MTX conjugation, tend to dissociate more easily than LYD045

These results clearly demonstrated the effect of MTX substitution. A higher degree of drug conjugation enhances the hydrophobicity of block copolymer; therefore, the micelles are more stable in terms of dissociation. It should be pointed out that the results from SEC-HPLC do not reflect the real equilibria concentration of each species. However, the results are still valid in the demonstration of the time course of polymeric micelles and unimers.

The spacer effect on micelle dissociation is more significant than the effect of degree of drug conjugation. The conjugates with a $C_6$ spacer displayed remarkable stability. Regardless of the level of drug conjugation and the length of PHAA block, micelle dissociation was not observed for the conjugates with a $C_6$ spacer during the period of the experiment (26 days) (Figure 4.6). Only micelle and drug peaks appeared on the HPLC chromatograms. In contrast, polymeric micelles from the conjugates with a $C_2$ spacer dissociated more rapidly. For instance, after 26 days, only about 5 % LYD045 was in micelle form, while the micelle peak of LYD051 remained unchanged (Figure 4.7). Similarly, LYD038 with a $C_2$ spacer, exhibited slow but noticeable micelle dissociation and an increase

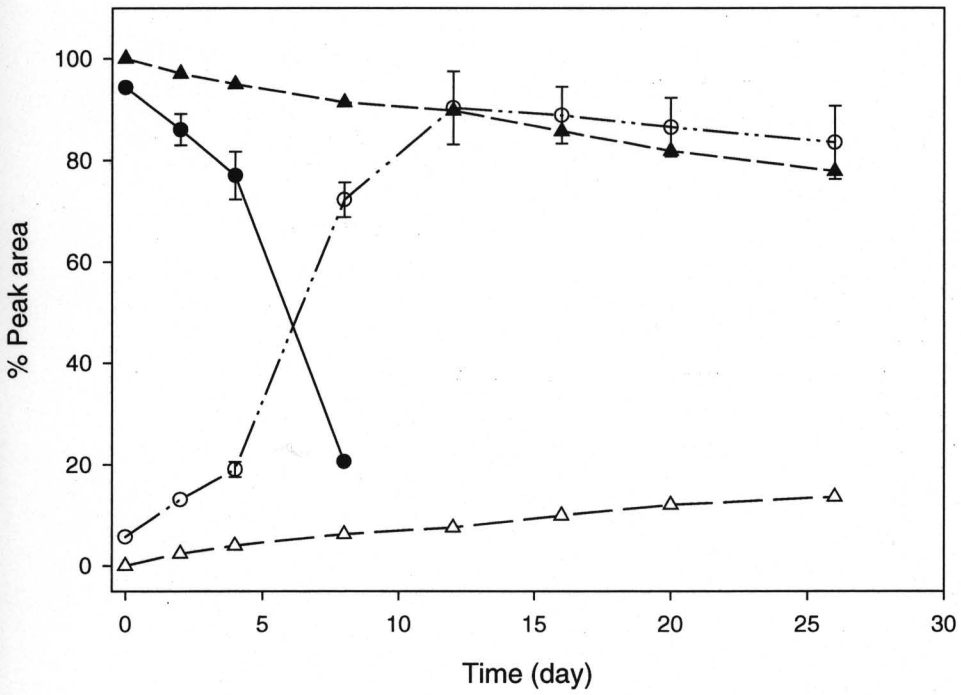


Figure 4.4. Effect of the level of MTX substitution on micelle dissociation ($C_2$-12-15). −●− micelle of LYD043($C_2$-12-15-23 % MTX); −▲− micelle of LYD038 ($C_2$-12-15-54 % MTX; -○- unimer of LYD043; −△− unimer of LYD038; Ultrahydrogel™ 500 GPC column; pH 7.4.

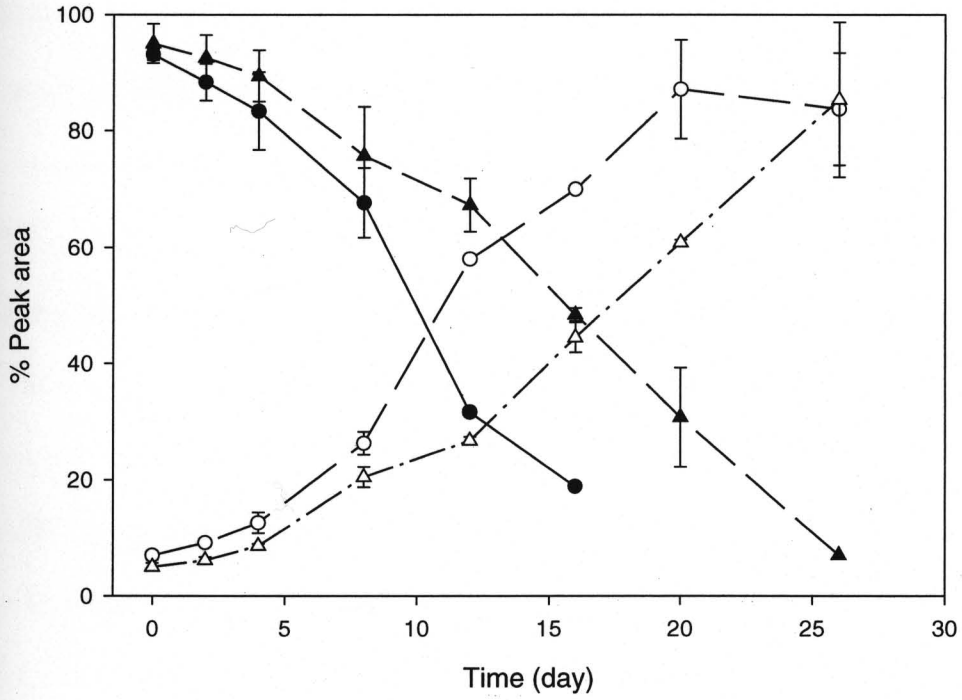


Figure 4.5. Effect of the level of MTX substitution on micelle dissociation ($C_2$-12-23). −●− Micelle of LYD044 ($C_2$-12-23-25 % MTX); −▲− micelle of LYD045 ($C_2$-12-23-51 % MTX; -o- unimer of LYD044; −Δ− unimer of LYD045; HPLC detection; pH 7.4.

of unimers; micelle dissociation of LYD050, which had a $C_6$ spacer, was negligible after 26 days (Figure 4.8)

The effect of the length of the PHAA block was not significant for the MTX esters with a $C_2$ spacer and ~ 25 % drug substitution (data not shown). However, for the conjugates with ~ 50 % of MTX substitution, LYD038, which had a shorter PHAA block (15 units of aspartic acid) demonstrated higher stability than LYD045, which had a PHAA block with 23 units of aspartic acid. After 26 days, about 85 % of LYD038 conjugate remained in micelle form, while only about 5 % of LYD045 were still in micelle form (Figure 4.9). Accordingly, LYD045 unimers increased more rapidly than LYD038. After 26 days, approximately 85 % of LYD045 conjugate was observed as unimers, while only about 10 % of LYD038 conjugates existed as unimers in the system.

Although the equilibrium between unimers and micelles in the conjugate system was complicated by the loss of hydrophobicity of the unimers due to the structural change caused by drug release, the change in micelle stability correlated nicely with the chemical structure of the conjugates. Adjusting the hydrophobicity of the drug polymer conjugates had a profound influence on the stability of the conjugate micelles in terms of their dissociation.

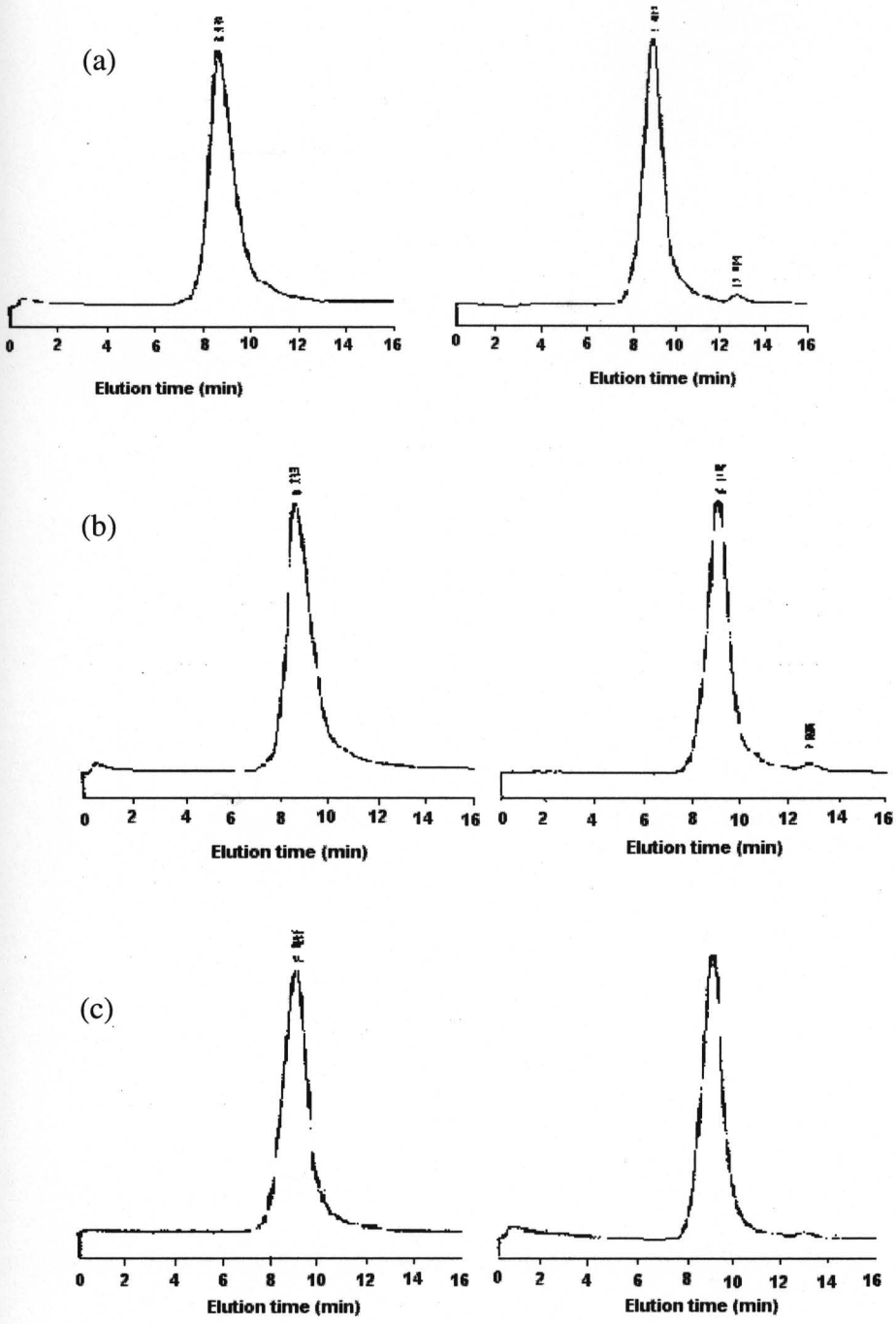


Figure 4. 6. SEC chromatograms of MTX esters of PEO-*b*-PHAA with $C_6$ spacer; LYD050 ($C_6$-12-15-37 % MTX); (b) LYD051 ($C_6$-12-23-36 % MTX); (c) LYD055 ($C_6$-12-23-55 % MTX). Left, day 0; right, day 26.

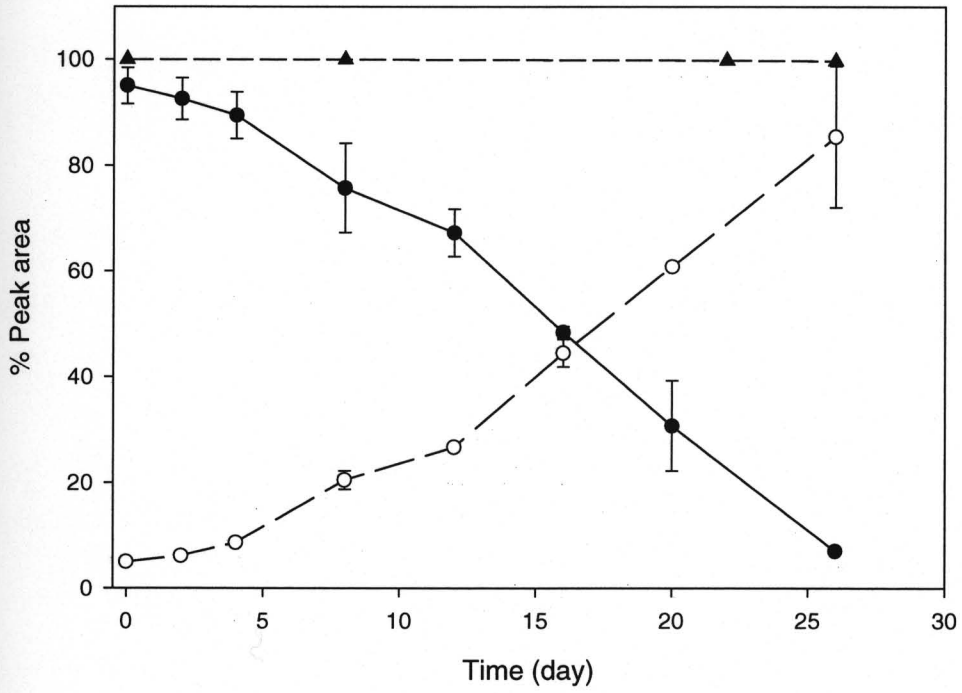


Figure 4.7. Effect of the length of alkyl spacer on micelle dissociation ($C_x$-12-23). -●-Micelle of LYD045 ($C_2$-12-23-51 % MTX); -▲- micelle of LYD055 ($C_6$-12-23-55 % MTX; -○- unimer of LYD045; unimer of LYD055 could not be detected; HPLC detection; pH 7.4.

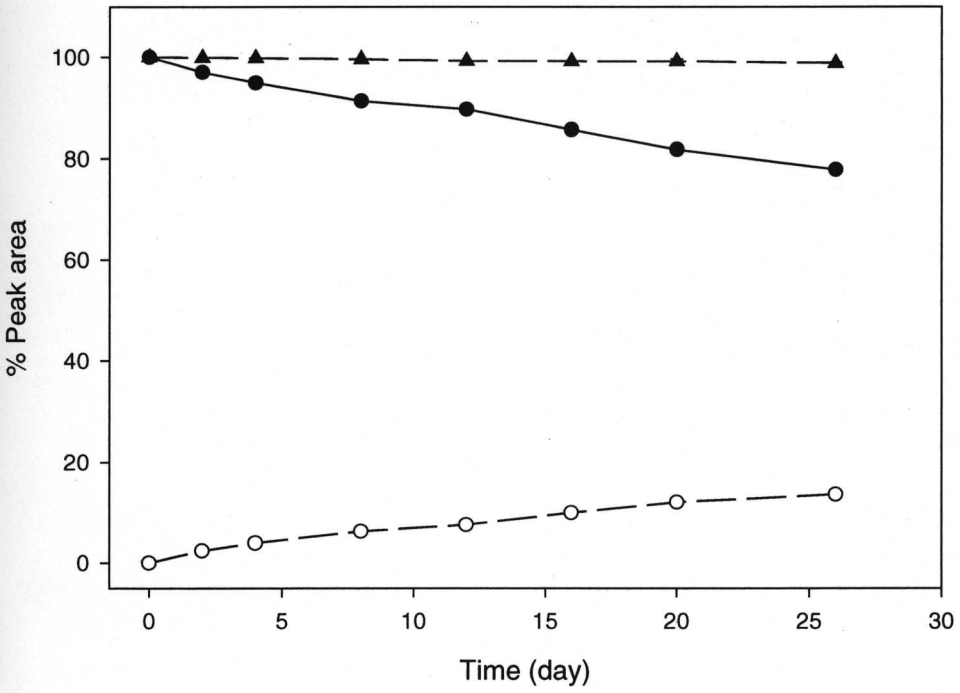


Figure 4.8. Effect of the length of alkyl spacer on micelle dissociation ($C_x$-12-15). −●− Micelle of LYD038 ($C_2$-12-15-54 % MTX); −▲− micelle of LYD050 ($C_6$-12-15-36 % MTX); −○− unimer of LYD038; unimer of LYD050 could not be detected; HPLC detection; pH 7.4.

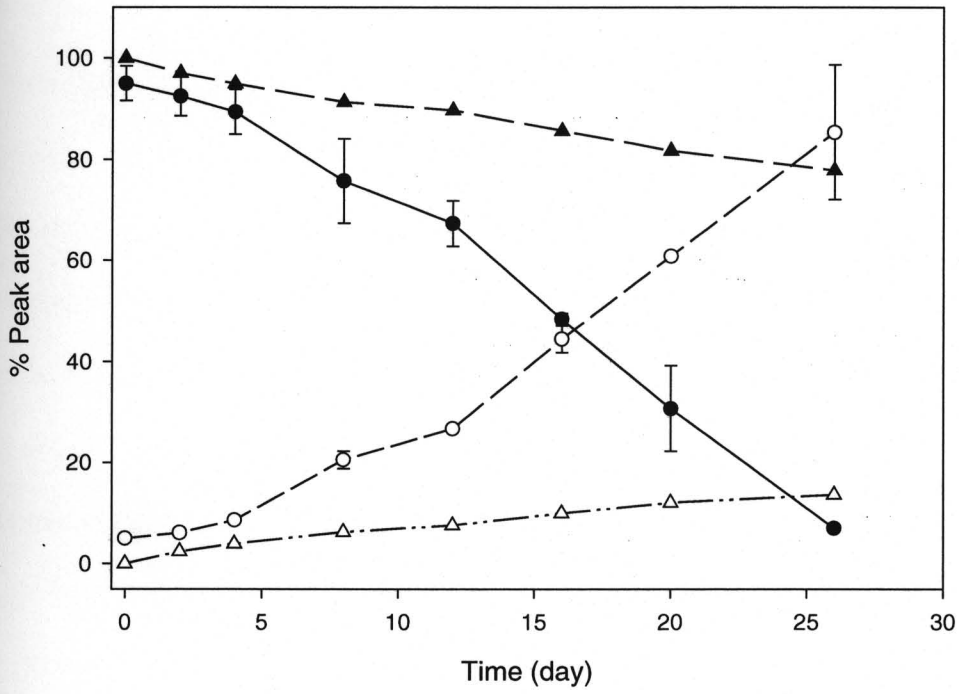


Figure 4.9. Effect of the length of PHAA block on micelle dissociation. −●− micelle of LYD038 ($C_2$-12-15-54 % MTX); −▲− micelle of LYD045 ($C_2$-12-23-51 % MTX; −○− unimer of LYD038; −△− unimer of LYD045; HPLC detection; pH 7.4.

### *4.3.3. Effect of pH on the release of MTX*

The *in vitro* release of MTX from the self-assembled MTX ester of PEO-*b*-PHAA ($C_2$-12-15-54 % MTX) at various pH values was carried out using the dialysis method, in which a micellar solution was equilibrated in a dialysis membrane. The molecular weight cut-off of the membrane is much higher than that of the molecular weight of the drug, but lower than that of the polymeric drug-carrier. The release of MTX was followed by absorption spectroscopy. The UV spectrum of MTX displayed three major bands at 265 nm, 304 nm, and 374 nm (Figure 4.11). These were the characteristic absorption bands of free MTX at the initial level of drug used for this study. As the release of MTX occurred, the absorption bands of MTX sampled from the medium increased in intensity. The *in vitro* release of MTX from self-assembled PEO-*b*-PHAA-MTX conjugate was slowest at pH = 5 and somewhat faster at pH = 2.2 and 7 (less than 20% released drug over 260 h). There was a greater level and a slightly higher rate of release of MTX in the presence of sodium dodecyl sulfate (SDS). At pH = 10, release of MTX was rapid and almost complete in 48 h. Lastly, there was a rapid loss of free MTX from the dialysis bag.

A micelle-like structure of PEO-*b*-PHAA-MTX conjugate was able to release MTX for a long duration (Fig. 4.10) at physiological pH. This reflects unfavorable ester hydrolysis in the nonpolar core of a micelle-like structure. MTX residues may be coiled or packed together in a core, making little contact with water. However, the mechanism for drug release is not clear so far. The presence of SDS slightly enhanced MTX release (Figure 4.10). The physical interaction of SDS is known to disrupt the supramolecular core/shell structure of a polymeric micelle. This leads to a slightly faster release of MTX from a PEO-*b*-PHAA-MTX

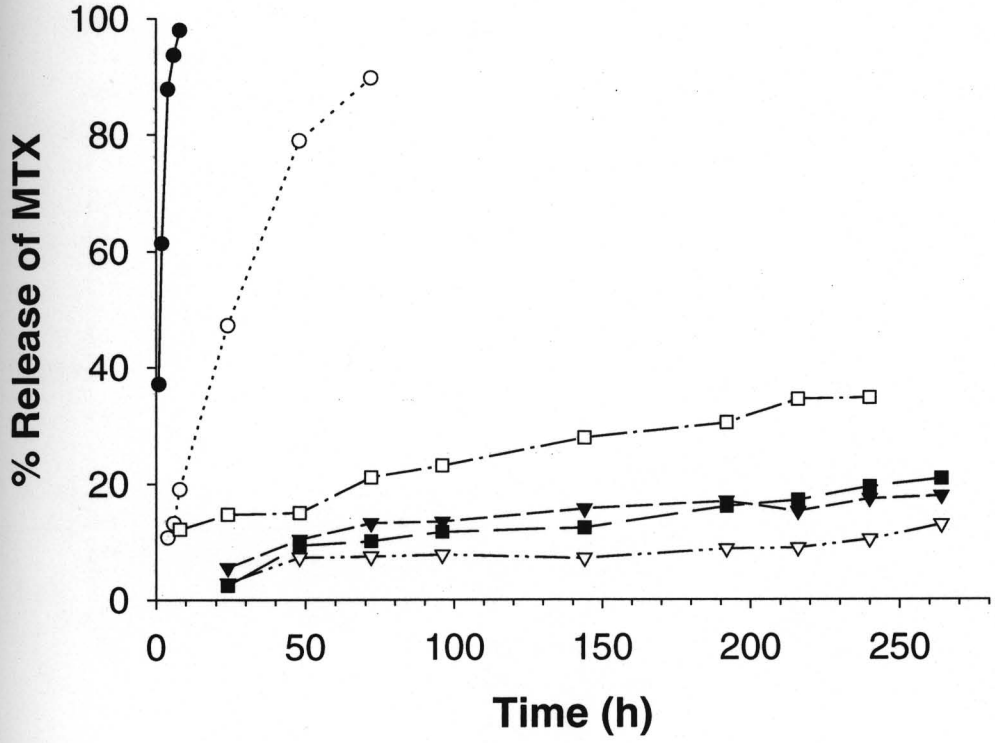


Figure 4.10. MTX release at various pH values by dialysis method (LYD038 ($C_2$-12-15-54 % MTX)). –●– free MTX as control; –o– pH 9.9; –■– pH 7; –▽– pH 5; –▼– pH 2.2; and –□– pH 7 and in presence of SDS.

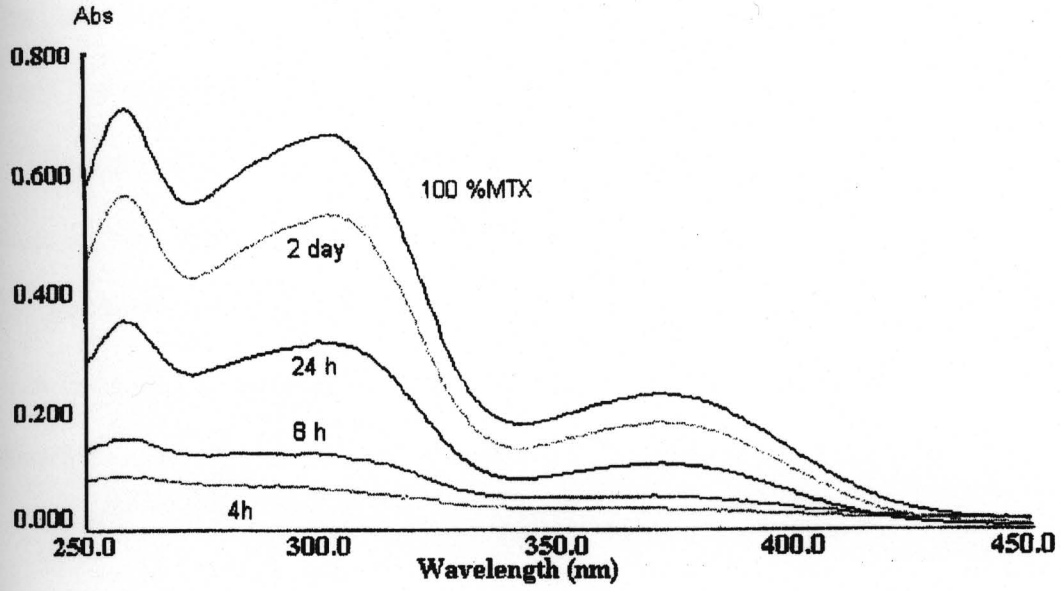


Figure 4.11. Absorption spectra of MTX during the release of MTX from LYD038 ($C_2$-12-15-54 % MTX) at pH 10.

conjugate, perhaps as a result of inducing the shift of equilibrium to the unimer side, or perhaps reflecting more exposure to water in a supramolecular structure with SDS.

The results can be compared to soluble polymer-drug conjugates, where an ester linkage has a $t_{1/2}$ of drug release on the order of 100 h (52). A dextran-MTX conjugate has a drug release half-life of 3 days when MTX is attached to dextran by an ester bond. In contrast, less than 20 % of MTX was released from a dextran-MTX conjugate after 6 days when MTX was attached to dextran by an amide bond.

Several factors govern the hydrolysis of ester bonds, such as chemical structure of the substrate, local environment of the ester bond and pH. The release of MTX was rapid at alkaline pH due to base-catalyzed ester hydrolysis and perhaps an alteration in micelle structure, owing to the ionization of the carboxyl group of MTX. Under neutral or acidic pH, less than 15% of MTX was released after 10 days. The slowest release of MTX occured at pH = 5 for a micelle-like structure of PEO-*b*-PHAA-MTX conjugate. At pH 2.2, release of MTX from a micelle-like structure of PEO-*b*-PHAA-MTX conjugate was similar to the profile at pH = 7. Dextran-drug conjugates exhibit the most rapid ester hydrolysis at elevated pH and maximum stability at ca. 5.0 (67). Acid-catalyzed hydrolysis of ester bonds also occurs at low pH, but at a rate slower than that which occurs at alkaline pH.

### *4.3.4. The effect of hydrophobicity on the release of MTX at pH 7.4*

The release of MTX from its esters of PEO-*b*-PHAA was monitored by SEC-HPLC under physiological pH 7.4. Concentrations of the conjugates for the release study were above their CMCs. The peak of free MTX appeared at about 13 min using an OHpak KB-805

column. The elution time for micelle and unimer peaks was about 9 min and 10 min, respectively. All conjugates showed remarkable stability in terms of *in vitro* drug release as a result of inter- or intramolecular self-association of the conjugate molecules. However, the rate of drug release was influenced by the hydrophobicity of the conjugates, which was closely related to the stability of the micelles in terms of dissociation.

Relatively unstable micelles released drug more freely (Figure 4.12). For the conjugates with PHAA of 15 units of aspartic acid and a $C_2$ spacer, a varied level of MTX substitution made a significant difference in drug release. After 10 days, 14 % MTX was released from LYD059 that had 7.4 % MTX substitution, while only 7 % of the drug was released from LYD043 that had 23 % MTX substitution and 3 % of the MTX from LYD038 that had 54 % substitution over the same time period.

Similarly, both LYD045 and LYD044 had PHAA of 23 aspartic acid and $C_2$ spacer. However, LYD045, with 51 % MTX, released MTX more slowly than LYD044, which had 25 % of MTX substitution (Figure 4.13). After 26 days, 18 % of MTX was released for LYD044, while 9 % of MTX released for LYD045.

The effect of the length of spacers is more significant. The release of MTX is much faster for the MTX esters that have a $C_2$ spacer than the ones that have a $C_6$ spacer. Approximately 9 % MTX was released after 26 days for LYD045, which has a $C_2$ spacer (Figure 4. 14). However, only less than 1 % of MTX was released from the conjugate with a $C_6$ spacer (LYD055) in the same period of time. Likewise, LYD038 had a $C_2$ spacer and released about 8 % MTX after 26 day, while LYD050 with a $C_6$ spacer liberated about 1% MTX (Figure 4.15). These results demonstrated that a long alkyl spacer significantly increased the hydrophobicity of the conjugates and resulted in slow drug release.

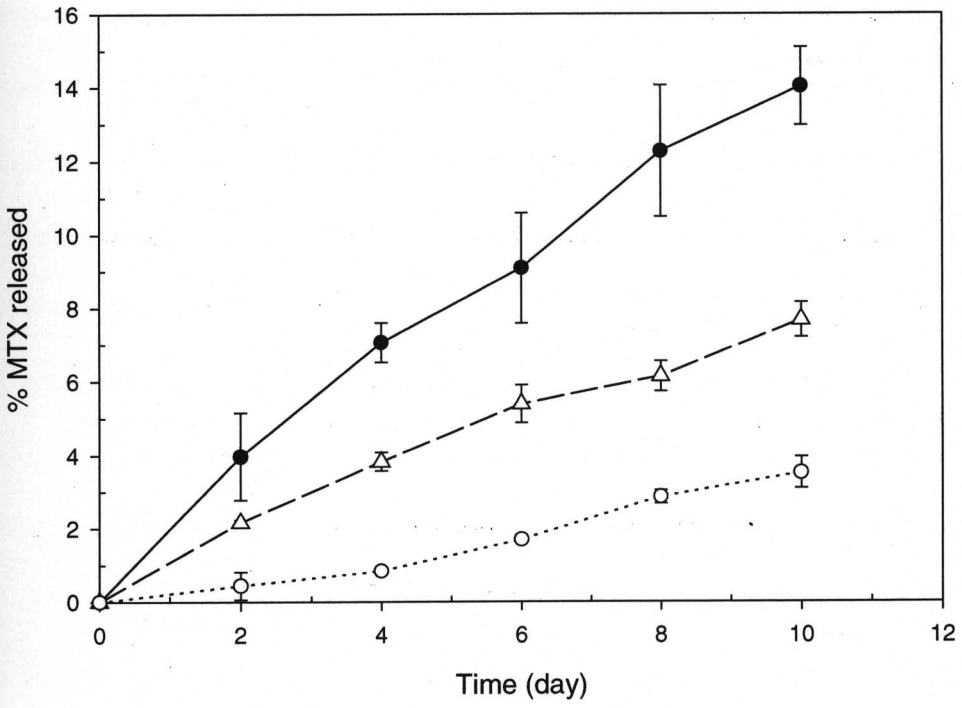


Figure 4.12. Effect of the level of MTX substitution on the release of MTX ($C_2$-12-15).

–•–LYD059 ($C_2$-12-15-7.4 % MTX); –▵– LYD043 ($C_2$-12-15-23 % MTX); –o– LYD038 ($C_2$-12-15-54 % MTX); HPLC detection; pH 7.4.

The length of PHAA block revealed a moderate effect on drug release. The effect was more significant for the conjugates with a higher degree of drug conjugation. With comparable level of MTX conjugation and the same length of spacer group, conjugate LYD038, which had 15 units of aspartic acid, was slightly more stable than LYD045, which had 23 units of aspartic acid. After 26 days, about 9.5 % MTX was released from LYD045, while about 8.5 % MTX was released from LYD038. Therefore, conjugates with a longer PHAA backbone seemed to release MTX faster. However, the effect was not as significant as the effect of spacer and drug level (Figure 4.16).

The release of MTX from MTX esters of PEO-*b*-PHAA occurred over several weeks. For MTX esters of PEO-*b*-PHAA, the hydrolyzable ester bonds were placed in a hydrophobic environment, the core of the micelles. Therefore, the drug is likely released through the hydrolysis of the unimers. As illustrated in Figure 4.17, at or above the CMC, micelles and unimers are in equilibrium, and the micellar form of the conjugate is available for circulation in biological systems. However, the release of the drug is more likely influenced by to the concentration of unimers. Adjustments of the equilibrium may be key to obtain a desired drug-release profile. Balancing the association and dissociation of the polymer micelles could be achieved via the modulation of the structure of MTX conjugates, particularly by adjusting the hydrophobicity of block copolymers. To achieve prolonged circulation of drug-polymer conjugates in blood, we can increase the level of MTX conjugation or use a long alkyl spacer. Consequently, the micelle-unimer equilibrium shifted to the micelle side. Lastly, as the release of MTX gradually occurred, polymeric micelles increasingly dissociated into unimers during elution in SEC-HPLC. The block copolymer

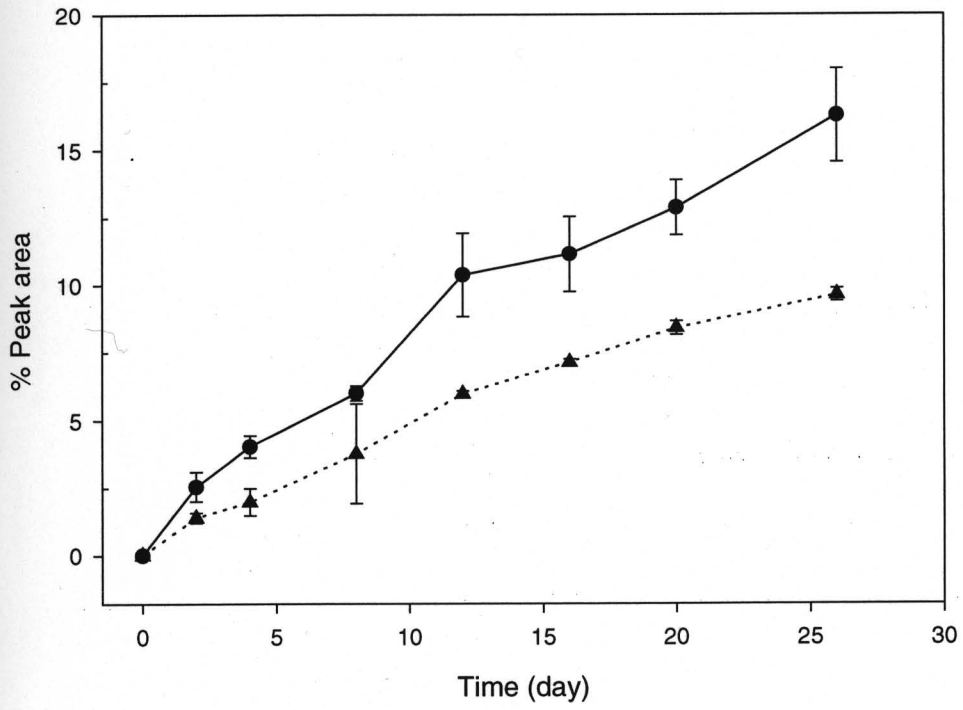


Figure 4.13. Effect of the level of MTX substitution on the release of MTX ($C_2$-12-23). −●− LYD044 ($C_2$-12-23-25 % MTX); −▲− LYD045 ($C_2$-12-23-51 % MTX).

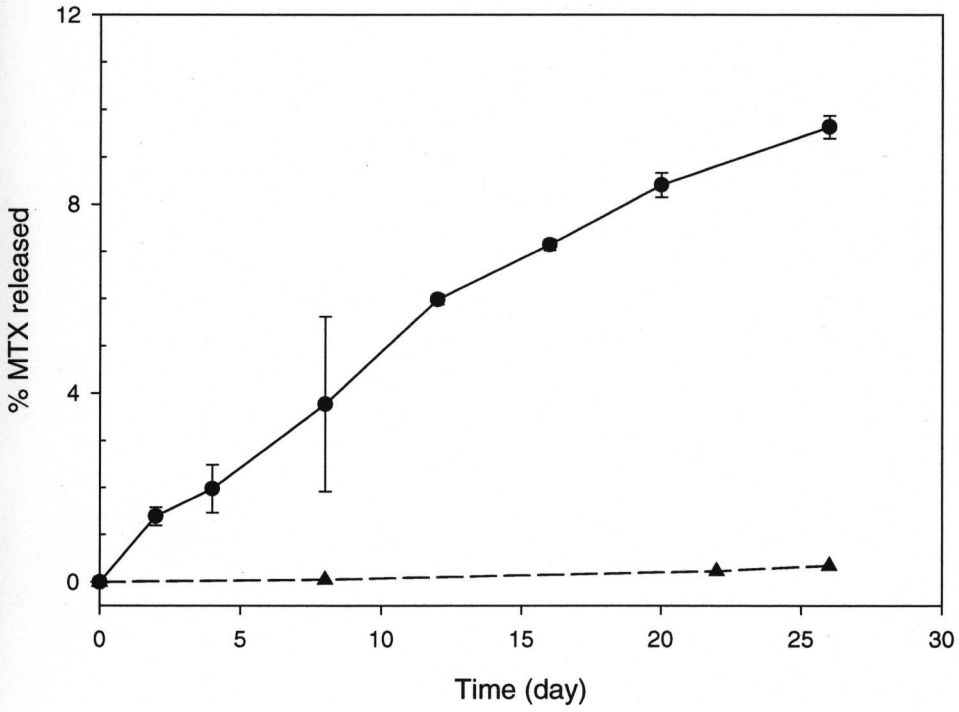


Figure 4.14. Effect of the length of spacer on the release of MTX ($C_x$-12-23). −●− LYD045 ($C_2$-12-23-51 % MTX); −▲− LYD055 ($C_6$-12-23-55 % MTX).

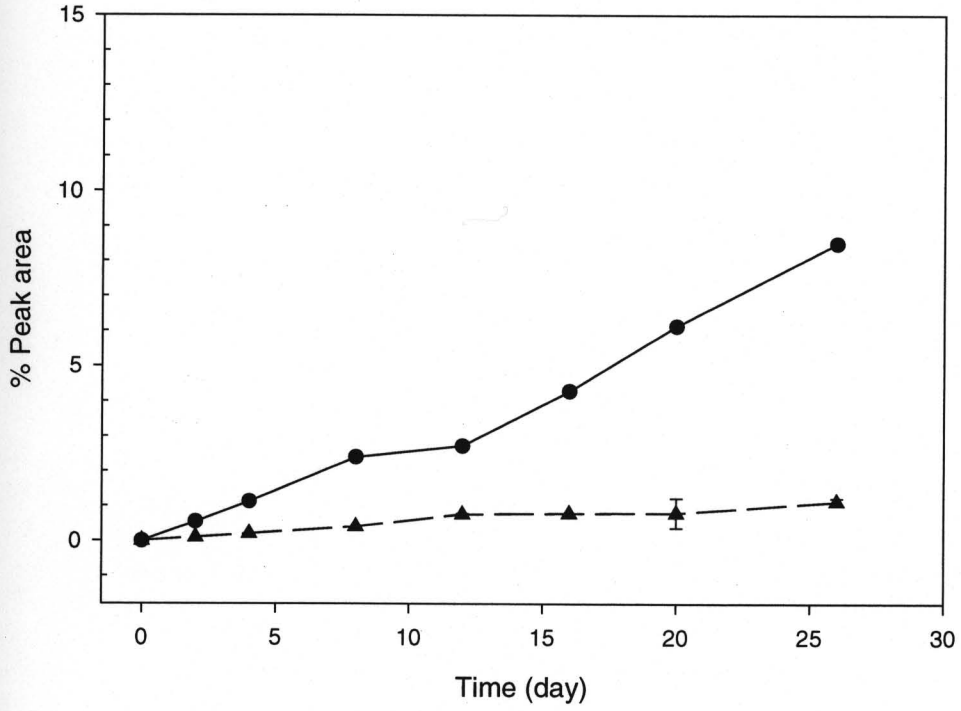


Figure 4.15. Effect of the length of spacer on the release of MTX ($C_x$-12-15). −●− LYD038 ($C_2$-12-15-54 % MTX); −▲− LYD050 ($C_6$-12-15-37 % MTX).

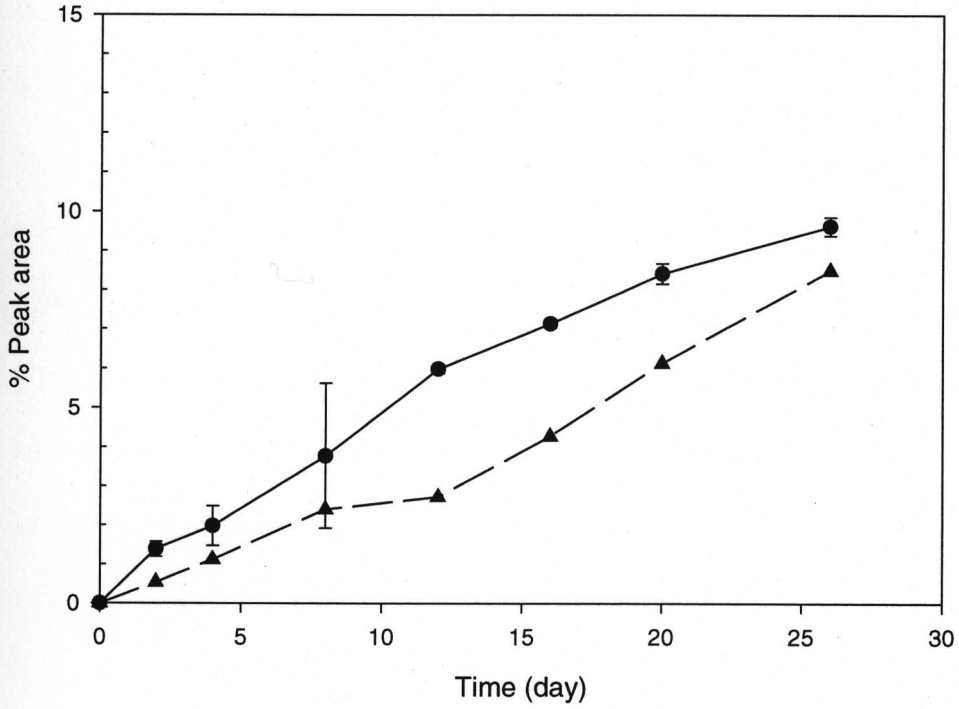


Figure 4.16. Effect of the length of PLAA block on the release of MTX. –●– LYD045 ($C_2$-12-23-51 % MTX); –▲– LYD038 ($C_2$-12-15-54 % MTX).

became less hydrophobic, which caused continuous dissociation of polymeric micelles into unimers, and drug release might be enhanced. However, under non-equilibrium conditions, such as in vascular systems, the release of MTX would be less affected by the equilibrium between the unimers and micelles.

On the other hand, drug release may also occur at the core/shell interface, where there is more likelihood of water being present than in the core. Thus, ester hydrolysis of MTX may gradually occur over time until the micelle-like structure breaks apart, exposing the ester linkage to water and perhaps to faster hydrolysis and release of MTX. Moreover, less stable micelles may contain more water molecules in the core than stable micelles; therefore, hydrolysis may partially occur and be more favorable for less stable micelles.

Drug release data have many potential applications. They can be used to try to understand the physicochemical structure of the delivery system and the release mechanism. Such data can also be used to predict the likely behavior of the system *in vivo*. This is a much more complex issue, which involves a knowledge of the interaction of many biological components with the carrier system. Consequentially this area is poorly understood at present.

In conclusion, MTX esters of PEO-*b*-PHAA can slowly release MTX under physiological conditions due to the hydrolyzable nature of ester bond. At elevated pH, the conjugates release MTX rapidly. The MTX esters can be structurally modulated by varying the level of MTX substitution, the length of spacer, and the length of PHAA block, which in turn modifies the hydrophobicity of the block copolymer conjugate. A higher percentage of MTX attachment and longer alkyl spacer resulted in slower dissociation and drug release.

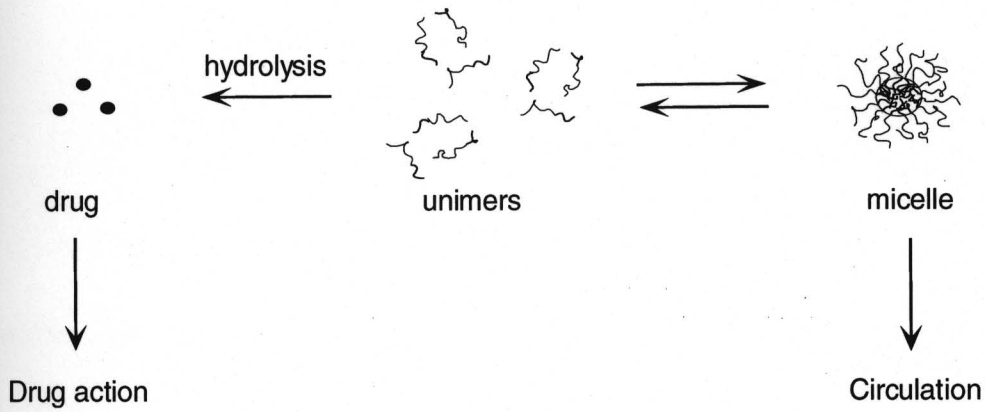


Figure 4.17. Speculated relationship between micelles and unimers and drug release.

# CHAPTER 5.

# Studies on the Biological Activities of MTX Esters of PEO-*b*-PHAA

## 5.1. Introduction

Many anticancer drugs are low molecular weight cytotoxic agents that exert their antitumor activity by interfering in one way or another with cell growth or multiplication. Because of the close similarity between cancer cells and normal cells, almost all currently available cytotoxic drugs are non-selective in their action. In therapeutic doses, they produce toxic side effects especially on rapidly dividing cells such as skin and bone marrow.

The conjugation of MTX to a polymer may yield a macromolecular derivative retaining many of the properties of this large molecule. Therefore, it is expected to circulate in blood over a long period of time. A constant high level of MTX, which could be therapeutically beneficial in the treatment of diseases, can be achieved by the slow hydrolysis of prodrugs.

We have prepared a series of micelle-forming MTX esters of PEO-*b*-PHAA and studied the physicochemical properties of these compounds. These esters are highly stable in aqueous media, and the release of MTX via hydrolysis is very slow. However, there is little known about how the hydrolyzable polymeric conjugates act in biological systems. The exploration of the biological aspects of the conjugates is thus necessary. We hypothesized that MTX esters of PEO-*b*-PHAA might exhibit anticancer activity in a similar manner as MTX. However, the conjugation of MTX to a polymeric carrier might alter the cellular uptake pathway of MTX from receptor-mediated endocytosis to a non-receptor mediated endocytotic pathway. Accordingly, we evaluated the inhibitory activity of a MTX ester on dihydrofolate reductase (DHFR), an enzyme that MTX acts on, and the cytotoxicity of three MTX esters of PEO-*b*-PHAA, which have a varied level of drug substitution, against a

murine leukemia cell line L1210. This cell line has been widely used for the screening of anticancer drugs including MTX. A tetrazolium colorimetric assay was used for the evaluation of cell viability. Furthermore, we tested the cytotoxicity of an ester in the presence of folate, which could competitively bind to the folate receptors used by MTX for cell entry. The folate may decrease the cytotoxicity of MTX as a result of reduced transport. However, it may not influence the activity of polymeric MTX esters, which may employ an altered cellular uptake pathway that is a non-receptor-mediated endocytotic pathway.

## 5.2. Experimental

### *5.2.1 Materials*

MTX, bovine liver DHFR, the tetrazolium compound (2,3-bis(2-methoxy-4-nitro-5-sulphonyl)-5-[(phenylamino)carbonyl]-2H-tetrazolium hydroxide; XTT), phenazine methosulfate (PMS), and dihydrofolic acid were purchased from Sigma (St. Louis, MO). Folic acid was purchased from Aldrich (Milwaukee, WI). Three MTX esters of PEO-*b*-PHAA used in the study were prepared as described in chapter 1. The structural properties of the conjugates and MTX are summarized in Table 2.2. The MTX conjugates were stored in the freeze-dried state at 4°C. L1012, a murine leukemia cell line, was obtained from the American Tissue Culture Collection, Rockville, MD. Horse serum and Dulbecco's Modified Eagle's medium (DMEM) containing 5.5 g/L glucose and 2 % glutamine were purchased from Gibco, Grand Island, NY. Cell culture plates (96 wells) were purchased from Fisher

Scientific, PA. The inhibitory activity of MTX and its ester of PEO-*b*-PHAA on DHFR was assayed by UV-Vis spectrophotometer (Pharmacia 4000).

### *5.2.2. DHFR inhibition assay*

MTX or freeze-dried MTX esters were dissolved in DMSO. The concentration used was in the range of $10^{-6}$ to $10^{-10}$ M for MTX and 1.0 mg/mL to $10^{-7}$ mg/mL for the conjugates, which is equivalent to $10^{-3}$ to $10^{-10}$M of MTX. DHFR activity was measured by following NADPH oxidation at 340 nm, according to a modified method of Peterson et al (68). DHFR and dihydrofolic acid in buffer solution were kept at 0°C during the experiment.

The assay mixture contained 1.5 M sodium acetate buffer (pH 6.0), 0.6 M KCl, 50 μM NADPH, 25 μL DMSO or the same volume of a DMSO solution of test compounds (whose final concentration is between 1 and $10^{-8}$ mg/mL), and 0.02 U of bovine liver DHFR, in a final volume of 3 mL. After enzyme addition, the mixture was incubated at 25°C for 5 min. The reaction was then started by adding 33 μM dihydrofolic acid. The change of absorbance of the reaction mixture at 340 nm ($\Delta_{Abs340}$) was followed for 10 min. Based on the enzyme activity in the absence of MTX (assuming 100 %), the percentage inhibition of the enzymatic activity of DHFR at various concentrations of MTX or MTX esters of PEO-*b*-PHAA was determined. The $IC_{50}$ was defined as the concentration at which 50 % enzyme activity remained and was estimated from the enzyme activity vs. concentration curve. Each value was the mean ± SD of three experiments.

*5.2.3. Cell inhibition assay*

The MTT tetrazolium colorimetric assay introduced by Mosmann (69) allows rapid measurement of cell viability. It reflects the metabolic activity of living cells. As the solubilization of MTT formazan, generated by cellular reduction of the MTT tetrazolium reagent, requires using DMSO and laborious mixing, a tetrazolium salt (XTT), which yields aqueous-soluble formazans upon the metabolic reduction by viable cells (70), was used in this study.

The freeze-dried MTX esters were dissolved in 0.1 M PBS buffer (pH 7.4). The solution was sonicated for 20 min in a water bath sonicator (FS 110, Fisher Scientific, Co., PA). The stock solution of MTX esters of PEO-*b*-PHAA was diluted by cell culture medium without serum to a series of concentrations in the range of 1.0 mg/mL to $10^{-7}$ mg/mL, which is equivalent to $10^{-3}$ to $10^{-10}$ M of MTX. A solution of MTX in cell culture medium without serum was diluted to concentrations in the range of $10^{-5}$ M to $10^{-10}$ M. XTT was freshly prepared at 1 mg/mL in a prewarmed (37°C) medium without serum before the experiment. PMS was prepared at 5 mM (1.53 mg/mL) in 0.1 M PBS (pH 7.4). The PMS solution was stored at 4°C for three weeks. It has been reported that PMS solution is stable at such conditions for at least three months. All solutions were filtered through a membrane with a size cutoff of 0.22 μm before use. The fresh XTT and PMS solutions were mixed together at an appropriate concentration. For a 0.025 mM PMS-XTT solution, 25 μL of the stock 5 mM PMS solution was added per 5 mL of XTT (1 mg/mL).

The murine leukemia L1012 cells (ATCC CCL 219) were maintained in DMEM media supplemented with 5 % horse serum and 2 mM glutamine, and were incubated at 37°C

in a 5 % $CO_2$, 95 % air atmosphere and at 95 % relative humidity. The cells were propagated by dilution into fresh media every 48 h. The cell number was maintained below 2 x $10^6$ cells/mL.

L1210 cells were collected by centrifugation and were resuspended in media and dispensed in 96 well plates. A suspension of cells (100 µL) was placed into each well (1000 ~ 3000 cells per well) using a multichannel pippete. A drug solution (50 µL) of various concentrations was added to the cells. Controls were only treated with the same volume of medium. After 24 to 72 h of exposure to drugs, 50 µL of XTT and PMS mixture (final concentration, 50 µg of XTT and 0.38 µg of PMS per well) was added to each well. After incubation at 37°C for 4 h, the OD of each well was measured with a microplate spectrophotometer (Kinetic Reader, EL312E, Biotek, Winooski, VT) at dual detection wavelength of 450 nm and 590 nm. The spectrophotometer was calibrated using wells that only contained cell culture medium and XTT reagents. The experiments were repeated three times, and each concentration was measured in quadruplet. The mean of OD and the standard deviation were determined for quadruplet samples. Assays defined the $IC_{50}$ value as the concentration of drug, which inhibits cell growth to 50 % of control (drug free). The *% cell viability* was calculated by the following equation:

$$\% \ cell \ viability = \frac{OD(drug)}{OD(control)} X100$$

% Cell growth inhibition is determined based on % cell viability, and the $IC_{50}$s of the esters are the mean of three experiments.

### *5.2.4. Cell inhibition in the presence of folate*

Folic acid was prepared at 0.8 mM in medium without serum. To 96 well plates were added 1000 cells (100 μL), 50 μL of drug solutions, and 50 μL of folic acid solution. Controls were treated with the same volume of cell culture medium instead of drugs. The cells were incubated for 24, 48, and 72 h. Cell viability was evaluated using the XTT assay as previously described.

## 5.3. Results and Discussion

### *5.3.1. DHFR inhibition by MTX esters of PEO-b-PHAA*

The major cytotoxic effect of MTX on proliferating cells is a consequence of its ability to inhibit DHFR, thereby blocking the reduction of dihydrofolate to tetrahydrofolic acid, the active form of folic acid. Thymidylate synthesis as well as various steps in de novo purine synthesis are inhibited, resulting in an arrest of DNA, RNA, and protein synthesis. The binding of MTX to DHFR is stoichiometric (one drug per enzyme molecule) and very tight with a binding affinity in *S. faecium* of $5.8 \times 10^{-11}$ M (68).

To demonstrate the pharmacological activity of the MTX esters on DHFR, the inhibitory activity of LYD043 ($C_2$-12-25-23 % MTX) was evaluated and compared with that of free MTX. The inhibitory activity of MTX or LYD043 against bovine liver DHFR at various concentrations was estimated based on the assumption that the activity of DHFR in the absence of the drug is 100 %. Compared to free MTX, the decreased activity of LYD043

was clearly demonstrated by a shift of its inhibition activity curve to a high concentration range (Figure 5.1).

The $IC_{50}$ of MTX, determined from the inhibition curve, is 10.4 nM, slightly higher than the reported values in the literature for DHFR from the same source (2.9 nM) (71) or from different sources (72). In most cases, the activity of MTX was determined using freshly extracted and purified DHFR from the same tumor cells as used in the *in vitro* and *in vivo* experiments. In this experiment, the commercial DHFR was used because our original purpose was to test if the conjugate had any activity toward DHFR, or if the release of free drug was required for the conjugate to exert its activity. The decreased sensitivity of MTX toward commercial DHFR might result from the denaturation of DHFR during extraction, delivery and storage. However, this decrease of the intrinsic activity of DHFR would not be too much concerned in the comparison of the conjugates with free MTX. The $IC_{50}$ of LYD043, interpreted as the equivalent MTX concentration, is 550 nM, approximately a 50-fold decrease when compared to MTX.

To exclude the possibility that the activity of LYD043 might result from the released MTX during the experiment, the sample was assayed by SEC-HPLC. A free MTX peak was not observed in the SEC chromatogram (data not shown), indicating that the observed inhibition activity is completely from the MTX conjugate.

The intrinsic activity of macromolecular conjugates was also observed in other MTX conjugate systems. Ryser and Shen's studies reveal that the intact conjugate MTX-poly(L-Lysine) binds less well to dihydrofolate reductase than does MTX itself (73).

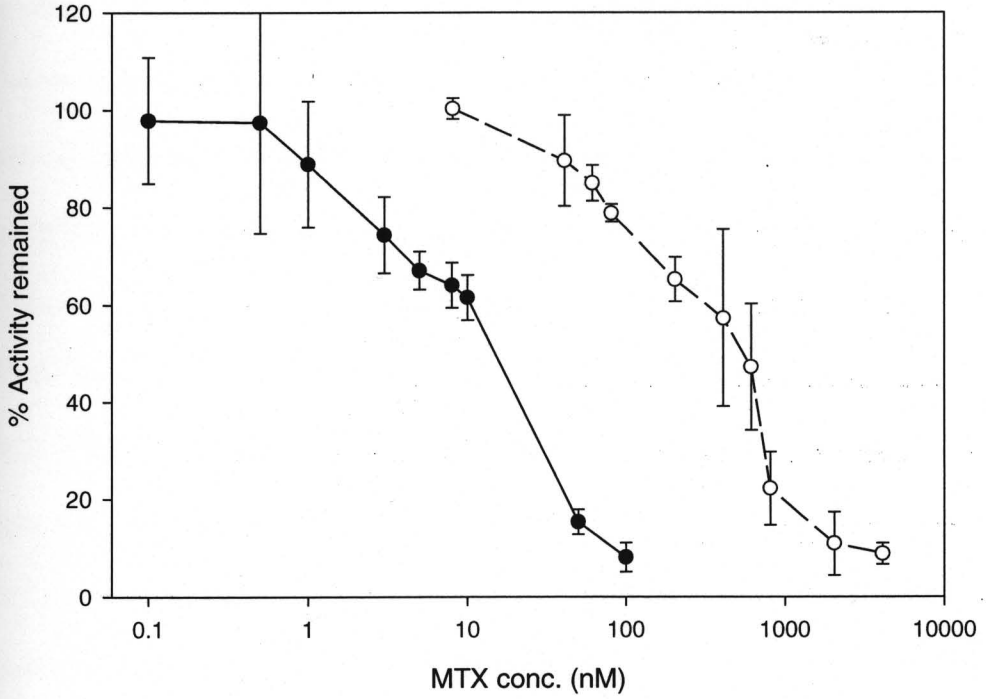


Figure 5. 1. Inhibition activity on DHFR of MTX conjugate and LYD043.−●− MTX; −○− LYD043.

The reduction in the activity of the ester of PEO-*b*-PHAA toward DHFR is not surprising, since the bulky derivatization of glutamate carboxyl groups of MTX would hinder the interaction of the drug with the binding site of enzyme (74). Furthermore, the amphiphilic nature of the conjugates results in self-association to minimize the unfavorable contact of the hydrophobic block with the aqueous media. The binding of MTX moieties with enzyme is greatly decreased. The decreased binding affinity of LYD043 results in decreased inhibitory activity on DHFR.

The concentration of LYD043 for the inhibitory activity study is in the range of 0.0167-3.33 x $10^{-5}$ mg/mL, which is below its CMC, 0.081 mg/mL. The activity of the conjugate at a concentration above its CMC was not evaluated. However, it can be predicted that the formation of micelles may cause MTX moieties inaccessible to DHFR, and the direct interaction of MTX moieties with DHFR may thus be prohibited. Therefore, only unimers with appropriate self-folding may elicit inhibition activity toward DHFR.

### *5.3.2. Cell growth inhibition of MTX esters of PEO-b-PHAA*

The L1210 cell line and its derived resistant cell lines have been widely used for the evaluation of the antagonistic activity and transport of MTX and its conjugates (75).

Three MTX esters were evaluated for their activity against L1210 cells. The PHAA block of the three esters has 15 units of aspartic acid residues, and a $C_2$ spacer bridging MTX to PEO-*b*-PHAA. However, the three esters have varied levels of MTX substitution, which is 7.4 % for LYD059, 23 % for LYD043, and 54 % for LYD038, respectively.

L1210 cells were exposed to various concentrations of MTX or MTX esters for 24, 48, and 72 h, and the viable cells were assayed by XTT reduction in the presence of PMS. The $IC_{50}$ of the conjugates is expressed as the equivalent MTX concentration. For free MTX, the incubation time did not influence its inhibitory activity significantly, as the $IC_{50}$s were close to 2 nM at 24 h, 48 h, and 74 h (Table 5.1). ). On the contrary, MTX esters showed a significant difference in their activity at different incubation times. As shown in Figure 5.2, the inhibition curve of LYD043 is in the higher concentration range at a shorter incubation time (24 h). The curve shifts to a high concentration range at longer incubation time (48 h and 72 h). This trend was also observed for LYD059 and LYD038. For all three conjugates, the $IC_{50}$ is lower at 72 h than at 48 h and 24 h (Figure 5.3). For example, at 72 h, the $IC_{50}$ of LYD059 is 284 nM, while at 48 h and 24 h, the $IC_{50}$ is 869 nM and 2838 nM, respectively.

There is no doubt that a longer incubation time allows more drugs to be released from the conjugate extracellularly which can exert activity toward cancer cells. On the other hand, it has been widely accepted that macromolecules can be taken up by cells through pinocytosis. Therefore, the intact conjugate of MTX may be pinocytosed, and a long incubation time also allows more conjugate molecules being endocytosed by and accumulated in the cells. The endocytosed conjugate may exert activity via direct, although weak, action on DHFR or may intracellularly release the cytotoxic MTX to elicit activity. Therefore, the total activity of the conjugates may be contributed by the extracellularly released drug, by the intracellularly released drugs after cellular uptake of the intact conjugates, and by the direct action of the intact conjugate on DHFR. However, based on present results, it is difficult to differentiate the contributions and determine the dominant processes that account for the total activity.

Table 5.1. $IC_{50}$ of MTX and MTX esters of PEO-*b*-PHAA

| Drug/ conjugates | composition | $IC_{50}$ (24 h, nM) | $IC_{50}$ (48 h, nM) | $IC_{50}$ (72 h, nM) |
|---|---|---|---|---|
| MTX | MTX | 2.1 ± 0.1 | 2.1 ± 0.1 | 1.1 ± 0.1 |
| LYD059 | $C_2$-12-15-7.4 % | 2838 ± 41 | 869 ± 42 | 284 ± 7 |
| LYD043 | $C_2$-12-15-23 % | 4092 ± 114 | 805 ± 11 | 282 ± 11 |
| LYD038 | $C_2$-12-15-54 % | n. d. | 812 ± 254 | 273 ± 47 |

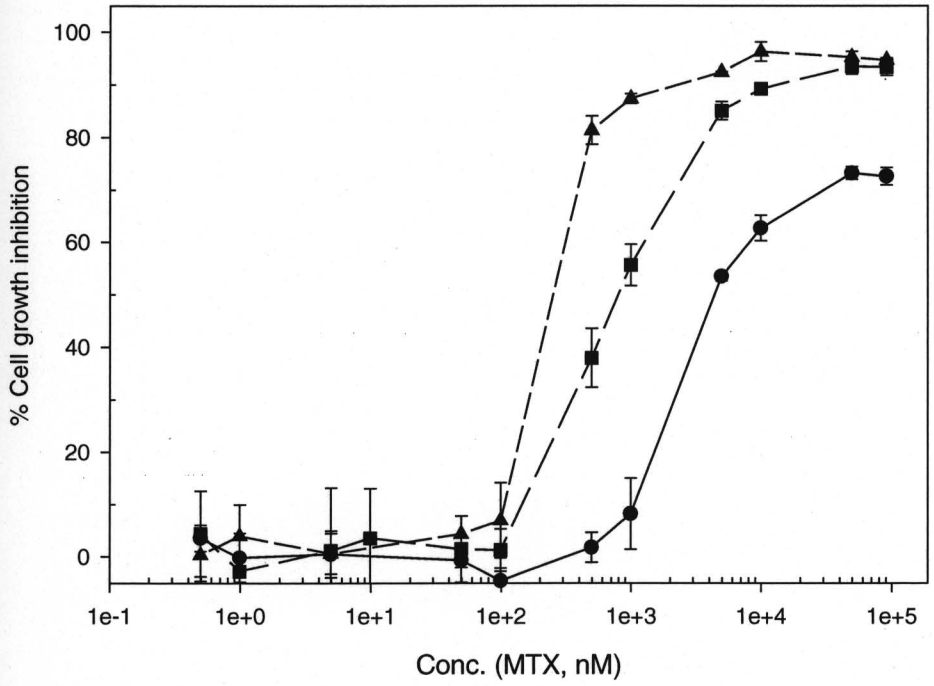


Figure 5.2. Cell growth inhibition of LYD043 at varied incubation time.

–●– 24 h; –■– 48 h; –▲– 72 h.

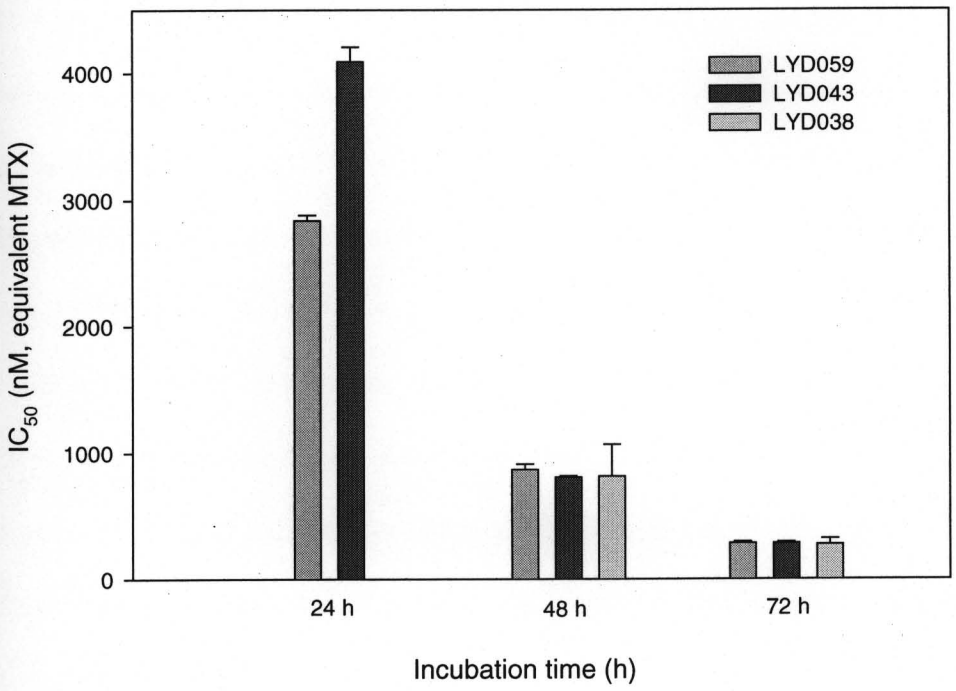


Figure 5. 3. $IC_{50}$ of the MTX esters at varied incubation time.

The $IC_{50}$s expressed as conjugate concentration (mg/mL) for the three conjugates are different (Figure 5.4). LYD038 ($C_2$-12-15-54 % MTX) showed lower $IC_{50}$ than LYD043 ($C_2$-12-15-23 % MTX) and LYD059 ($C_2$-12-15-7.4 % MTX), regardless of the incubation time. However, when the results were normalized and expressed on the equivalent MTX basis, the three conjugates displayed a similar activity in terms of the equivalent MTX concentration, except when the incubation was 24 h (Figure 5.3). When the incubation time was 24 h, both LYD043 and LYD038 showed low activity toward L1210 cells. Compared to free MTX, the anticancer activity of the MTX esters decreased significantly regardless of the incubation time (Figure 5.5 and Figure 5.6).

It should be mentioned that the concentrations of MTX esters for the anticancer activity assay covered a wide range of concentrations above and below CMC. The $IC_{50}$s for all conjugates, in terms of the conjugate concentration, were below the CMC. Therefore, the effect of micelles on the conjugate activity was not counted. The intramolecular association of the conjugates might also affect their activity.

The conjugation of MTX to macromolecular carriers usually decreases the inhibitory activity of the parent drug (76). For example, approximately 1000-fold decrease of activity is observed for the conjugates of MTX and branched polypeptides. Polycationic conjugates exhibited less decrease in the activity. The MTX-poly(L-lysine) conjugates only showed a 10-fold decrease in the activity compared to free MTX. The decreased activity is attributed to the decreased binding to the target enzyme.

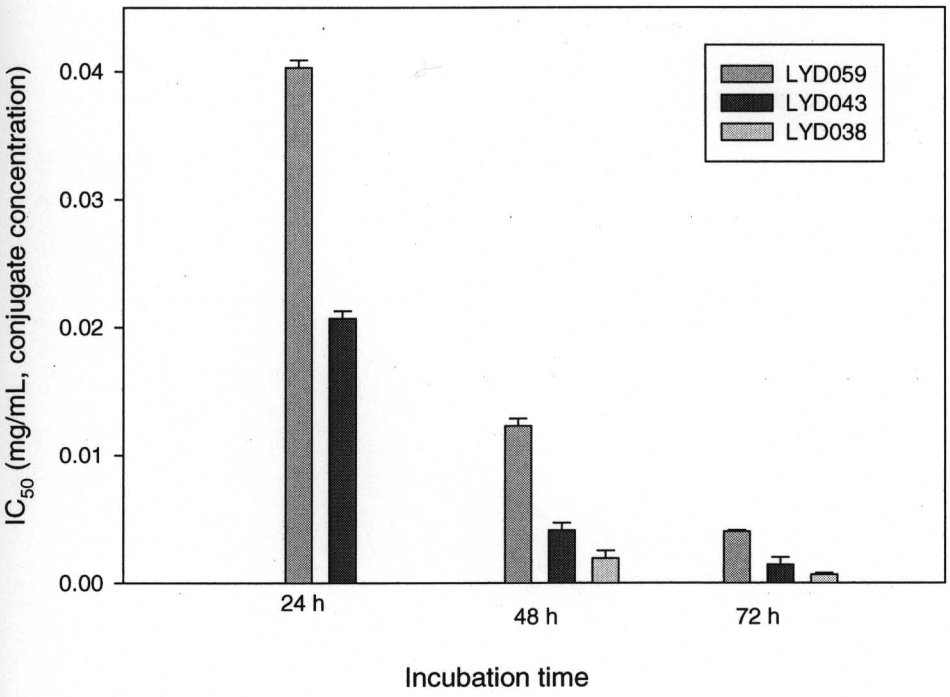


Figure 5. 4. $IC_{50}$ of the MTX esters expressed as polymer concentration

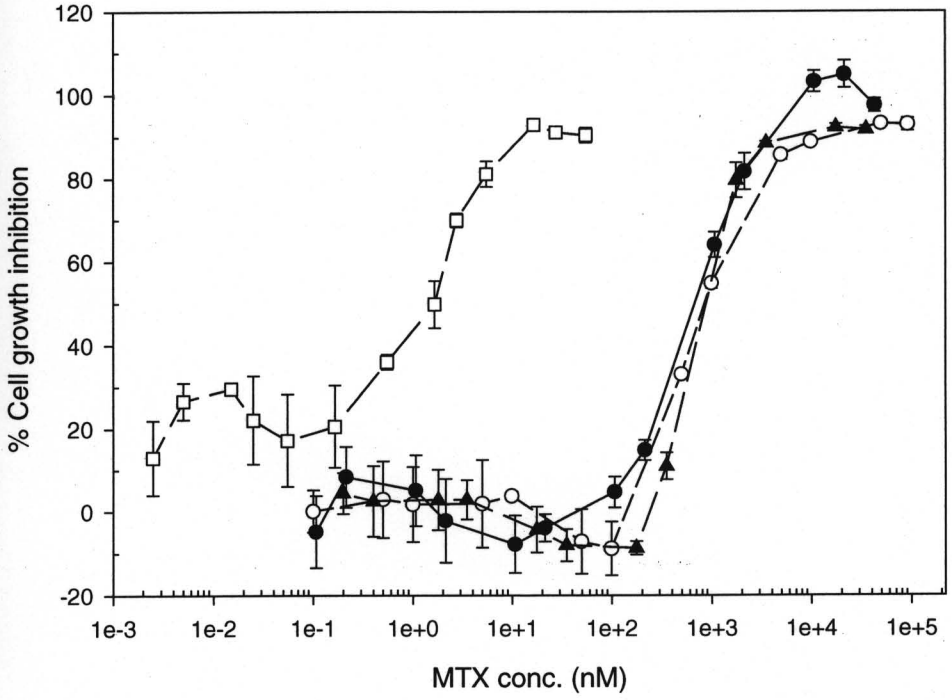


Figure 5.5. Cell growth inhibition of MTX esters. Incubation time was 48 h; –●– LYD038 with 54 % MTX substitution; –o– LYD043 with 23 % MTX substitution; –▲– LYD059 with 7.4 % MTX substitution; –□– MTX.

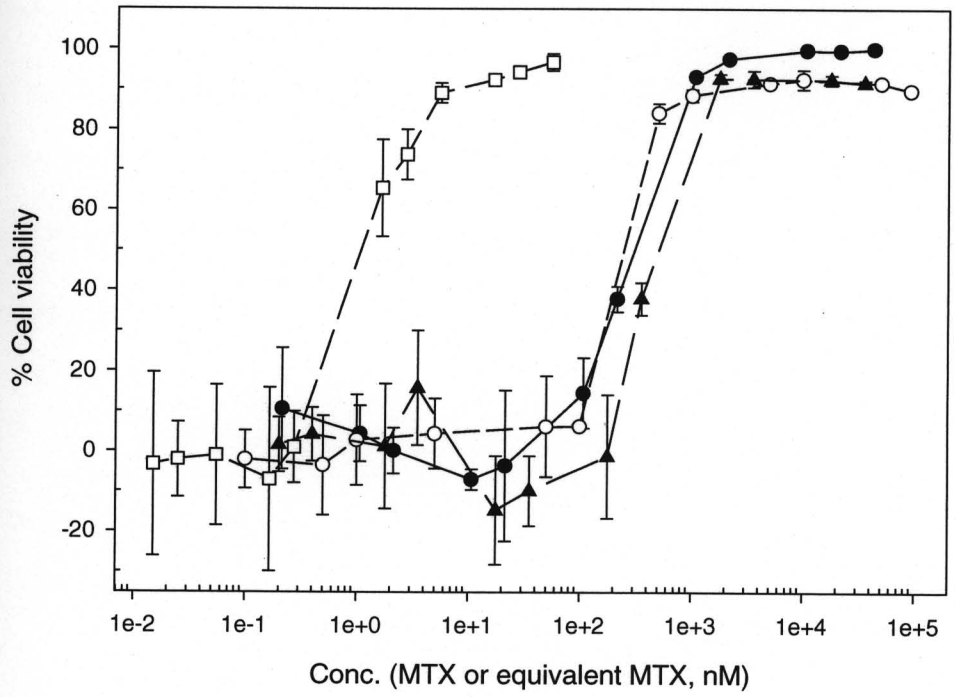


Figure 5.6. Cell growth inhibition of MTX esters. Incubation time was 72 h; –●– LYD038 with 54 % MTX substitution; –o– LYD043 with 23 % MTX substitution; –▲– LYD059 with 7.4 % MTX substitution; –□– MTX.

### *5.3.3 Inhibitory activity of MTX and MTX esters of PEO-b-PHAA in the presence of folate*

MTX is an analogue of folic acid, a natural product participating in the synthesis of nuclear bases. MTX differs from folic acid in two substitutions: (1) an amino group for a hydroxyl in the pteridine portion of the molecule and (2) a methyl group on the amino nitrogen between the pteridine nucleus and the benzoyl group (Figure 5.7). Both MTX and folate bind to folate receptors on the cell surface and are taken up by cells via receptor mediated endocytosis.

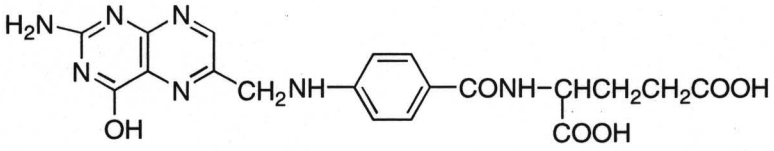


folic acid

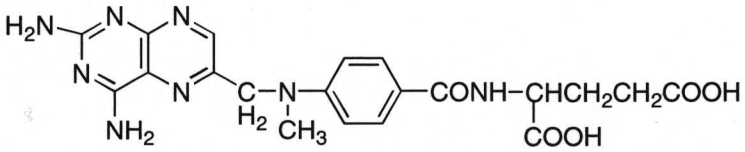


MTX

Figure 5.7. Chemical structure of folic acid and MTX.

Folate has been used as a competitor for the studies of MTX transport (77). The presence of high concentration of folate (0.8 mM) revealed a notable effect on MTX activity, observed as a shift of the inhibition curve of MTX to a higher concentration range (Figure 5.8). Regardless of the incubation times, the $IC_{50}$ of MTX increased from ~ 2.0 nM in the absence of folate to ~ 10.0 nM in the presence of folate (Figure 5.9). The decreased activity of MTX in the presence of folate is caused by the reduced cell entry of MTX.

However, folate showed a slight effect on the activity of MTX esters. LYD043 exhibited similar activity against the L1210 cells in the presence and the absence of folate at an incubation time of 48 h or 72 h (Figure 5.10). The $IC_{50}$s of LYD043 in the presence of folate were 996 nM and 395 nM at 48 h and 72 h, respectively. The $IC_{50}$s in the absence of folate were 805 nm and 282 nM at 48h and 72 h, respectively (Figure 5.11, Table 5.2).

The results suggest that the conjugation of MTX to a polymeric carrier might alter its cellular uptake pathway. MTX enters cells via receptor-mediated endocytosis. A large number of folate molecules will competitively bind to the folate receptors. Consequently, the available receptors for MTX may be greatly reduced. On the other hand, the cell-entry of polymeric conjugates of MTX may not use the folate carriers, but rather occur through a non-receptor mediated endocytotic pathway. Hence, the availability of folate receptors for the drugs may have less effect on the cell entry of conjugates and their $IC_{50}$s.

Table 5.2. Cell growth inhibition of LYD043 ($C_2$-12-15-23 % MTX)

in the presence of 0.8 mM folate

| $IC_{50}$ | 24 h (nM) | 48 h (nM) | 72 h (nM) |
|---|---|---|---|
| MTX | 2.1 ± 0.1 | 2.1 ± 0.1 | 1.1 ± 0.1 |
| MTX & folate | 8.1 ± 0.2 | 9.7 ± 0.5 | 10.2 ± 0.3 |
| LYD043 | 4092 ± 114 | 805 ± 11 | 282 ± 11 |
| LYD043 & folate | n. d. | 996 ± 275 | 385 ± 24 |

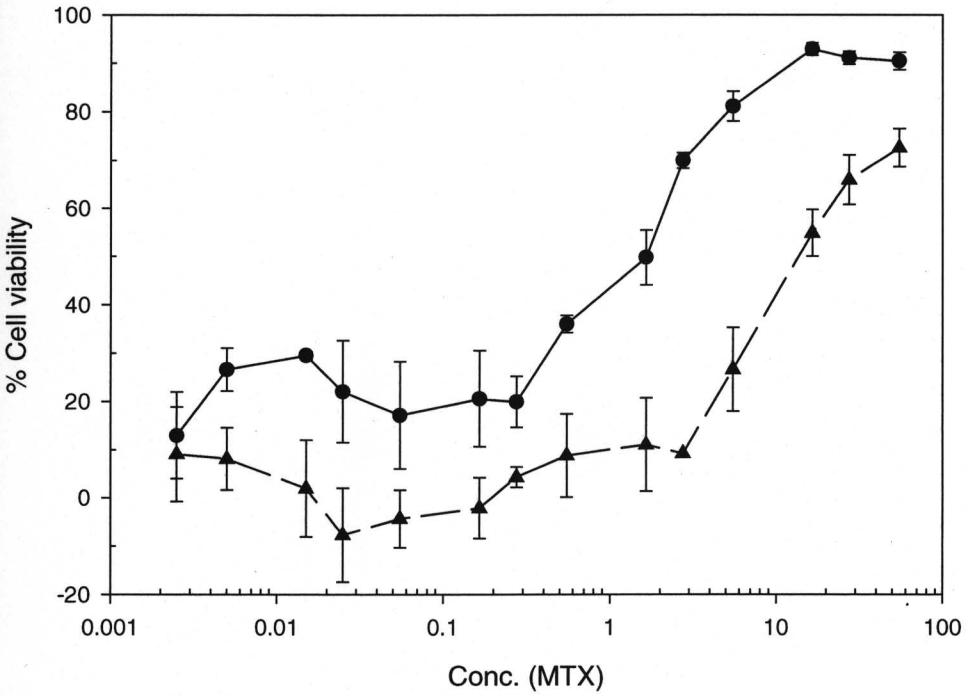


Figure 5.8. Inhibition curve of MTX in the absence (●) and the presence of folate (▲).

Incubation time was 48 h.

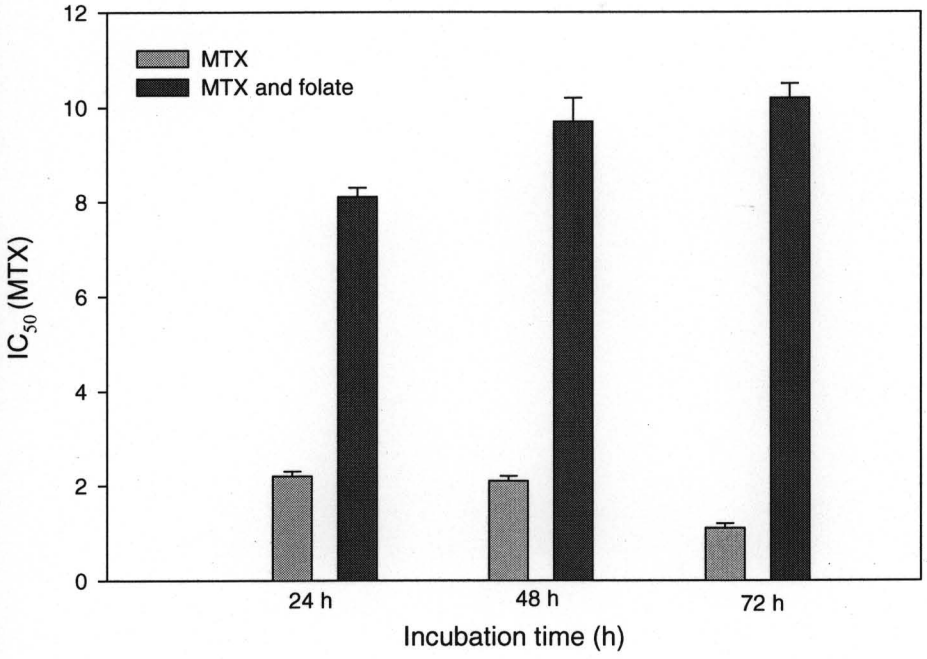


Figure 5.9. Effect of the presence of folate on the $IC_{50}$ of MTX.

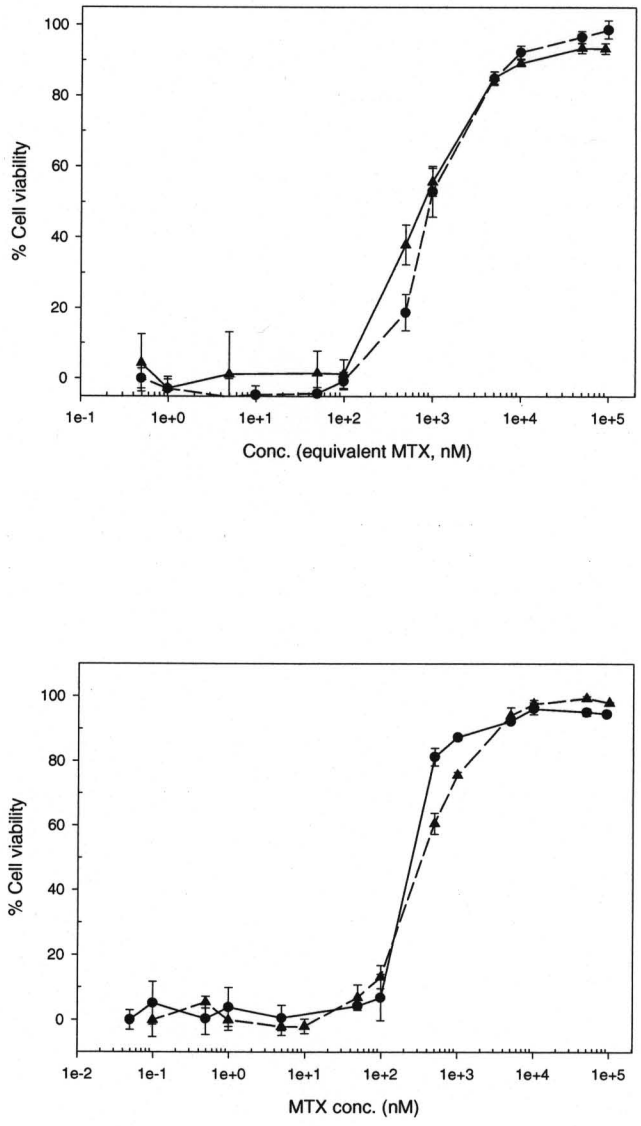


Figure 5.10. Cell viability of LYD043 ($C_2$-12-15-23 % MTX) in the presence of folate at 48 h (upper panel) and 72 h (lower panel). –●– MTX ester alone; –▲– in presence of 8 x $10^{-4}$M folate.

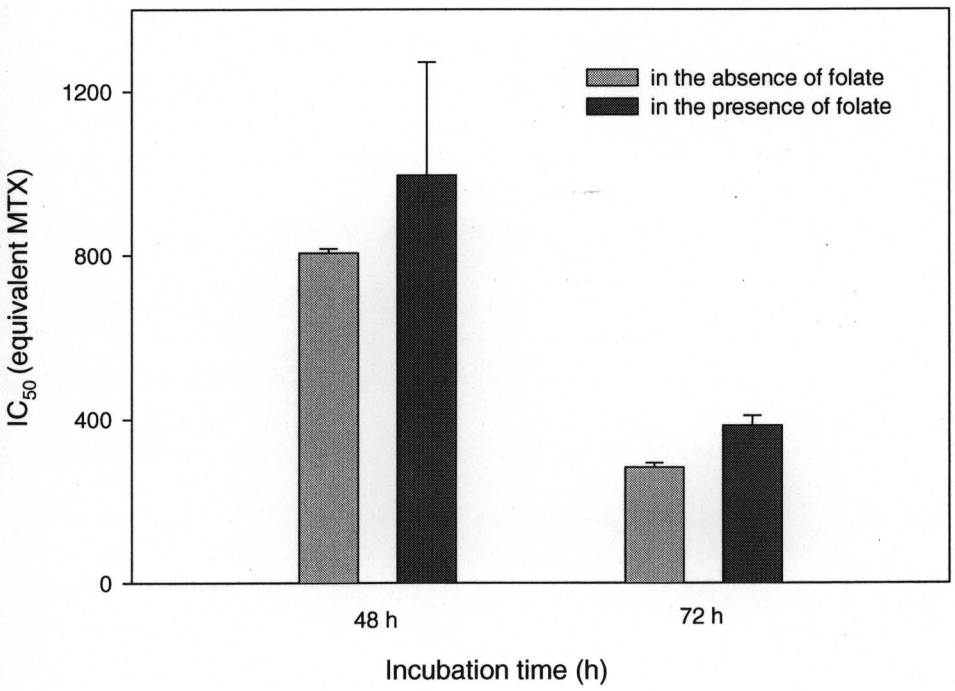


Figure 5.9. Effect of folate on the activity of LYD043 at 48 h and 72 h.

The conclusion that using a polymeric carrier for MTX can change the cell entry pathway of the drug is consistent with the work reported by Ryser and Shen. (78). They covalently attached MTX to poly(L-lysine) to alter the mode of cellular uptake and to overcome MTX resistance. They demonstrated that uptake of MTX-poly(lysine) is unaffected by inhibitors of MTX transport, and is efficient especially in cells with impaired MTX transport, e.g., in MTX resistant cells. They conclude that the conjugate of MTX is probably taken up by cells via pinocytosis.

This study has demonstrated the biological activity of the MTX esters toward DHFR and murine leukemia L1210 cells. The intact conjugate in unimer form exhibited a low inhibitory activity toward DHFR, as a result of weak binding affinity due to chemical structural modification of MTX. The conjugates showed decreased activity against L1210 cells compared to free MTX. The cell inhibitory activity is sensitive to drug exposure time. The presence of folate reduced the activity of MTX significantly, but demonstrated less effect on MTX esters. Extracellularly released MTX may contribute to the activity of the conjugates. However, the cellular uptake and function of the intact conjugates offer alternative mechanisms for the action of the conjugate system. Based on these results, it can be predicted that a higher dose of the conjugates can be used to provide an efficient amount of drugs for a long period of time due to sustained drug release.

# CHAPTER 6.

## Paclitaxel Conjugate of Poly(ethylene oxide)-*block*-Poly(L-aspartic acid)

## 6.1. Introduction

Paclitaxel is a diterpenoid taxane derivative (Figure 6.1), which was first isolated from *Taxus brevifolia* (79). Paclitaxel has shown high activity against a variety of tumors and has been used clinically in the treatment of metastatic breast cancer (80), refractory ovarian cancer and several other malignancies (81). The antitumor activity of paclitaxel comes from its ability to promote assembly of tubulin into microtubules and stabilize microtubules from depolymerization, thus interfering with the G2 and M phases of the cell cycle. In spite of its excellent antitumor activity, there are considerable problems in the clinical application of paclitaxel, resulting from its formulation.

Paclitaxel is a highly hydrophobic drug with very low water solubility. In order to enhance paclitaxel solubility, a mixture of 50:50 Cremophor EL (a polyoxyethylated caster oil) and ethanol is used in the current clinical formulation. The formulation is diluted 5- to 20- fold with saline or other aqueous intravenous solution before infusion. This results in the administration of a significant amount of Cremophor (about 80 mg Cremophor for 1 mg paclitaxel) (82). Serious side effects (such as hypersensitivity and extraction of plasticizer from the i.v. infusion line) arising from the formulation have been observed (83). Consequently, a variety of formulation systems have been studied to enhance the solubility with minimal formulation-related toxicity. Cosolvents (ethanol/polysorbate-80, polyethylene glycol or polyvinylpyrolidone), oil-in-water emulsions, liposomes (84), cyclodextrins (85) (86), and surfactants (pluronic L64) (87), and polymeric micelles (polyethylene oxide-poly(lactic acid)) (PEO-PLA)) (44) have all been employed to enhance paclitaxel solubility.

In particular, PEO-PLA micelles can increase the concentration of paclitaxel to 50 mg/mL without precipitation upon dilution.

In the mean time, a great deal of chemical research has gone into structural modification of paclitaxel to create a more soluble and, therefore, a more easily formulated and delivered drug. Of all approaches, prodrug technology seems most promising (88). Prodrug strategies modify the structure of problematic drugs (89). Such chemical modification is usually designed to alter aqueous solubility and biodistribution while the inherent pharmacological properties of the parent drug remain intact (90). Prodrugs, or transport forms as they are sometimes referred to, can be designed to reliably function, i.e., to self-destruct in a predictable fashion *in vivo* to the active drug by either an enzymatic mechanism or by simple hydrolysis initiated under physiological pH conditions, once the barrier to delivery has been circumvented.

Macromolecules are able to accumulate at tumor sites due to the physiological characteristics of tumor tissues. Conjugation of paclitaxel to polymeric carriers provides a potential approach to not only resolve the solubility problem, but also to achieve controlled drug release and tumor targeting. 2-Hydroxypropylmethacrylamide (HPMA) copolymers containing oligopeptide side chains terminating in paclitaxel generated a system in which the conjugated paclitaxel can be released in a controlled rate by lysosomal enzymes after cellular uptake of the conjugate. *In vivo* data for this paclitaxel-copolymer conjugate employing a solid tumor model (murine melanoma B16F10) has revealed greater efficacy than paclitaxel control (91).

The attachment of Paclitaxel to PEG yielded a prodrug, in which an ester linkage was used. The prodrug was highly water-soluble. pH-dependent hydrolysis of the linkage would

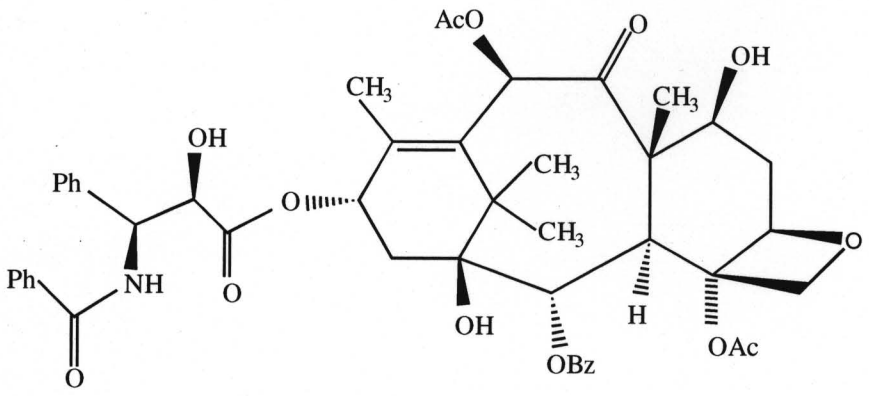


Figure 6. 1. Chemical structure of paclitaxel.

release the conjugated drug. Substantial enhancement in the rate of drug release due to non-specific esterase occurred *in vivo,* which add the effective use of the prodrug. The half-life of the esters in PBS buffer was more than 50 hours. In human plasma, however, the half-life was about 1 h (92).

Amphiphilic block copolymer PEO-*b*-PBLA is able to physically solubilize paclitaxel. However, the system is limited by drug loading capacity and systemic stability, which inspired us to develop a conjugate system. We hypothesized that chemical attachment of paclitaxel to poly(ethylene oxide)-*block*-poly(L-aspartic acids) (PEO-*b*-PLAsp) might result in an amphiphilic polymeric drug conjugate. In aqueous media, the conjugate might self-assemble into a micelle-like structure. As ester bonds were used for drug conjugation, paclitaxel might be released upon hydrolysis of the ester linkage in a physiological environment.

# 6.2. Experimental

### *6.2.1. Materials*

Unless stated otherwise, all reagents and solvents were used as purchased without further purification. $^1$H NMR was measured on a 400 MHz NMR instrument (JEOL EX400, Japan) in DMSO-$d_6$ containing 0.05 % of tetramethylsilane (TMS) at 25°C for paclitaxel and its derivatives and at 80° C for polymers. HPLC analyses (TKO-1 system, Japan) were performed using a $C_{18}$ reverse phase column (Inerrtsil ODS-II, 4.6 mm id x 150 mm, Japan) at 40°C. The detection wavelength was set at 227 nm. A mixed solvent of 55 % acetonitrile (v/v) and 2 nM phosphoric acid in water solution was used as the mobile phase. The flow rate was 1 mL/min, and the injection volume was 10 μL.

### *6.2.2. Synthesis*

#### *6.2.2a. Synthesis of PEO-b-PLAsp*

The synthesis and characterization of poly(ethylene oxide)-*block*-poly(β-benzyl-L-aspartate) (PEO-*b*-PBLA) was described in 1.2.1. Briefly, α-methoxy-ω-amino-PEO ($M_w$ = 12,000 g/mol, $M_w/M_n$ = 1.05, functionality of amino group = 0.96) acts as an initiator for the polymerization of β-benzyl-L-aspartate N-carboxyanhydride. The PBLA block has a degree of polymerization of 24 based on $^1$H NMR measurement. The conversion of PEO-*b*-PBLA to

PEO-*b*-PLAsp was completed by hydrogenolysis. In a typical procedure, a dried round bottom flask was purged with argon, a solution of PEO-*b*-PBLA (1.50 g) in DMF (45 mL) was added. A portion of 10 % Pd/C catalyst (0.50 g) was added to the solution in several portions. The system was then purged with $H_2$, and kept under $H_2$ with stirring for 48 h at room temperature. The reaction mixture was filtered through a pad of celite (the celite was layered on a piece of filter paper and thoroughly washed with DMF until DMF became colorless) to remove catalyst. The filter pad was washed with DMF three times. The viscous brownish solution obtained was concentrated by rotary evaporator until the volume was about10 mL, and then poured into cold ether with stirring. The precipitate was collected by filtration and dried in vacuum to give a gray powder (yield 1.37g, 90 %). The product was characterized by UV-Vis spectrometer (JASCO model V-550, Japan) and $^1$H NMR spectroscopy.

*6.2.2b. 2'-N-(Carbobenzyloxy)-γ-aminobutyryl paclitaxel (79)*

Acetonitrile (HPLC grade, Sigma) was refluxed with $CaH_2$ and distilled. γ-(N-benzyloxycarbonyl (CBz))-aminobutyric acid (50 mg, 0.21 mmol), dicyclohexylcarbodiimide (40 mg, 0.19 mmol), and DMAP (50 mg, 0.19 mmol) were added to a solution of paclitaxel (50 mg, 0.059 mmol) in anhydrous acetonitrile (10 ml) at 0°C. The reaction mixture was slowly warmed to room temperature and stirred for 22 hours. The urea salt formed in solution was filtered off, and the resulting solution was concentrated under vacuum. The crude product was purified on silica gel by flash chromatography, and recrystallized from hexane/ethyl acetate (1:1) to give a white crystalline product (55 mg, 86%). m.p.: 164–

167°C; $R_f$ = 0.37 (ethyl acetate/Hexane, 60:40). The $^1$H NMR spectrum was measured at 25°C in $d_6$-DMSO (contains 0.05% TMS).

*6.2.2c. 2'-(γ-Aminobutyryl) paclitaxel*

2'-N-CBz-γ-aminobutyryl) paclitaxel (68 mg, 0.063 mmol) was dissolved in methanol (50 mL). Formic acid (3.5 mL) and a catalytic amount of 10 % Pd/C (17.5 mg) were then added. The reaction mixture was stirred at room temperature for 4 h. The resulting mixture was filtered, washed with methanol (3 x 10 mL). After removing the solvent, the remaining product (50 mg) was then used immediately for the synthesis of the conjugate.

*6.2.2d. 2'-N-CBz-γ-aminocaproyl paclitaxel*

*N*-CBz-γ-aminocaproic acid (35 mg, 0.13 mmol), dicyclohexylcarbodiimide (80 mg, 0.38 mmol), and DMAP (23.5 mg, 0.089 mmol) were added to a solution of paclitaxel (100 mg, 0.12 mmol) in anhydrous acetonitrile (40 ml) at 0°C. The reaction mixture was slowly warmed to room temperature and stirred for 48 hours. The resulting solution was filtered and concentrated. The residue was purified on silica gel by flash chromatography, recrystallized from hexane/ethyl acetate (1:1) to give a white crystalline product (127 mg, 98%). $R_f$ = 0.37 (ethyl acetate /Hexane, 75:25). The $^1$H NMR spectrum was measured at 25°C in $d_6$-DMSO (contains 0.05% TMS).

*6.2.2e. 2'-(6-Aminocaproyl) paclitaxel*

2'-(6-N-CBz-aminocaproyl) paclitaxel (68 mg, 0.063 mmol) was dissolved in methanol (50 mL). Formic acid (3.5 mL) and a catalytic amount of 10 % Pd/C (30 mg) were

added. Stirring at room temperature for 4 h, the reaction mixture was filtered through a pad of celite, and washed with methanol (3 x 10 mL). The solvent was then evaporated under vacuum. The product (50 mg) was used immediately for the synthesis of the conjugate.

*6.2.2f. Paclitaxel conjugate of PEO-b-PLAsp*

In a typical procedure, PEO-*b*-PLAsp (85.5 mg) was dissolved in N-methylpyrolidone (NMP) (5.0 mL) and heated at 35°C to obtain a clear solution. A solution of 2'-(γ-aminobutyryl) paclitaxel (85.5 mg) in NMP (3.0 mL), benzotriazolyl-N-oxy-tris(dimethylamino)-phosphonium hexafluorophosphate (BOP reagent, 76.0 mg), and a solution of lithium chloride (4.3 mg) in NMP (3 mL) were added to the polymer solution. triethylamine (80 μL) was then added. The reaction mixture was stirred for 24 h, and monitored by TLC. The resulting mixture was dialyzed exhaustively against DMSO containing 10 mmol lithium chloride (3x1L, MWSO 3500 g/mol)), DMSO (1L), and then water (3 x 1 L). The obtained solution was freeze-dried (yield 60 mg). Free paclitaxel was not observed on TLC plate (ethyl acetate/Hexane 60/40, paclitaxel: $R_f = 0.22$, conjugate: $R_f = 0$).

The product was characterized by $^1$H NMR spectroscopy in DMSO-$d_6$. Characteristic peaks of polymer and paclitaxel were present in the $^1$H NMR spectra. The content of paclitaxel was estimated based on a standard curve generated with known concentrations of paclitaxel in methanol. The secondary differentiation of the UV spectra was used for quantitation. Briefly, 1.0 mg of conjugate was dissolved in methanol (spectrometric purity). The solution was diluted and measured by a UV spectrometer. UV spectra were converted to their secondary differentiation, and the height of the characteristic peak of paclitaxel was

measured to determine the content of paclitaxel. The level of paclitaxel substitution was then calculated. The substitution level was also estimated from $^1$H NMR.

### *6.2.3. Self-assembly of the conjugate in aqueous solution*

Paclitaxel conjugate (10 mg) was dissolved in 2.5, 5 or 20 ml of solvent (DMSO, DMAc or methanol) to form a clear solution. 10 % (volume) water was slowly added. The resulting solution was dialyzed against water (3 x 1 L). The obtained solution was directly used for DLS or concentrated five times with an ultrafiltration membrane (molecular weight cut-off: 30,000 g/mol). The final concentration of the conjugates was in the range of 0.3-0.8 mg/mL. The concentrated solution of the conjugates was used for further analysis or freeze-dried.

### *6.2.4. Dynamic light scattering measurements*

The size distribution of paclitaxel conjugate micelles was determined by dynamic light scattering measurements. A light scattering spectrophotometer (DLS-700, Photal, Otsuka Electronics, Japan) equipped with a He-Ne laser was used at a wavelength of 633 nm. The scattering angle was set at 90°. The concentrations of the conjugates were in the range of 0.5 to 1.0 mg/mL). Before measurement, the solution was filtered through a membrane with size cut-off 0.45 μm (Millipore). All measurements were carried out at 25°C.

### *6.2.5. Fluorescence measurements*

Fluorescence measurements were carried out on a fluorometer (770F, JASCO, Japan) at 25°C. Pyrene (Wako Chemicals, Japan) was used as a probe to study micelle formation. The concentration was 6.0 x $10^{-7}$M. Emission spectra were recorded at varied concentrations of the conjugate at the excitation wavelength of 339 nm. Excitation and emission bandwidths were 3.0 and 1.5 nm, respectively. The polymer solutions were purged with argon to remove dissolved oxygen prior to measurements.

### *6.2.6. Drug release*

Freeze-dried conjugates (5.0 mg) were redissolved in PBS buffer (10.0 mL) by the aid of sonication. Drug release was carried out at pH 3, 5, 7, and 12. Drug release in the presence of two lysosomal enzymes, capthesin B and capthesin D, was also tested at pH 5. Drug released from the conjugate was monitored by HPLC equipped with a reverse phase column (Inertsil ODS-II, Japan). The paclitaxel peak was monitored and plotted as a function of time (Figure 6.10).

## 6.3. Results and discussion

### *6.3.1 Conjugation of paclitaxel to PEO-b-Pasp*

Paclitaxel possesses two hydroxyl groups that can be used for its structural modification (Figure 6.1). The hydroxyl group at the 2'– position of paclitaxel is more reactive than the sterically hindered 7-hydroxyl group. Therefore, it is possible to use this difference in reactivity to introduce chemical moieties at the 2'- position to enhance the solubility of paclitaxel. PEO-*b*-PLAsp obtained from its benzyl ester has pendent carboxyl groups at the side chains. The carboxyl groups can be used for the conjugation of drugs to block copolymer. Hence, PEO-*b*-PLAsp can react with paclitaxel forming a polymer-drug conjugate with an ester linkage.

The conversion of PEO-*b*-PBLA to PEO-*b*-PAsp was achieved through either hydrolysis (Figure 6.2) or hydrogenolysis (Figure 6.3). Alkaline hydrolysis of PEO-*b*-PBLA resulted in PEO-*b*-PAsp in high yield (>90 %). However, α-amide bonds of the BLA units were partially transformed into β amide bonds. The isomerization may vary the reactivity of the carboxyl groups. The carboxyl groups at the β peptide side chains were closer to the backbone, and, thus, more hindered for reactions. The overall reactivity of the polymer may be decreased.

The hydrogenolysis of PEO-*b*-PBLA yielded PEO-*b*-PLAsp, in which, all peptides were α form, and the carboxyl groups were away from the polymer backbone (Figure 6.3). The hydrogenolysis was carried out using 10 % Pd/C as catalyst. The removal of the catalyst

from the reaction mixture was difficult. The product was thus slightly contaminated by the catalyst, and a grayish polymer was obtained instead of a white product.

The successful debenzylation was confirmed by $^1$H NMR and UV spectroscopic analysis. As in Figure 6.4, characteristic absorption bands of BLA were not detectable for PEO-*b*-PLAsp. Similarly, phenyl proton signals (7.3 ppm) due to benzyl groups were absent in the $^1$H NMR spectrum of PEO-*b*-PLAsp (Figure 6.5).

The direct conjugation of paclitaxel to PEO-*b*-PLAsp resulted in low level of drug substitution due to the steric hindrance (data not shown). Therefore, paclitaxel was preactivated by coupling its 2'-hydroxyl group to an aliphatic acid that had a terminal protected amino group, which yielded a derivative of paclitaxel (Figure 6.6).

The introduced amino groups were more reactive toward carboxyl groups on PEO-*b*-PLAsp. The aliphatic acid also served as a linker for paclitaxel and the polymer, so the reaction would be less hindered. The reaction of paclitaxel with N-protected amino acid yielded an ester in excellent yield (> 80 %). CBz, a protecting group for amino groups, could be easily removed via hydrogenolysis in formic acid in the presence of 10 % Pd/C. The deprotection of the CBz group yielded a paclitaxel derivative with an amino group, which was reacted with PEO-*b*-PLAsp. Using N-CBz-γ-amino butyric acid, the obtained intermediate, γ-amino butyroyl ester of paclitaxel was not stable and underwent intramolecular nucleophilic reaction, in which a six-member ring transition state might form easily. As a result, the initial reactant, paclitaxel, was recovered as observed from the TLC of the reaction mixture over time. Therefore, the preactivated paclitaxel was reacted with PEP-*b*-PLAsp right after it was prepared. A six-carbon amino acid was also used as a linker for the conjugation of paclitaxel and the polymer backbone. Intramolecular reaction of

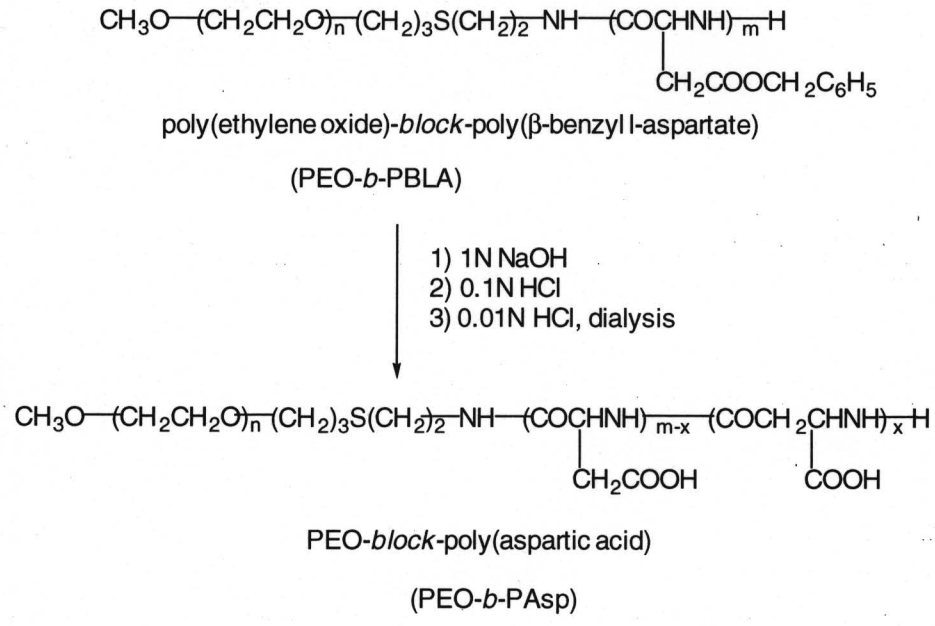


Figure 6. 2. Hydrolysis of PEO-*b*-PBLA.

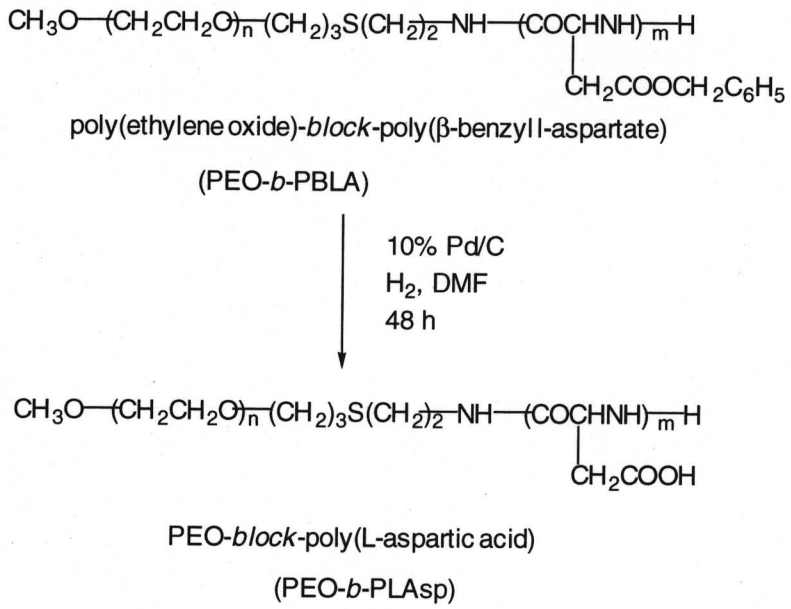


Figure 6. 3. Hydrogenolysis of PEO-*b*-PBLA.

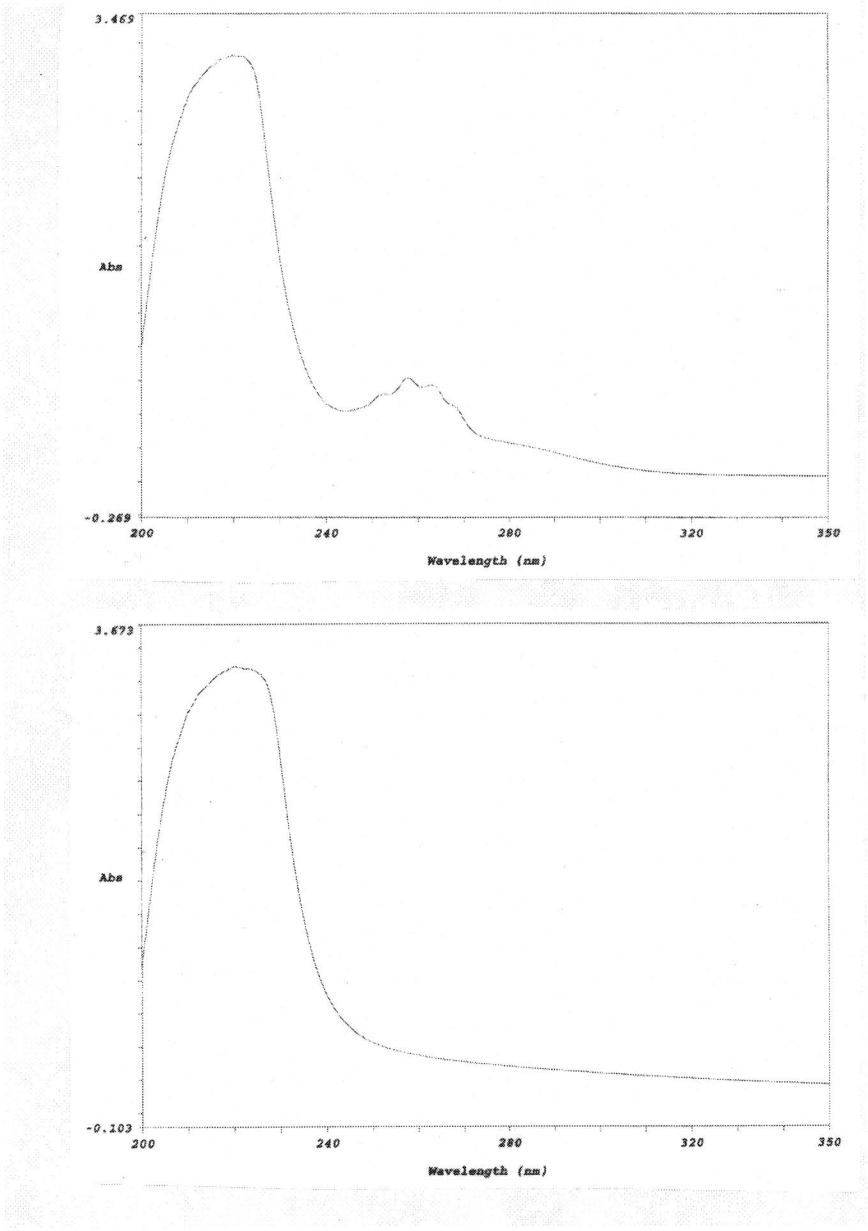


Figure 6. 4. UV spectrum of PEO-*b*-PBLA (upper panel) and PEO-*b*-PLAsp (lower panel).

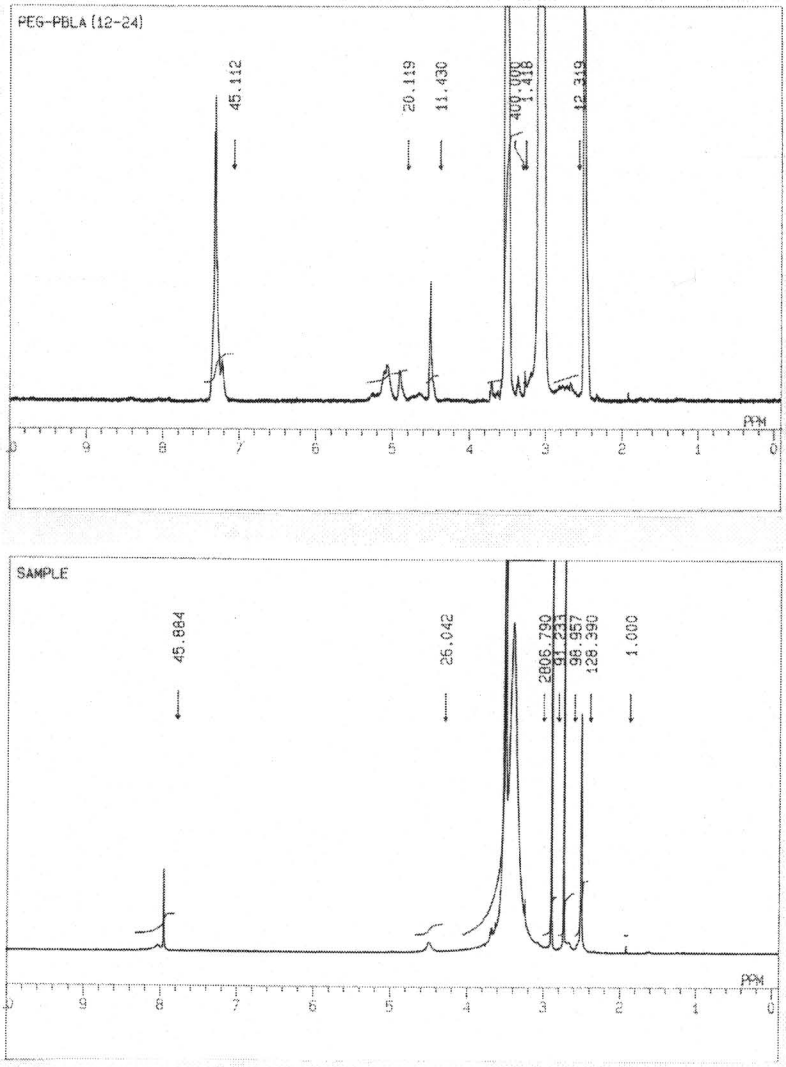


Figure 6. 5. $^{1}$H NMR of PEO-*b*-PBLA and PEO-*b*-PLAsp

(6-aminocaproyl) paclitaxel was not favored. Therefore, the level of drug substitution was significantly improved from 21 % to 38 % (Table 1).

The conjugation of paclitaxel to PEO-*b*-PLAsp was carried out using BOP as a coupling reagent and DMSO containing 1 mM LiCl as solvent in the presence of DMAP (Figure 6.7). TLC was used to monitor the reaction. The product was purified by exhaustive dialysis against DMSO to remove unreacted reactants and by-products, then dialyzed against water, and freeze-dried. TLC of the obtained conjugate did not show the existence of free paclitaxel. The conjugate was characterized by $^1$H NMR spectroscopy (Figure 6.8), and the presence of the characteristic peaks for both polymeric backbone and paclitaxel moieties revealed that the chemistry was successful. The conjugates were analyzed using reverse phase HPLC. Contrary to the TLC result, a certain amount of free paclitaxel was detected in the conjugate sample, which might be explained because of the limitation of the sensitivity for TLC or as a result of hydrolysis of the conjugate at the HPLC operating conditions. Nevertheless, strong interaction between paclitaxel and the hydrophobic segment of the conjugates might be significant, and, thus, make the purification difficult.

The level of paclitaxel substitution was determined by UV analysis. As the UV absorption of paclitaxel and PEO-*b*-PLAsp overlapped, the secondary differentiation of UV spectra was used to separate the two (Figure 6.9). The height of the paclitaxel peak was used for quantitation, using free paclitaxel as a standard. Average levels of paclitaxel conjugation were 12 % or 21 % for the $C_4$ carbon linker, and 38 % for the $C_6$ carbon linker. A higher level of paclitaxel using the $C_6$ linker was achieved as a result of a more stable intermediate, which allowed a longer reaction time. $^1$H NMR was also used to estimate the level of drug

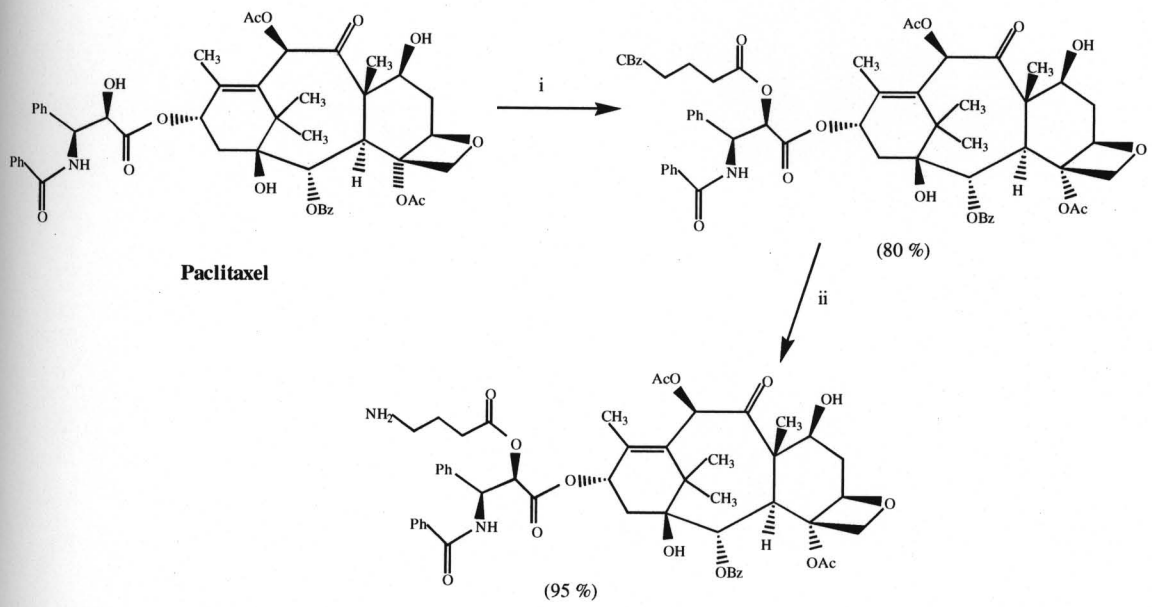


**Paclitaxel**

(i) DCC, DMAP, N-CBz-r-aminobury ric acid, $CH_3CN$, 24 hr; Flash Chromatography, EtOAc/Hexane (60/40), Rf=0.37, m.p. 167-170°C
(ii) 10 % Pd/C, HCOOH, $CH_3OH$, 4 hr, r.t.

Figure 6. 6. Preactivation of paclitaxel.

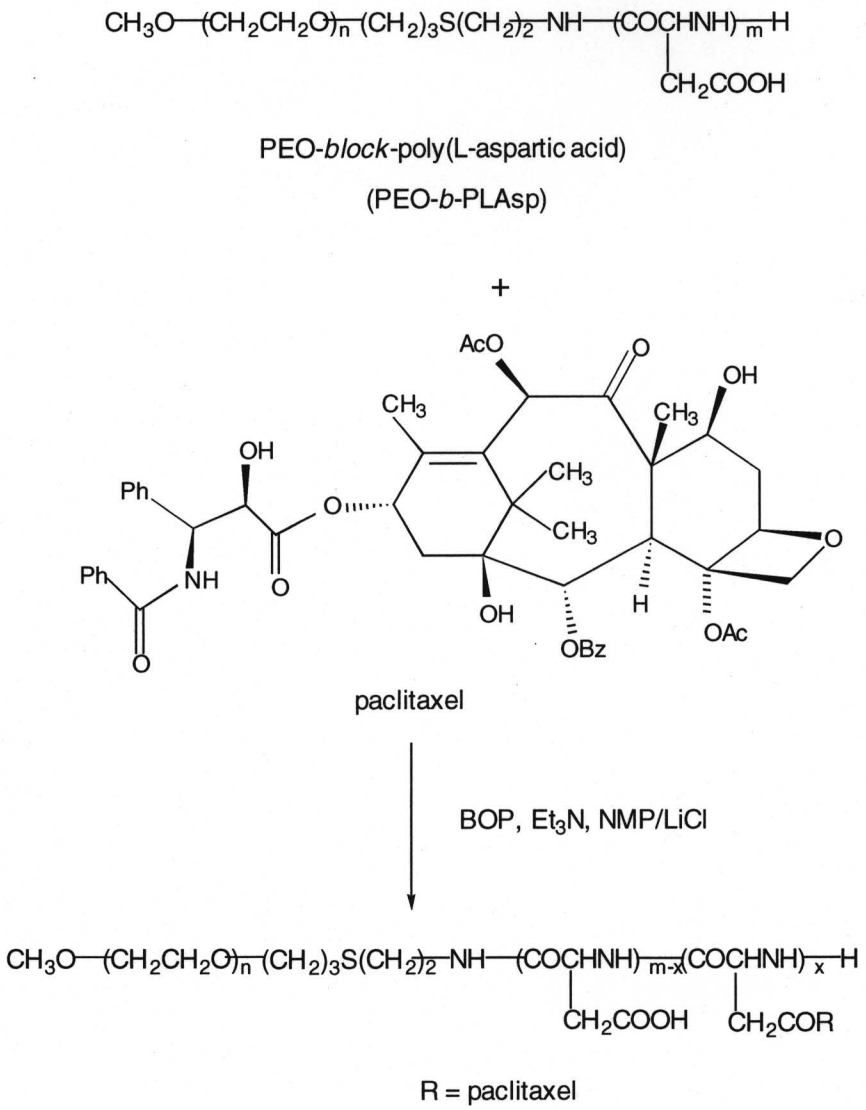


Figure 6. 7. Conjugation of paclitaxel to PEO-*b*-PLAsp

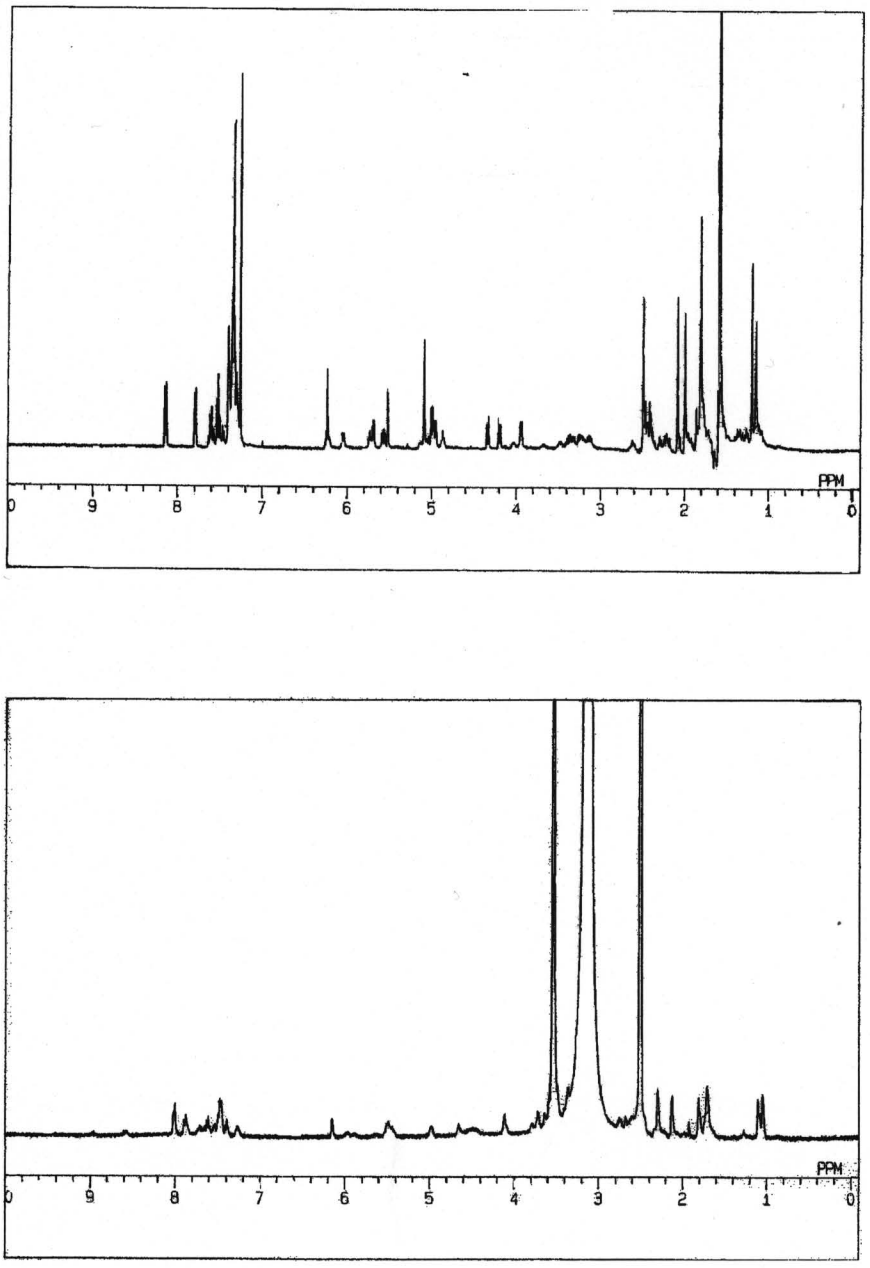


Figure 6. 8. $^{1}$H NMR of the paclitaxel intermediate (upper panel) and PEO-*b*-PLAsp conjugate (lower panel) in $d_6$-DMSO.

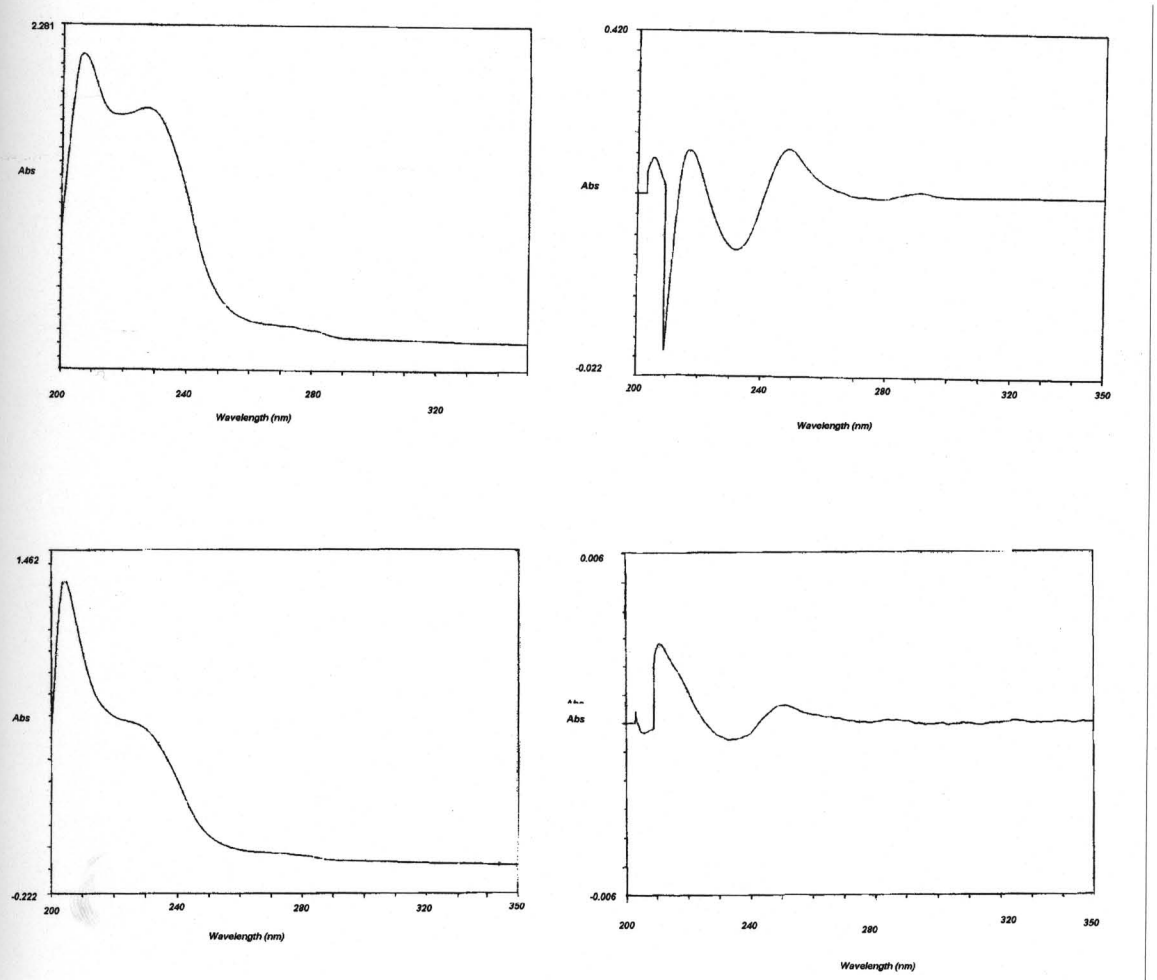


Figure 6. 9. UV spectra of paclitaxel and its conjugate. (a) Paclitaxel; (b) Secondary differentiation of UV spectrum of paclitaxel. (c ) Paclitaxel conjugate of PEO-*b*-PLAsp. (d) Secondary differentiation of UV spectrum of paclitaxel conjugate.

Table 6.1. Conjugate of paclitaxel with PEO-*b*-PLAsp

| Conjugate | Structural | Paclitaxel content (UV-Vis) | | mol % ($^1$H NMR) |
|---|---|---|---|---|
| | | mol% | weight% | |
| LYJ010 | 12-24-C4 | 12.5 | 15.5 | n.d. |
| LYJ040 | 12-24-C4 | 21.0 | 24.3 | 15.4 |
| LYJ034 | 12-24-C6 | 38.8 | 40.0 | 22.5 |

substitution; however, UV analysis yielded more reliable results, since $^1$H NMR for quantitation was believed to have high systematic error. Error also resulted from the large difference in the molecular weight of PEO and the conjugated paclitaxel moieties, as error introduced from signal integration might be significant.

### *6.3.2. Association of the conjugates to form aggregates*

The conjugation of paclitaxel to PEO-*b*-PLAsp greatly changed hydrophobicity of the polymer exhibited as micelle formation. PEO-*b*-PLAsp was not hydrophobic enough to form micelles. With conjugated paclitaxel, however, micelle formation could occur under proper conditions. The assembly of the block copolymer conjugates was carried out under different conditions. Because of strong interaction among the paclitaxel moieties, an aqueous solution of the conjugate prepared from concentrated polymer in organic solution appeared cloudy. Therefore, instead of 5 mg/mL polymer in DMAC, a typical concentration used for preparation of micelles, five or ten times diluted polymer solution in several organic solvents was employed (about 0.5 mg/mL). After dialysis, the conjugate aqueous solution was very dilute, and hardly detected micelles using the DLS technique (< 2 nm). The solution was then concentrated by ultrafiltration by three- to four-fold, and micelle size was determined (Table 6.2 and 6.3). In DMSO, micelles from sample LYJ010 had a size of 194.5 ± 79 nm based on weight or 156.4 ± 35 nm based on number ($d_w/d_n$ was 1.24) (Figure 6.10). Using DMAC as solvent micelles of the conjugates resulted in a small size and narrow size distribution (Table 6.2). The size of micelles was 15 to about 70, depending on the composition of the conjugates. When $CH_3OH$ was used as the solvent, the resulting micelle showed a larger size,

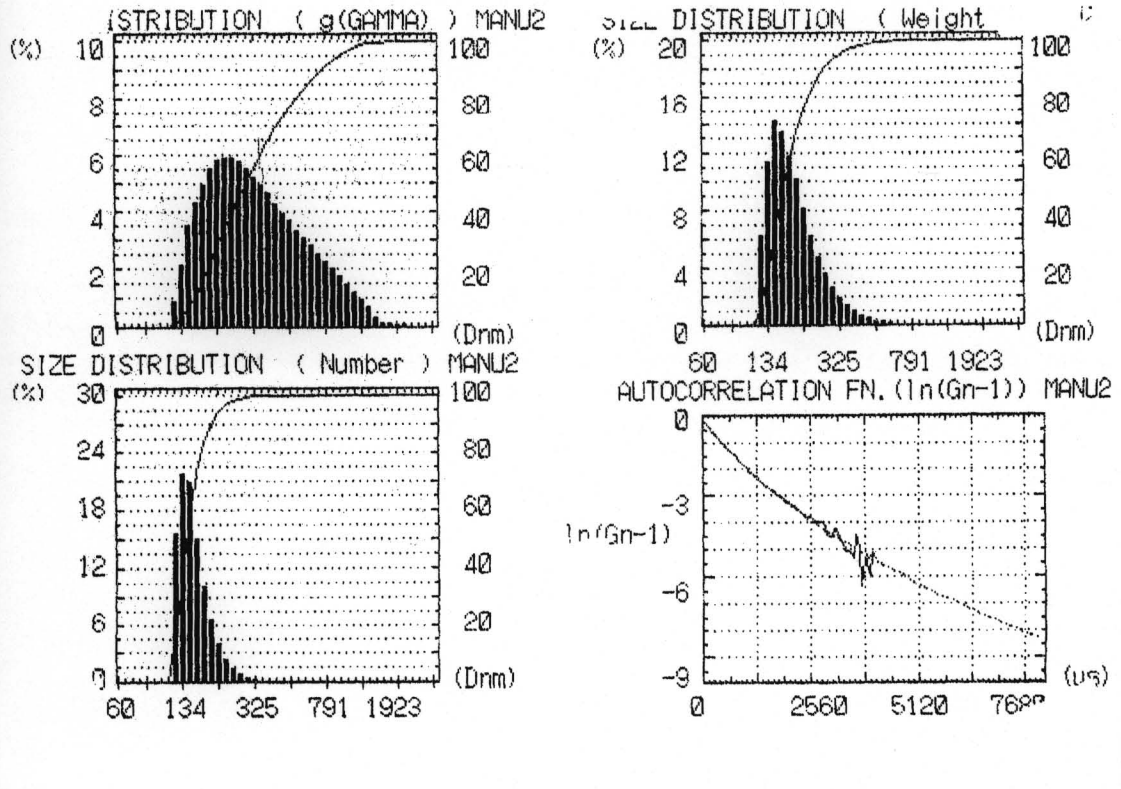


Figure 6. 10. Size distribution of LYJ010 micelles by DLS.

Table 6.2. Size of micelles prepared from DMAC

| Sample | Size ($D_{Wt}$) concentrated | Size ($D_{No}$) concentrated | $D_w/D_{no}$ |
|---|---|---|---|
| LYJ010 | 18.8±1.0 125.9±3.6 | 18.6±1.0 107±1.0 | |
| LYJ040 | 48.3±16.9 | 45.4±4.2 | 1.06 |
| LYJ032 | 68.0±24.1 | 64.0±6.7 | 1.06 |

Table 6.3 Size of micelles prepared from methanol

| Sample | Size ($D_w$) | Size ($D_{no}$) | $D_w/D_{no}$ |
|---|---|---|---|
| LYJ010 | n.d. | n.d. | |
| LYJ040 | 126.0±33.1 | 107.9±22.9 | 1.17 |
| LYJ032 | 123.2±38.2 | 102.2±23.6 | 1.21 |

about 100 nm (based on number). Occasionally, the secondary association of micelles was observed. For LYJ010, sizes based on number were 18.6 nm and 107 nm, which might represent a single micelle size and aggregated micelle size, respectively.

The self-association of paclitaxel conjugates was also confirmed by a fluorescent probe, pyrene. Pyrene has been widely used as a fluorescence probe because its vibrational structure is sensitive to polarity. Thus, a variety of micelle properties, such as critical micelle concentration, micropolarity or mobility can be estimated following the photophysical behavior of pyrene in micelle solutions. Usually the relative change of the first band and the third band in the pyrene emission spectrum, which is defined as $I_1/I_3$, reveals the microenvironmental change of pyrene. The solubilization of pyrene by conjugate micelles (LYJ049) was revealed by the change of $I_1/I_3$. As the concentration of conjugate increased, the $I_1/I_3$ value shifted from 1.62 to 1.02, indicating a change, after uptake of pyrene molecules by micelles, from polar to non polar (Figure 6.11). The CMC of the solution was about 0.02 mg/mL extrapolated from the plot.

### *6.3.3. Release of paclitaxel from the conjugates*

The stability of paclitaxel-PEO-*b*-PLAsp was evaluated at various pH values and in the presence of two lysosomal enzymes, capthesin B and capthesin D (Figure 6.12). At pH 12, both conjugate and paclitaxel were degraded in two hours. However, at pH 3 and 5, the conjugate was relatively stable, compared to pH 7. The presence of the two lysosomal enzymes did not influence the stability of the conjugates significantly. As the self-assembly of paclitaxel-PEG-*b*-PLAsp resulted in a core/shell structure and the drug moieties would

reside in a hydrophobic environment. Therefore, the hydrolysis of the ester bonds in micelles might be slow, especially compared to ester prodrugs with ester bonds exposed to the surrounding media.

These results demonstrated the potential of using block copolymer as a carrier for paclitaxel to circumvent the solubility problem and achieve sustained drug release. Paclitaxel was successfully conjugated to PEO-*b*-PLAsp. The resulting conjugates formed micelles in aqueous solution with a nanoscopic size. In such a solution, the paclitaxel concentration reached up to 0.15 mg/mL for the conjugate with 21 % (mol/mol) paclitaxel. The conjugates slowly released drug at neutral pH 7.4. However, more research needs to be done in the aspects of drug release behavior and the biological and pharmacological properties of the conjugates.

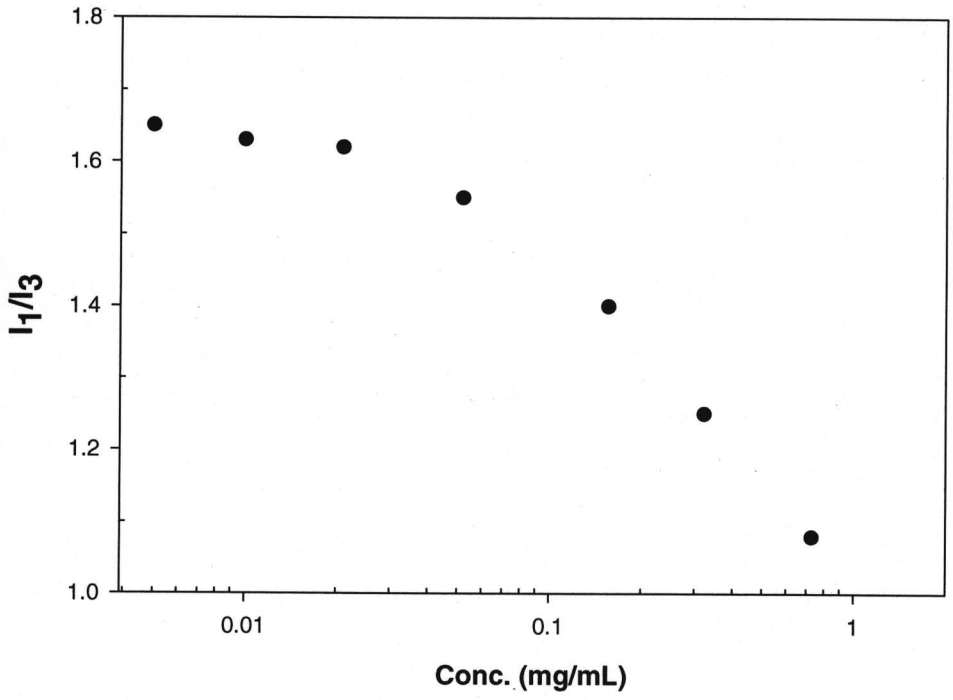


Figure 6. 11. Plot of $I_1/I_3$ of fluorescence spectrum of pyrene as a function of concentration.

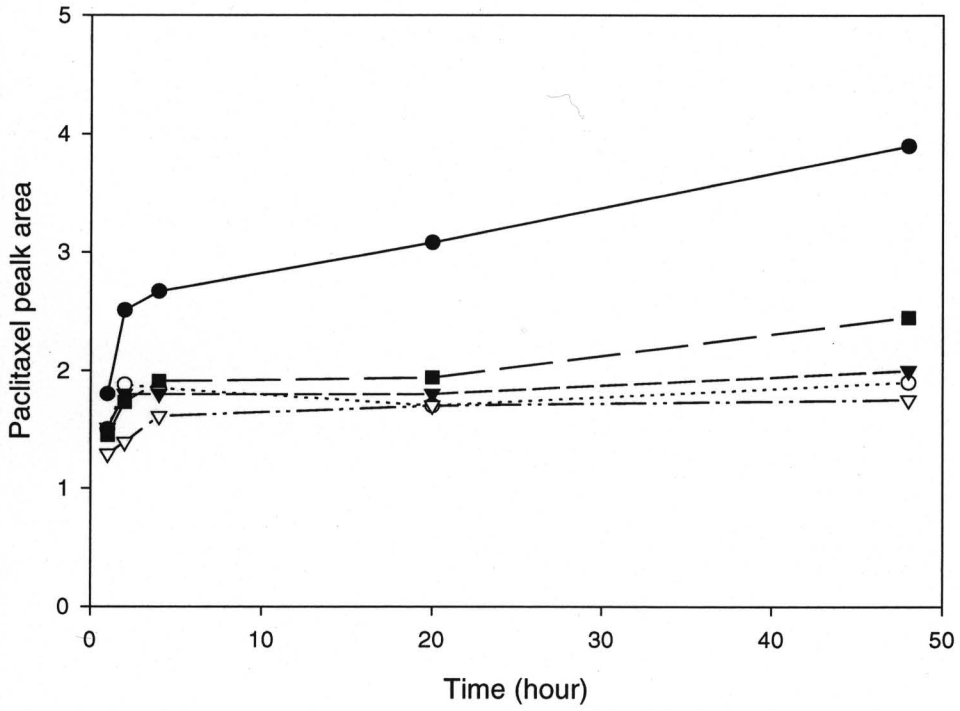


Figure 6. 12. Release of paclitaxel from the conjugates at varied conditions. -●- pH 7.4; -■- pH 2.0; -▼- in the presence of capthesin D (pH 5.0); -○- in the presence of capthesin B (pH 5.0); -▽- pH 5.0.

# CHAPTER 7.

# Conclusions and Suggestions for Future Work

## 7.1. Conclusions

In the previous chapters, we have discussed the design and synthesis of micelle-forming drug-polymer conjugates, the characterization of the conjugates and the resulting micelle systems, the assessment of micelle stability and drug release, and the evaluation of some of the biological properties of such systems. The following conclusions can be derived from this thesis work:

1. The application of amphiphilic block copolymer PEO-*b*-PBLA can be expanded by the chemistry on the hydrophobic block, including aminolysis to introduce a functional hydroxyl group and hydrolysis or hydrogenolysis to release the protected carboxyl groups. These functional groups are the potential sites for the conjugation of drugs, such as methotrexate and paclitaxel, and for the structural modification of block copolymer to facilitate physical drug loading.
2. A model of micelle-forming drug-polymer conjugate has been designed. In this model, the drug molecules are covalently bonded to the block copolymer backbone via a hydrolyzable ester linkage. An alkyl spacer group is also utilized in the model with dual functions: bridging the drug moieties with polymeric backbone and modifying the amphiphilicity of the block copolymer. Two anticancer drugs, methotrexate and paclitaxel, have been used as examples of drugs to illustrate the designed model. Due to

the structural difference between the two drugs, two synthetic routes have been developed for the conjugation of the drugs to block copolymer PEO-*b*-PLAA. For paclitaxel conjugation, a spacer with amino and carboxyl groups at its termini was used. For mothotrexate conjugation, a two- or six-carbon spacer with amino and hydroxyl groups at its termini was used, and the conjugation of methotrexate to PEO-*b*-PLAA was achieved with good yield and a controllable level of drug substitution. A variety of MTX conjugates of PEO-*b*-PLAA have been synthesized, which vary in the structure of the hydrophobic PLAA block: degree of polymerization, length of alkyl spacer group and degree of drug substitution.

3. MTX esters self-assemble into spherical micelles with a core/shell structure in aqueous media. The formation of micelles is demonstrated by the restricted movement of the hydrophobic block in $^{1}H$ NMR studies, due to the participation from the aqueous media. The hydrophobic nature of the core is evidenced by the partition of the fluorescent probe, nile red. However, the method for micelle preparation is critical for achieving small sizes of micelles with a narrow size distribution. The gradual addition of water to the solution of block copolymers in organic solvents such as DMAc allows the slow orientation of the amphiphilic molecules favored for the formation of spherical nanoscopic micelles. Regardless of the chemical compositions, the size of micelles of MTX esters of PEO-*b*-PLAA falls in the range of 10-100 nm, the desired size for macromolecules to be maintained in circulation without being recognized by the RES system. The conjugates with higher molecular weight tended to form micelles with larger sizes. The critical micelle concentration (CMC), an indicator of the thermodynamic stability of a micelle system, showed a notable dependency on the structure of the hydrophobic block. The

conjugates with a high level of MTX substitution and a long spacer group (six-carbon) exhibited low CMCs. It can be deduced that the micelles from the conjugates with high hydrophobicity have low CMC and vice versa.

4. The unimers and micelles of MTX esters of PEO-*b*-PLAA exist in equilibria. The unimer-micelle equilibria of MTX esters of PEO-*b*-PLAA are strongly influenced by the structure of the core-forming PLAA block, namely the degree of drug substitution, the length of spacer groups, and the lengths of polymeric backbone. Polymeric micelles based on the conjugates with a low level of MTX tend to dissociate rapidly compared to the micelles with a high level of drug conjugation. The alkyl spacer displayed a remarkable effect on the micelle stability in terms of dissociation. The micelles formed from the conjugates with long spacer groups showed extraordinary stability. The dissociation of micelles was not observed in SEC-HPLC studies for several weeks. The micelle stability was closely related to the rate of drug release. The rate of MTX release (ester hydrolysis) was slow and was influenced by alterations in the chemical structure of the core-forming PLAA block. The micelles with high stability displayed slow drug release. Accordingly, the conjugate with a high level of drug substitution and a long spacer group released the drug slowly. The relationship between the micelle stability and drug release may indicate the mechanism of drug release from the polymeric micelles. Since the release of MTX requires nucleophilic attack at the ester bond, the hydrophobic core is not a good environment for releasing the drug. Therefore, the dissociation of micelles is required to liberate the unimers and release the drugs. This mechanism may also be applicable to a physical loading system. On the other hand, a certain amount of aqueous molecules may also be entrapped in the micelle core, and those molecules may

serve as the nucleophiles for hydrolysis and release of the drugs. Less stable micelle may trap more water into the core and facilitate drug release. Based on these results, it is difficult to differentiate the dominant process.

5. The conjugation of MTX on PEO-*b*-PHAA resulted in decreased inhibitory activity toward DHFR and L1210 cells of the drug and altered the cellular uptake pathway of MTX from receptor-mediated endocytosis to a non receptor-mediated endocytotic process.
6. When paclitaxel is conjugated to PEO-*b*-PLAA, the resulting conjugate is water-soluble and forms micelles in aqueous solution with the size smaller than 100 nm. The conjugate releases the drug slowly, which is an advantage of micelle-forming drug conjugate technology. The successful conjugation of paclitaxel to PEO-*b*-PLAA provided a feasible approach to solve the solubility problem of this drug as well as to provide slow drug release system. Although several systems have been reported with improved solubility, there is no system yet that provides a slow release property.

## 7.2. Summary of contributions

1. Established a methodology for the modification of the side chain of poly(ethylene oxide)-*block*-poly(β-benzyl-L-aspartate). Based on the established methods, functional groups can be introduced to the block copolymer, and a variety of molecules such as drugs and structurally modifying moieties can be conjugated to the polymer. The application of the block copolymer in drug delivery is greatly broadened.

2. Developed the first example of micelle-forming drug-polymer conjugates which possess a hydrolyzable ester linkage for conjugating and releasing drugs. Such conjugates can be used for the delivery of hydrophobic drugs, e.g., paclitaxel, protect the drugs from degradation due to the formation of micelles, and slowly release the drugs.
3. Demonstrated the relationship of the structure of a micelle-forming block copolymer and the properties of polymeric micelles. These properties were correlated, for the first time, with drug release from the micelle-forming conjugates. This relationship has a profound impact on revealing the mechanism of drug release and achieving controlled drug release. The outcome brought by such structural changes is of great importance in drug delivery.

## 7.3. Suggestions for future work

Block copolymer micelles bearing small drug molecules conjugated through ester bonds provide a new and practical approach for controlled drug delivery due to the hydrolyzable nature of ester bonds, the physicochemical properties of polymeric micelles; the feasibility of altering the structure of the block copolymer, and the potential of the micelles in biological system for a prolonged circulation.

Although we have demonstrated some fundamental aspects of a micelle-forming drug conjugate system using MTX esters as a model system, particularly on the impact of the hydrophobicity on micelle stability, numerous studies can be further carried out. These can include developing new drug conjugate systems based on the established chemistry, and continuing the studies on paclitaxel conjugate system. However, revealing the mechanism of drug release from polymeric micelles and the mechanism of biological action should be the

primary goal for future studies. Such studies can provide the fundamentals for the clinical application of polymeric micelles as drug carriers.

Studies on MTX esters of PEO-*b*-PHAA have provided some insight on the issues of polymeric micelles in drug delivery. The studies should be continued in following aspects:

1. further understanding of the physicochemical properties of the micelle system such as the internal structure of micelles, the packing of the hydrophobic block, the aggregation number of unimers per micelle, and the volume available for drug loading;
2. the dynamics of unimer-micelle equilibria and its impact on drug release, and the dynamics of the hydrophobic block in the micelle core to provide the mechanism of micelle dissociation;
3. the mechanisms and the kinetics of drug release, including the demonstration of the drug release process, the determination of the rate limiting step; and adjusting variables in controlled drug release;
4. the interactions of the amphiphilic drug conjugates with the cell membrane. The current belief is that the cellular uptake occurs via pinocytosis. However, the amphiphilic nature of the block copolymer may interfere or disturb the structure of the cell membrane and facilitate cellular uptake of the conjugate;
5. the *in vivo* mechanism of action of micelle-forming conjugates;
6. passive tumor accumulation of such conjugates and the impact of structural changes on the pharmacokinetics and *in vivo* activity.

# REFERENECES


1. Sander, C. **2000.** Genomic medicine and the future of health care. *Science* 287:1977-1978

2. Rosamond, J., Allsop, A. **2000.** Harnessing the power of the genome in the search of new antibiotics. *Science* 287:1973-1976

3. Alberts, B., Bray, D., Lewis, J., Raff, M., Roberts, K., et al. **1994**. Molecular biology of the cell, pp. 621. New York: Garland Publishing, Inc.

4. Pouton, C. W., Seymour, L. W. **1998.** Key issues in non-viral gene delivery. *Advanced Drug Delivery Reviews.* 34:3-19

5. Yokoyama, M., Okano, T., Sakurai, Y., Ekimoto, H., Skibazaki, C., et al. **1991.** Toxicity and antitumor activity against solid tumors of micelle-forming polmeric anticancer drug and its extremely long circulation in blood. *Cancer Research* 29:17-23

6. Ringsdorf, H. **1975.** Structure and properties of pharmacologically active polymers. *J. Polymer. Sci.: Symposium* 51:135

7. Duncan, R., Seymour, L. W., O'Hare, K. B., Flanagan, P. A., Wedge, S., et al. **1992.** Preclinical evaluation of polymer-bound doxorubicin. *J. Control. Rel.* 19:331-346

8. Gregoriadis, G., Florence, A. T. **1993.** Recent advances in drug targeting. *TIBTECH* :11

9. Allen, C., Eisenberg, A., Maysinger, D. **1999.** Copolymer drug carriers: conjugates, micelles and microspheres. *S. T. P. Pharm. Sci.* 9:139-151

10. Dundan, R., Spreafico, F. **1994.** Polymer conjugates. *Clin. Pharmacokinet.* 27:290-306

11. Seymour, L. W., Ulbrich, K., Steyger, P. S., Brereton, M., Subr, V., et al. **1994.** Tumor tropism and anti-cancer efficacy of polymer-based doxorubicin prodrugs in the treatment of subcutaneous murine B16F10 melanoma. *Br. J. Cancer* 70:636-641

12. Kabanov, A. V., Alakhov, V. Y. 1993. Micelles of amphiphilic block copolymers as vehicles for drug delivery. In *Amphiphilic block copolymers: self-assembly and applications*, ed. P. Alexamdris, B. Lindman. Amstrdam: Elsevier

13. Kataoka, K., Kwon, G. S., Yokoyama, M., Okano, T., Sakurai, Y. **1993.** Block copolymer micelles as vehicles for drug delivery. *Journal of Controlled Release* 24:119-132

14. Patten, M. K., Lloyd, J. B., Horpel, G., Ringsdorf, H. **1985.** Micelle-forming block copolymers: pinocytosis by macrophages and interaction with model membranes. *Makromol. Chem.* 186:725-733.

15. Yokoyama, M., Miyauchi, M., Yamada, N., Okano, T., Sakurai, Y., et al. **1990.** Characterization and anticancer activity of the micelle-forming polymeric anticancer drug adriamycin-conjugated poly(ethylene glycol)-poly(aspartic acid) *block* copolymer. *Cancer Research* 50:1693-1700

16. Kwon, G. S., Naito, M., Kataoka, K., Yokoyama, M., Sakurai, Y., et al. **1994.** Block copolymer micelles as vehicles for hydrophobic drugs. *Colloids and Surfaces B: Biointerfaces* 2:429-434

17. Yokoyama, M., Sugiyama, T., Okano, T., Sakurai, Y., Naito, M., et al. **1993.** Analysis of micelle formation of an adriamycin-conjugated poly(ethylene glycol)-poly(aspartic

Acid) block copolymer by gel permeation chromatography. *Pharmaceutical Research* 10:895-899

18. Yokoyama, M., Okano, T., Sakurai, Y., Kataoka, K. **1994.** Improved synthesis of adriamycin-conjugated poly(ethylene oxide)-poly(aspartic acid) block copolymer and formation of unimodal micelles structure with controlled amount of physically entrapped adriamycin. *J. Controlled Rel.* 32:269-276

19. Lin, S., Kawashima, Y. **1985.** The influence of three poly(oxyethylene) poly-(oxypropylene) surface-active block copolymers to the solubility behavior of indomethacin. *Pharm. Acta Helv.* 60:339

20. Forster, S., Antonietti, M. **1998.** Amphiphilic block copolymers in structure controlled nanomaterial hybrids. *Advanced Materials* 10:195-217

21. Miller, D. W., Batrakova, E. V., Waltner, T. O., Alakhov, Y. V., Kabanov, A. V. **1997.** Interactions of Pluronic block copolymers with brain microvessel endothelial cells: evidence of two potential pathways for drug absorption. *Bioconjugate Chem.* 8:649-657

22. Alakhov, V. Y., Moskaleva, E. Y., Batrakova, E. V., Kabanov, A. **1996.** Hypersensitization of multidrug resistant human ovarian carcinoma cells by Pluronic P85 block copolymer. *Bioconjugate Chem.* 7:209-216

23. Cammas, S., Suzuki, K., Sone, C., Sakurai, Y., Kataoka, K., et al. **1997.** Thermo-responsive polymer nanoparticles with a core-shell micelle structure as site-specific drug carriers. *Journal of Controlled Release* 48:157-164

24. Heskins, M., Guillet, J. E. **1968.** Solution properties of poly(N-isopropylacrylamide). *J. Macromol. Sci. Chem.* A2:1441-1455

25. Kohori, F., K. Sakai, T. Aoyagi, M. Yokoyama, Y. Sakurai, et al. **1998.** Preparation and characterization of thermally responsive block copolymer micelles comprising poly(N-isopropylacrylamide-*b*-d,l-latide). *J. Control. Rel.* 55:87-98

26. Kohori, F., K. Sakai, T. Aoyagi, M. Yokoyama, M. Yamato, et al. **1999.** Control of adriamycin cytotoxic activity using thermally responsive polymeric micelles composed of poly(N-isopropylacrylamide-*co*-N, N-dimethylacrylamide)-*b*-poly(d, l-lactide). *Colloids and Surfaces B: Biointerfaces* 16:195-205

27. Scholz, C., Iijima, M., Nagasaki, Y., Kataoka, K. **1995.** A novel reactive polymeric micelle with aldehyde groups on its surface. *Macromolecules* 28:7295-7297

28. Cammas-Marion, S., Okano, T., Kataoka, K. **1999.** Functional and site-specific macromolecular micelles as high potential drug carriers. *Colloids and Surfaces B: Biointerfaces* 16:207-215

29. Li, Y., Kwon, G. S. **1999**. Conjugation of targeting molecules to the surface of poly(ethylene oxide)-*block*-poly(D, L-lactic acid) micelles. *The 31st Pharmaceutics Graduates Students Research Meeting, Kansas City, Missouri,* PS26

30. Kabanov, A. V., Batrakova, E. V., Melik-Nubarov, N. S., Fedoseev, N. A., Dorodnich, T. Y., et al. **1992.** A new class of drug carriers: micelles of poly(oxyethylene)-poly(oxypropylene) block copolymers as microcontainers for drug targeting from blood in brain. *J. Controlled Rel.* 22:141-158

31. Philp, D., Stoddart, J. F. **1996.** Self-assembly in natural and unnatural systems. *Angew. Chem. Int. Ed. Engl.* 35:1154-1196

32. Francis, G. E., Delgado, C., Fisher, D., Nakuj, F., Agrawal, A. K. **1996.** Polyethylene glycol modification: relevance of improved methodology to tumor targeting. *Journal of Drug Targeting* 3:321-340

33. Zhang, L., Shen, H., Eisenberg, A. **1997.** Phase separation behavior and crew cut micelles formation of polystyrene-*b*-poly(acrylic acid) copolymers in solutions. *Macromolecules* 30:1001-1011

34. Kozlov, M. Y., Melik-Nubarov, N. S., Batrakova, E., Kabanov, A. **2000.** Relationship between pluronic block copolymer structure, critical micellization concentration and partitioning coefficients of low molecular mass solute. *Macromolecules* 33:3305-3313

35. Allen, C., Maysinger, D., Eisenberg, A. **1999.** Nano-engineering block copolymer aggregates for drug delivery. *Colloids and Sufaces B: Biointerfaces* 16:3-27

36. La, S. B., Okano, T., Kataoka, K. **1996.** Preparation and characterization of the micelle-forming polymeric drug indomethacin-incorporated poly(ethylene oxide)-poly(β-benzyl L-aspartate) *block* copolymer micelles. *Journal of Pharmaceutical Sciences* 85:85-90

37. Creutz, S., Stam, J., De Schryver, F. C., Jerome, R. **1998.** Dynamics of poly((dimethylamino)alkyl methacrylate-*block*-sodium methacrylate) micelles. Influence of hydrophobicity and molecular architecture on the exchange rate of copolymer molecules. *Macromolecules* 31:681-689

38. Hagan, S. A., Coombes, A. G. A., Garnett, M. C., Dunn, S. E., Davies, M. C., et al. **1996.** Polylactide-poly(ethylene glycol) copolymers as drug delivery systems. 1.

Characterization of water dispersible micelle-forming systems. *Langmuir* 12:2153-2161

39. Nogochi, Y., Wu, J., Duncan, R., Strohalm, J., Ulbrich, K., et al. **1998.** Early phase tumor accumulation of macromolecules: A great difference in clearance rate between tumor and normal tissues. *Jpn. J. Cancer Res.* 89:307-314

40. Baban, D. F., Seymour, L. W. **1998.** Control of tumor vascular permeability. *Advanced Drug Deliver Reviews* 34:109-119

41. Jain, R. K. **1997.** Delivery of molecular and cellular medicine to solid tumors. *Advanced Drug Delivery* 26:71-90

42. Kataoka, K. 1997. Targetable polymeric drugs. In *Controlled drug delivery: Challenges and strategies*, ed. K. Park, pp. 49-71. Washington, D. C.: American Chemical Society

43. Kwon, G. S., Naito, M., Yokoyama, M., Okano, M., Sakurai, Y., et al. **1995.** Physical entrapment of adriamycin in AB block copolymer micelles. *Pharm. Res.* 12:192-195

44. Zhang, X., Burt, H. M., Mangold, G., Dexter, D., Hoff, V. D., et al. **1997.** Anti-tumor efficacy and biodistribution of intravenous polymeric micellar paclitaxel. *Anti-Cancer Drugs* 8:696-701

45. Burt, H. M., Zhang, X., P. Toleikis, L. Embree, Hunter., W. L. **1999.** Development of copolymers of poly(D, L-lactide) and methoxypolyethylene glycol as micellar carriers of paclitaxel. *Colloids and Surfaces B: Biointerfaces* 16:161-171

46. Forster, S. Antonietti, M. **1998.** Amphiphilic block copolymers in structure controlled nanomaterial hybrids. *Advanced Materials.* 10:195-217

47. Sela, M., Katachalski, E. **1987.** Biological properties of poly(amino acids). *Adv. Protein Chem.* 14:391-478

48. Li, Y., Kwon, G. S. **1999.** Micelle-like structure of poly(ethylene oxide)-*block*-poly(2-hydroxyethyl aspartamide)-methotrexate conjugates. *Colloids and Surfaces B: Biointerfaces* 16:217-226

49. Yokoyama, M., Kwon, G. S., Okano, T., Sakurai, Y., Seto, T., et al. **1992.** Preparation of micelle-forming polymer-drug conjugates. *Bioconjugate Chemistry* 3:295-301

50. Marre, A. D., Soyez, H., Schacht, E. **1994.** Improved method for the preparation of poly[$N^5$-(2-hydroxyethyl)-L-glutamine] by aminolysis of poly(β-benzyl-L-glutamate). *Polymer* 35:2443-2446

51. Feijen, J., Gregonis, D., Anderson, C., Peterson, R. V., Anderson, J. **1980.** Coupling of steroid hormones to biodegradable poly(α-amino acids) I: norethindrone coupled to poly-$N^5$-(3-hydroxypropyl)-L-glutamate. *J. Pharm. Sci.* 69:871-872

52. Dang, W., Colvin, O. M., Brem, H., Saltzman, W. M. **1994.** Covalent coupling of methotrexate to dextran enhances the penetration of cytotoxicity into a tissue-like matrix. *Cancer Research* 54:1729-1735

53. Gao, Z., Varshney, S. K., Wong, S., Eisenberg, A. **1994.** Block copolymer "crew cut" micelles in water. *Macromolecules* 27:7923-7927

54. Goldmints, I., Von Gottberg, F. K., Smith, K. A., Hatton, T. A. **1997.** Small-angle neutron scattering study of PEO-PPO-PEO micelle structure in the unimer-to-micelle transition region. *Langmuir* 13:3659-3664

55. Allen, C., Yu, Y., Maysinger, D., Eisenberg, A. **1998.** Polycaprolactone-*b*-poly(ethylene oxide) block copolymer micelles as a novel drug delivery vehicle for neurotrophic agents FK506 and L-685,818. *Bioconjugate Chemistry* 9:564-572

56. Yokoyama, M., Satoh, A., Sakurai, Y., Okano, T., Matsumura, Y., et al. **1998.** Incorporation of water-insoluble anticancer drug into polymeric micelles and control of their particle size. *J. Control. Rel.* 55:219-229

57. Deye, J. F., Berger, T. A. **1990.** Nile red as a solvatochromic dye for measuring solvent strength in normal liquids and mixtures of normal liquids with supercritical and near critical fluids. *Anal. Chem.* 62:615-622

58. Haynes, L. C., Cho, M. J. **1988.** Mechanism of nile red transfer from o/w emulsions as carriers for passive drug targeting to peritoneal macrophages in vitro. *International J. Pharm.* 45:169-177

59. Sackett, D. L., Wolff, J. **1987.** Nile red as a polarity-sensitive fluorescent probe of hydrophobic protein surfaces. *Anal. Biochem.* 167:228-234

60. Tancrede, P., Barwicz, J., Jutras, S., Gruda, I. **1990.** The effect of surfactants on the aggregation state of amphotericin B. *Biochimica et Biophysica Acta* 1030:289-295

61. Szczubialka, K., Ishikawa, K., Morishima, Y. **1999.** Micelle formation of diblock copolymer of styrene and sulfonated isoprene in aqueous solution. *Langmuir* 15:454-492

62. Teng, Y., Morrison, M. E., Munk, P., Webber, S. E. **1998.** Release kinetics studies of aromatic molecules into water from block polymer micelles. *Macromolecules* 31:3578-3587

63. Hurter, P. N., Hatton, T. A. **1992.** Solubilization of polycyclic aromatic hydrocarbons by poly(ethylene oxide-propylene oxide) block copolymer micelles: Effect of polymer structure. *Langmuir* 8:1291-1299

64. Gorshkova, M. Y., Stoskaya, L. L. **1998.** Micelle-like macromolecular systems for controlled release of daunomycin. *Polym. Adv. Technol.* 9:362-367

65. Wang, Y., Balaji, R., Quirk, R. P., Mattice, W. L. **1992.** Detection of the rate of exchange of chains between micelles formed by diblock copolymers in aqueous solution. *Polymer Bulletin* 28:333-338

66. Winnik, M. A., Yekata, A. **1997.** Associative polymers in aqueous solution. *Current Opinion in Colloid & Interface Sciences* 2:424-436

67. Williams, A., Love, W. G., Williams, B. D. **1992.** Synthesis of methotrexate-dimyristoylphosphatidylethanolamine analogs and characterization of methotrexate release *in vitro*. *International J. Pharm.* 85:189-197

68. Peterson, D. L., Gleisner, J. M., Blakley, R. L. **1975.** Bovine liver dihydrofolate reductase: purification and properties of the enzyme. *Biochemistry* 14:526

69. Mosmann, T. **1983.** Rapid colorimetric assay for cellular growth and survival: application to proliferation and cytotoxicity assays. *J. Immunological Methods* 65:55-63

70. Scudiero, D. A., Shoemaker, R. H., Paull, K. D., Monks, A., Tierney, S., et al. **1988.** Evaluation of a soluble tetrazolium/formazan assay for cell growth and drug sensitivity in culture using human and other cell lines. *Cancer Res.* 48:4827-4833

71. Pignatello, R., Sorrenti, V., Spampinato, G., Pecora, T., Panico, A., et al. **1996.** Synthesis and preliminary *in vitro* screening of lipophilic a, γ-bis(amides) as potential prodrugs of methotrexate. *Anti-Cancer Drug Design* 11:253-264

72. McCormack, J. J. 1990. Reductases. In *Comprehensive Medicinal Chemistry*, ed. C. Hansch, P. G. Sammes, J. B. Taylor, pp. 271. Oxford: Pergamon

73. Shen, W. C., Ryser, H. J. P. **1979.** Poly(L-Lysine) and poly(D-Lysine) conjugates of methotrexate: different inhibitory effect on drug resistant cells. *Mol. Pharmacol.* 16:614-622

74. Taira, K., Benkovic, S. J. **1988.** Evaluation of the importance of hydrophobic interactions in drug binding to dihydrofolate reductase. *J. Med. Chem.* 31:129-134

75. Rosowsky, A., Forsch, R. A., Galivan, J., Susten, S. S., Freisheim, J. H. **1985.** Regiospecific γ-conjugation of methotrexate to poly(L-lysine) chemical and biological studies. *Mol. Pharmacol.* 27:141-147

76. Hudecz, F., Clegg, J. A., Kajtar, J., Embleton, M. J., Pimm, M. V., et al. **1993.** Influence of carrier on biodistribution and *in vitro* cytotoxicity of methotrexate-branched polypeptide conjugates. *Bioconjugate Chem.* 4:25-33

77. Kamen, B., Eibl, B., Cashmore, A., Bertino, J. **1984.** Uptake and efficacy of trimetrexate (TMQ, 2,4-diamino-5-methyl-6-[(3,4,5-trimethoxyanilino)methyl] quinazolite), a non-classical antifolate in methotrexate-resistant leukemia cells *in vitro*. *Biochemical Pharmacology* 33:1697-1699

78. Ryser, H. J. P., Shen, W. C. **1978.** Conjugation of methotrexate to poly(L-lysine) increases drug transport and overcomes drug resistance in cultured cells. *Proc. Natl. Acad. Sci. U. S. A.* 75:3867-3870

79. Drori, S., Eytan, G. D., Assaraf, Y. G. **1995.** Potentiation of anticancer drug cytotoxicity by multidrug-resistance chemsensitizers involves alterations in membrane fluidity leading to increased membrane permeability. *Eur. J. Biochem* 228:1020-1029

80. Rowinsky, E. K., Donehower, R. C. **1995.** Paclitaxel. *N. Engl. J. Med.* 332:1004-1014

81. Spencer, C. M., Faulds, D. **1994.** Paclitaxel. *Drugs* 48:794-847

82. Fjallskog, M. L., Frii, L., Bergh, J. **1993.** Is cremophor, solvent for paclitaxel, cytotoxic? *Lancet* 342:876

83. Weiss, R. B., Donehower, R. C., Wiernik, P. H., Ohnuma, T., Gralla, R. L., et al. **1990.** Hypersensitivity reactions from taxol. *J. Clin. Oncol.* 8:1263-1268

84. Riondel, J., Jacrot, M., Fessi, H., Puisieux, F. **1992.** Effects of free and liposomes-encapsulated taxol on two brain tumors xenografted in nude mice. *In vivo* 6:23-28

85. Sharma, A., Balasubramianian, S. V., Straubingen, R. M. **1995.** Pharmaceutical and physical properties of paclitaxel (taxol) complexes with cyclodextrins. *J. Pharm. Sci.* 84:1223-1230

86. Cserhati, T., Forgacs, E., Hollo, J. **1995.** Interaction of taxol and other anticancer drugs with α-cyclodextrin. *Pharm. Res.* 13:533-541

87. Alkan-Onyuksel, H., Ramakrishnan, S., Chai, H. B., Pezzuto, J. M. **1994.** A mixed micellar formulation suitable for the parenteral administration of taxol. *Pharm. Res.* 11:206-212

88. Connors, T. A., Knox, R. J. **1995.** Prodrugs in cancer chemotherapy. *Stem Cells* 13:501-511

89. Sinhababu, A. K., Thakker, D. R. **1996.** Prodrugs of anticancer agents. *Advanced Drug Delivery Review* 19:241-273

90. Balant, L. P., Doelker, E., Buri, P. **1991**. *Pharmacokinetics strategies in the development of prodrugs*. New trends in pharmacokinetics. New York

91. Mongelli, N., Pesenti, E., Suarato, A., Biasoli, G. **1994**. Polymer bound paclitaxel derivatives. US 5,362,861

92. Greenwald, R. B., Gilbert, C. W., Pendri, A., Conover, C. D., Xia, J., et al. **1996.** Drug delivery systems: water soluble taxol 2'-poly(ethylene glycol) ester prodrugs-design and in *vivo* effectiveness. *J. Med. Chem.* 39:424-431